



## University of Bradford eThesis

This thesis is hosted in [Bradford Scholars](#) – The University of Bradford Open Access repository. Visit the repository for full metadata or to contact the repository team



© University of Bradford. This work is licenced for reuse under a [Creative Commons Licence](#).

**SIMULATION, OPTIMISATION AND FLEXIBLE  
SCHEDULING OF MSF DESALINATION PROCESS  
UNDER FOULING**

Optimal Design and Operation of MSF Desalination Process with  
Brine Heater and Demister Fouling, Flexible Design Operation and  
Scheduling under Variable Demand and Seawater Temperature  
using gPROMS

**EBRAHIM Ali M. HAWAIDI**

*BSc. Chem. Eng and MSc.*

Submitted for the Degree of

Doctor of Philosophy

School of Engineering, Design and Technology

University of Bradford

United Kingdom

2011

## Abstract

Keywords: Modelling, Optimisation, MSF desalination process, Neural Networks, Seawater temperature, Freshwater demand, Fouling, Flexible Scheduling, gPROMS

Among many seawater desalination processes, the multistage flash (MSF) desalination process is a major source of fresh water around the world. The most costly design and operation problem in seawater desalination is due to scale formation and corrosion problems. Fouling factor is one of the many important parameters that affect the operation of MSF processes. This thesis therefore focuses on determining the optimal design and operation strategy of MSF desalination processes under fouling which will meet variable demand of freshwater.

First, a steady state model of MSF is developed based on the basic laws of mass balance, energy balance, and heat transfer equations with supporting correlations for physical properties. gPROMS software is used to develop the model which is validated against the results reported in the literature. The model is then used in further investigations.

Based on actual plant data, a simple dynamic fouling factor profile is developed which allows calculation of fouling factor at different time (season of the year). The role of changing brine heater fouling factor with varying seawater temperatures (during the year) on the plant performance and the monthly operating costs for fixed water demand and fixed top brine temperature are then studied. The total monthly operation cost of the process are minimised while the operating parameters such as make up, brine recycle flow rate and steam temperature are optimised. It was found that the seasonal variation in seawater temperature and brine heater fouling factor results in significant variations in the operating parameters and operating costs.

The design and operation of the MSF process are optimized in order to meet variable demands of freshwater with changing seawater temperature throughout the day and throughout the year. On the basis of actual data, the neural network (NN) technique has been used to develop a correlation for calculating dynamic freshwater demand/consumption profiles at different times of the day and season. Also, a simple polynomial based dynamic seawater temperature correlation is developed based on actual data. An intermediate storage tank between the plant and the client is considered. The MSF process model developed earlier is coupled with the dynamic model for the storage tank and is incorporated into the optimization framework within gPROMS. Four main seasons are considered in a year and for each season, with variable freshwater demand and seawater temperature, the operating parameters are optimized at discrete time intervals, while minimizing the total daily costs. The intermediate storage tank adds flexible scheduling and maintenance opportunity of individual flash stages and makes it possible to meet variable freshwater demand with varying seawater temperatures without interrupting or fully shutting down the plant at any-time during the day and for any season.

Finally, the purity of freshwater coming from MSF desalination plants is very important when the water is used for industrial services such as feed of boiler to produce steam. In this work, for fixed water demand and top brine temperature, the effect of separation efficiency of demister with seasonal variation of seawater temperatures on the final purity of freshwater for both cleaned and fouled demister conditions is studied. It was found that the purity of freshwater is affected by the total number of stages. Also to maintain the purity of freshwater product, comparatively large number of flash stage is required for fouled demister.

## **Acknowledgements**

I would like to express my sincere gratitude to Professor I.M. Mujtaba for his invaluable guidance and advice, continuous co-operation, valuable comments, suggestions, unlimited help and support throughout this work.

Thanks also go to all staff members of School of Engineering Design and Technology.

I want to express my gratitude to my parents for their enormous love, brothers and sisters for their unconditional support and encouragement. My warmest thanks go to my wife, my son and my daughters for their love, understanding, and patience, during my study.

Above all, I am very much grateful to almighty Allah for giving me courage and good health for completing the venture.

## Table of Contents

Contents	pages
<b>Abstract</b>	<b>i</b>
<b>Acknowledgement</b>	<b>ii</b>
<b>Table of Contents</b>	<b>viii</b>
<b>List of Tables</b>	<b>ix</b>
<b>List of Figure</b>	<b>xiv</b>
<b>Nomenclature</b>	<b>xv</b>
<b>Chapter 1: Introduction</b>	<b>1</b>
1.1 Background	1
1.2 Desalination Market	4
1.3 Classification of Desalination Processes	5
1.3.1 Thermal Processes	6
1.3.1.1 Multistage Flash Distillation (MSF)	6
1.3.1.2 Multi-Effect Evaporator (MEE) Process	9
1.3.2 Membrane Process	10
1.4 Scope of this Research	10
1.5 The Aims and the Objective of this Work	13
1.6 Thesis Organisation	15
<b>Chapter 2: Literature Review</b>	<b>18</b>
2.1 Introduction	18
2.2 MSF Process Configuration	18
2.3 Parameters Affecting the Performance of MSF	20
2.4 Fouling Factor	23
2.4.1 Prediction of Scaling Tendency	25

2.4.2	Factors Affecting the Rate of Scale Formation	26
2.4.2.1	Temperature	26
2.4.2.2	Flow Velocity	27
2.4.2.3	Concentration of scale	27
2.4.3	Scale Control Additives	28
2.4.3.1	Acid dosing	28
2.4.3.2	Anti scaling	28
2.4.4	Review of Previous Work on Fouling Problems in MSF Process	30
2.5	Corrosion in MSF Desalination Plants	32
2.6	Application of Neural Networks in Process Engineering	32
2.6.1	Neural Network Architecture	34
2.6.2	Neural network based physical properties	35
2.7	Modelling and Simulation of MSF Desalination Process	36
2.7.1	Steady State Modelling	36
2.7.2	Dynamic Modelling	38
2.7.3	Numerical Methods and Computational Tools Employed for Simulation of MSF process	39
2.7.4	Summary	40
2.8	Optimization of MSF Desalination Process	40
2.8.1	Optimization Framework	42
2.10	Conclusion	44
	<b>Chapter 3: gPROMS: An Equation Oriented Tool for Modelling Simulation and Optimisation</b>	<b>47</b>
3.1	Introductions	47
3.2	The Features of gPROMS	47
3.3	The Advantages of gPROMS	49
3.4	Model Development using gPROMS	49

3.5	gPROMS Entities	50
3.5.1	Model Entity	50
3.5.2	Task/Process Entity	52
3.6	Simulation in gPROMS	53
3.7	Optimisation Entity	54
3.8	Control Variable Profiles in gPROMS	54
3.9	Comparison of gPROMS with Other Commercial Software	56
3.10	Conclusion	56
<b>Chapter 4: Modelling MSF Desalination Process</b>		<b>58</b>
4.1	Introduction	58
4.2	Steady State Model of MSF Process	59
4.2.1	MSF Process Description	59
4.2.2	Model Equations	60
4.2.2.1	Stage Model	61
4.2.2.2	Brine Heater Model	63
4.2.2.3	Mixer and Splitters Model	64
4.3	Model Validation	68
4.4	Conclusion	72
<b>Chapter 5: Simulation of MSF Desalination Process: Impact of Brine Heater Fouling</b>		<b>73</b>
5.1	Introduction	73
5.2	Understanding Scaling and Fouling Factor	73
5.3	Seawater Temperature Profile throughout the Year	74

5.4	Estimation of Dynamic Brine Heater Fouling Profile	75
5.5	Effect of Brine Heater Fouling on the Performance of MSF Process	76
5.5.1	Fixed Seawater Temperature, Steam Temperature and Steam Consumption Rate	77
5.5.2	Fixed Seawater Temperature, Top Brine Temperature (TBT) and Fresh Water Demand	81
5.5.3	Variable Seawater Temperature, Fixed Freshwater Demand and Fixed Steam Temperature	82
5.5.4	Fixed TBT and Fixed Freshwater Demand throughout the Year	87
5.6	Conclusion	90
<b>Chapter 6: Effect of Brine Heater Fouling on Optimal Design and Operation of MSF Process</b>		<b>92</b>
<b>6.1</b>	<b>Introduction</b>	<b>92</b>
6.2	Fixed Design and Fixed Freshwater Demand Throughout the Year	93
6.2.1	Optimization Problem Formulation	93
6.2.2	Case Study	95
6.3	Variable Design and Freshwater Demand throughout the Year	99
6.3.1	Optimization Problem Formulation	99
6.3.2	Results and Discussions	100
6.4	Conclusions	104
<b>Chapter 7: Meeting Variable Freshwater Demand by Flexible Design and Operation of MSF Desalination Process</b>		<b>106</b>
7.1	Introduction	106
7.2	Estimation of Dynamic Freshwater Demand/Consumption Profile Using NN	107
7.3	Estimation of Dynamic Seawater Temperature Profile	115
7.4	MSF Process Model	116
7.4.1	Tank Model	117



7.5	Storage Tank Level Constraints	117
7.6	Description of Case Studies	119
7.7	Case Study 1: Minimise Total Daily Operating Cost under Fixed Design	120
7.7.1	Optimisation Problem Formulation	120
7.7.2	Results and Discussions	122
7.8	Case Study 2: Minimise Total Daily Operating Cost with Variable Design	127
7.9	Case Study 3: Sensitivity of Seawater Temperature Profile	131
7.10	Case study 4: Flexible Design and Operation of MSF Process with Variable Seasonal Demand during a Year	135
7.10.1	Results and Discussions Case Study	137
7.11	Conclusions	145
	<b>Chapter 8: Effect of Demister Separation Efficiency on the Freshwater Purity in MSF Process</b>	<b>147</b>
8.1	Introduction	147
8.2	Demister Model	149
8.3	Case Study	151
8.4	Results and Discussions	152
8.4.1	Variation in the Product Salinity for an MSF Process for Different Seawater Temperature	152
8.4.2	Effect of Total Number of Stages on the Purity of Freshwater for Clean Demister	156
8.5	Conclusion	158
	<b>Chapter 9: Conclusions and Future Work</b>	<b>159</b>
9.1	Conclusions	159
9.2	Future Work	163
	<b>Reference</b>	<b>165</b>
	<b>Appendix</b>	<b>181</b>

## List of Tables

Table 2.1	Predication of water characteristics by LSI and RSI	26
Table 2.2	Commonly used transfer function (Hagan et al., 1996)	36
Table 4.1	Constant parameters and input data	68
Table 4.2	Summary of the simulation results by (Rosso et al., 1996)	69
Table 4.3	Summary of the simulation results by using model in gPROMS	70
Table 6.1	Pre-treatments for make-up	94
Table 6.2	Summary of optimization results (Case 1)	96
Table 6.3	Summary of optimization results (Case 2)	97
Table 6.4	Summary of optimization results	103
Table 7.1	Demand Profile from Alvisi et al. (2007)	109
Table 7.2	Weights, biases, transfer functions ( <i>TF</i> ) and Scaled up parameters for 4-layerd	112
Table 7.3	Summarised of all case studies in this chapter	120
Table 7.4	Constant parameters and input data	123
Table 7.5	Summary of optimisation results using different intervals	124
Table 7.6	Summary of optimisation results	128
Table 7.7	Summary of optimisation results	133
Table 7.8	Summary of optimisation results for all seasons	140
Table 8.1	Constant parameters and input data	152
Table 8.2	Demister features	152

## List of Figures

Figure 1.1	The variation in world population from 1823 to 2050	2
Figure 1.2	Freshwater consumption in Libya from 2006 to 2020	3
Figure 1.3	Market share of the main desalination process for desalination of seawater	5
Figure 1.4	Classification of desalting processes	5
Figure 1.5	MSF-Once Through Multi Stage Flash	7
Figure 1.6	Multi Stage Flash with brine circulation (MSF-BR)	8
Figure 1.7	Multi-Effect Evaporator (MME) process	9
Figure 1.8	Reverse Osmosis process (RO)	10
Figure 2.1	A typical MSF process	19
Figure 2.2	A typical flash stage	20
Figure 2.3	Fouling classification	23
Figure 2.4	Fouling in brine heater after operation for a period of time at	25
Figure 2.5	Solubility of $\text{CaCO}_3$ in pure water at 1 bar $\text{CO}_2$ partial pressure	27
Figure 2.6	The process of nucleation of calcium carbonate and crystallisation without anti-scaling	29
Figure 2.7	General action mode of anti-scalent	30
Figure 2.8	A Multilayered feed forward Neural network	35
Figure 2.9	Typical simulation and optimisation Architecture	40
Figure 2.10	Pictorial representation of the NLP optimization framework	43
Figure 3.1	Screenshot of the Model Entity for the MSF Process gPROMS Mode	51
Figure 3.2	Screenshot Showing The gPROMS Process Entity	52
Figure 3.3	Screenshot Showing The gPROMS Optimisation Entity	55
Figure 3.4	Piecewise Constant seawater make up F (kg/h)	55

Figure 4.1	Typical MSF Process	60
Figure 4.2	A general stage in a MSF plant	61
Figure 4.3	Typical brine heater	63
Figure 4.4	Mixing and splitting points in the MSF desalination unit	64
Figure 4.5	Comparison of gPROMS results and Rosso et al., 1996 results for stage profiles of flow rate, salinity, temperature and overall heat transfer coefficient	71
Figure 5.1	Monthly average seawater temperature during the year in Kuwait	74
Figure 5.2	Brine Heater Fouling $f_{bh}$ Profile	75
Figure 5.3	Effect of brine heater fouling factor on freshwater flow rate and T BT at fixed steam temperature and fixed steam consumption	78
Figure 5.4	Effect of brine heater fouling factor on brine recycle flow rate at fixed steam temperature and fixed steam consumption	79
Figure 5.5	Temperature variation of brine through stages	79
Figure 5.6	Temperature variation of feed saline water through condenser	80
Figure 5.7	Temperature variation of freshwater through stages	80
Figure 5.8	Effect of brine heater fouling on plant performance (GOR)	81
Figure 5.9	Effect of brine heater fouling factor on steam consumption and steam Temperature	82
Figure 5.10	Effect of the brine heater fouling on top brine temperature (TBT)	84
Figure 5.11	Effect of brine heater fouling on steam flow rate	85
Figure 5.12	Effect of brine heater fouling on brine recycle flow rate	85
Figure 5.13	Effect of brine heater fouling on temperature of feed saline water inlet brine heater	86
Figure 5.14	Effect of brine heater fouling on total brine feed inlet to recovery section ( $W_R$ )	86
Figure 5.15	Effect of brine heater fouling on performance	87
Figure 5.16	Variation of steam temperature throughout the year	88
Figure 5.17	Variation of steam flow rate throughout the year	89
Figure 5.18	Variation of brine recycle throughout the year	89

Figure 5.19	Variation of performance ‘GOR’ throughout the year	90
Figure 6.1	Variation of optimal monthly anti-scalant consumption throughout the year	98
Figure 6.2	Average monthly seawater temperature and freshwater demand /consumption profiles during a year	101
Figure 6.3	The variation of total monthly cost with total number of stages during a year	103
Figure 7.1	A typical MSF desalination process with storage tank	107
Figure 7.2	A Four layer neural network	111
Figure 7.3	Neural Network back propagation training scheme	113
Figure 7.4	Freshwater demand/consumption( <i>flow_out</i> ) profiles at different season	114
Figure 7.5	Calculated and measured freshwater demand/consumption ( <i>flow_out</i> )	114
Figure 7.6	Actual freshwater demand/consumption by Alvisi et al. (2007) and predicted profile	115
Figure 7.7	Seawater temperature profiles	116
Figure 7.8	Storage Tank	117
Figure 7.9	(a) A typical storage tank level profile (b) Tank level Violations during the operation	119
Figure 7.10	Variations of seawater temperature and freshwater demand/consumption Profiles	123
Figure 7.11	Optimum seawater makeup (F) and brine recycle flow rate (R) profiles at two and three intervals	125
Figure 7.12	Variations of steam temperature and consumption profiles at two and three intervals time	125
Figure 7.13	Freshwater production and consumption profile at different intervals	126
Figure 7.14	Storage tank level profiles at different intervals	126
Figure 7.15	Variations of blow down temperature profiles at different intervals	127

Figure 7.16	Optimum seawater makeup and brine recycle flow rates throughout Profiles	129
Figure 7.17	Steam temperature and consumption profile	129
Figure 7.18	Freshwater production and consumption profile (N=16)	130
Figure 7.19	Storage tank level profiles at different number of stages	130
Figure 7.20	Seawater temperature profile during 24 h	132
Figure 7.21	Optimum seawater makeup and brine recycle flow rates at different seawater temperature profiles	133
Figure 7.22	Steam temperature and consumption profile at different seawater temperature profiles	134
Figure 7.23	Variations of blow down temperature profiles at different seawater temperature profiles	134
Figure 7.24	Seawater temperature Profiles for different season	138
Figure 7.25	Fresh water consumption demand profiles for different season	138
Figure 7.26	The variation of total annual cost with total number of stages at different season	140
Figure 7.27	Variation of optimal operation cost at different season	141
Figure 7.28	Variation of optimal steam cost at different season	141
Figure 7.29	Optimum seawater makeup (F) and brine recycle flow rate (R)	142
Figure 7.30	Variations of steam temperature and consumption profiles at different season	142
Figure 7.31	Storage tank level profiles for all seasons	144
Figure 7.32	Variations of freshwater production of MSF, consumption and freshwater hold up during a day for all seasons	144
Figure 8.1	A typical MSF Process	149
Figure 8.2	Wire-mesh mist eliminator	149
Figure 8.3	Typical flash stage	150
Figure 8.4	The variation in the product salinity as function of the intake seawater temperature and number of stage for (a) clean demister, (b) fouled demister	153
Figure 8.5	Temperature and pressure variation through stages	154

Figure 8.6	Variation of vapour velocity and density through stages	154
Figure 8.7	The variation in the demister efficiency through stages at seawater temperature 30°C	155
Figure 8.8	The variation in the product salinity with seawater temperature	155
Figure 8.9	The variation in product salinity with total stages at 35°C and 20°C for clean demister	157
Figure 8.10	The variation in the product salinity with total fresh water production at 20 °C for clean demister	157

## Nomenclature

$A_H$	Heat transfer area of brine heater ( $m^2$ )
$A_j$	Heat transfer area of stage $j$ ( $m^2$ )
$A_s$	cross section area of storage tank ( $m^2$ )
$A_{ss}$	Demister specific surface ( $m^2/m^3$ )
$B_0$	Flashing brine mass flow rate leaving brine heater (kg/h)
BBT	Bottom brine temperature ( $^{\circ}C$ )
$B_D$	Blow-down mass flow rate (kg/h)
BHF	Brine heater fouling factor ( $h\ m^2K/kcal$ )
$B_j$	Flashing brine mass flow rate leaving stage $j$ (kg/h)
$B_N$	Flashing brine mass flow rate leaving last stage $j$ (kg/h)
$CP_{Bj}$	Heat capacity of flashing brine leaving stage $j$ (kcal/kg $^{\circ}C$ )
CPC	MSF Annual capital cost (\$/year)
$CP_{Dj}$	Heat capacity of distillate leaving stage $j$ (kcal/kg $^{\circ}C$ )
$CP_j$	Heat capacity of cooling brine leaving stage $j$ (kcal/kg $^{\circ}C$ )
$CP_{RH}$	Heat capacity of brine leaving brine heater (kcal/kg $^{\circ}C$ )
$C_w$	Rejected seawater mass flow rate (kg/h)
$D_j$	Distillate flow rate leaving stage $j$ (kg/h)
$D_N$	Total distillate flow rate (kg/h)
$D_z$	Demister thickness (m)
E	liquid entertained vapour ratio (ppm)
F	Make-up seawater mass flow rate (kg/h)
$f_{bh}$	Brine heater fouling factor ( $m^2K/kw$ )
$f_j$	Fouling factor at stage $j$ ( $m^2\ h\ K /kcal$ )
Flow_in	Total distillate flow rate (ton/h)
Flow_out	Freshwater demand/consumption (ton/h)



Flow <sub>out</sub> <sub>mean</sub>	Mean of the freshwater demand/consumption data for NN correlation
G	Specific evaporation (kg/h m <sup>2</sup> )
GOR	Gained out ratio or performance ratio
h	Storage tank level (m)
h <sub>Bj</sub>	Specific enthalpy of flashing brine at stage j (kcal/kg)
h <sub>F</sub>	Specific enthalpy of make-up water (kcal/kg)
H <sub>j</sub>	Height of brine pool at stage j (m)
h <sub>m</sub>	Specific enthalpy of brine at T <sub>FM</sub> (kcal/kg)
h <sub>max</sub>	Maximum storage tank level (m)
h <sub>min</sub>	Minimum storage tank level (m)
h <sub>R</sub>	Specific enthalpy of flashing brine recycle (kcal/kg)
h <sub>vj</sub>	Specific enthalpy of flashing vapour at stage j (kcal/kg)
ID	Internal diameter of tubes (m)
J	Objective function
K <sub>f</sub>	Shape coefficient
L <sub>H</sub>	Length of brine heater tubes (m)
L <sub>j</sub>	length of tubes at stage j (m)
M	Tank holdup (ton)
M <sub>in</sub>	Mass of entrained brine droplet by the vapour in (kg/h)
M <sub>out</sub>	Mass of entrained brine droplet by the vapour out (kg/h)
N	Total number of stages
OD	External diameter of tubes (m)
P <sub>c</sub>	Critical pressure (atm)
P <sub>j</sub>	Stage pressure (atm)
R	Recycle stream mass flow rate (kg/h)
S	Season

$S_{\text{mean}}$	Mean of the season data for NN correlation
$S_{\text{std}}$	Standard deviation of the season data for NN correlation
STC	Storage tank cost (\$/year)
TAC	Total annual cost (\$/year)
$T_{Bj}$	Temperature of flashing brine leaving stage j ( $^{\circ}\text{C}$ )
$T_{\text{BN}}$	Temperature of blow-down ( $^{\circ}\text{C}$ )
$T_{\text{BO}}$	Temperature of flashing brine leaving brine heater ( $^{\circ}\text{C}$ )
TBT	Top brine temperature ( $^{\circ}\text{C}$ )
$T_c$	Critical temperature (K)
TDC	Total daily cost (\$/day)
$T_{Dj}$	Temperature of distillate leaving stage j ( $^{\circ}\text{C}$ )
$TE_j$	Boiling point elevation at stage j ( $^{\circ}\text{C}$ )
$T_{Fj}$	Temperature of cooling brine leaving stage j ( $^{\circ}\text{C}$ )
$T_{\text{FM}}$	Temperature of cooling brine to the heat recovery section ( $^{\circ}\text{C}$ )
$T_{\text{FNR}}$	Temperature of make-up ( $^{\circ}\text{C}$ )
$\text{Time}_{\text{mean}}$	Mean of the time data for NN correlation (h)
$\text{Time}_{\text{std}}$	Standard deviation of the time data for NN correlation (h)
TMC	Total operating cost (\$/Month)
TOC	Total operating cost (\$/year)
$T_s$	Steam temperature ( $^{\circ}\text{C}$ )
$T_{\text{sw}}$	Seawater temperature ( $^{\circ}\text{C}$ )
$T_{Vj}$	Temperature of flashed vapour at stage j ( $^{\circ}\text{C}$ )
$U_H$	Overall heat transfer coefficient at brine heater ( $\text{kcal} / \text{m}^2 \text{ h K}$ )
$U_j$	Overall heat transfer coefficient at stage ( $\text{kcal} / \text{m}^2 \text{ h K}$ )
V	Vapours specific volume ( $\text{m}^3/\text{kg}$ )
$V_{Bj}$	Linear velocity of brine (m/sec)

$V_S$	Superficial vapour velocity (m/sec)
$V_T$	Tank level violation ( $m^2$ )
$W_j$	Width of stage (m)
$W_R$	Total brine recirculating flow rate to the heat recovery section (kg/h)
$W_s$	Steam mass flow rate (kg/h)
$W_{sw}$	Seawater mass flow rate (kg/h)
$X$	Salt concentration (wt %)
$X_{Bj}$	Salt concentration in flashing brine leaving stage j (wt %)
$X_{BN}$	Salt concentration in flashing brine leaving last stage (wt %)
$X_F$	Salt concentration in make-up water (wt %)
$X_R$	Salt concentration in cooling brine (wt %)
$X_{sw}$	Salt concentration in seawater (wt %)
$X$	Temperature difference
$Y$	Thermal resistance of brine film
$Z$	Thermal resistance
$\Delta_j$	Temperature loss due to demister ( $^{\circ}C$ )
$\lambda_s$	Latent heat of steam to the brine heater (kcal/kg)
$\Delta T_{Bj}$	Flashed down per stage (F)
$\mu_L$	Brine viscosity (cpoise)
$\delta_j$	Non- equilibrium of tubes ( $^{\circ}C$ )
$\varepsilon$	Demister void fraction
$\eta$	Demister separation efficiency
$\rho_j$	Water density ( $kg/ m^3$ )
$\omega$	Load per unit length of the stage width

## **IDEX**

L	Liquid
V	vapour
H	Brine heater
j	Stage index
*	Reference value
s	Steam
R	Recycle
sw	Seawater
mean	Average
std	Stranded deviation
min	Minimum
max	Maximum

# Chapter 1

## Introduction

### 1.1 Background

Water is the most precious chemical compound because it is indispensable for all living things (life also originates from it) at least according to accredited scientific theories. At the same time, it is the fluid most widely used in industry for two types of opposite processes for example cooling and the production of steam. Unfortunately drinking water, like most other natural resources, is unequally distributed in the world (EL-Dessouky and Bingulac, 1996). However, the percentage of saltwater in the world is about 94% and freshwater is about 6%. About 27% of total freshwater resource is glaciers and 73% of it is underground (Buros, 2000). About 65% of total amount of freshwater is used for agriculture, 10 % is consumed for drinking and 25% is used for industry. However, ground water is already excessively exploited, while surface waters are prone to pollution (sewage, industry waste, agriculture and drainage water). Moreover, using unhealthy water in developing countries causes 80 to 90% of all diseases and 30% of all deaths (Ustun and Corvalan, 2006).

The shortage of freshwater is not a temporary problem in specific area or in one country, but a long-term and substantial problem concerning the survival of human beings and development of society in most countries (Buros, 2000). About forty percent of the world's population such as the countries of the Middle East and Africa, majority of these states suffer from a shortage of freshwater and this trend is expected to increase in the future (EL-Dessouky and Ettouney, 2002). This is due to the continuous rise in world population (Figure 1.1), industrialization, change in the lifestyle, increased

economic activities and water pollution. The continuous line in Figure 1.1 is based on population data available until 2002 (EL–Dessouky and Ettouney, 2002) and the dotted line represents the population trend based on prediction by EL–Dessouky and Ettouney (2002) until 2010 and the additional population information recently available (7 billion on 25 October 2011, [www.telegraph.co.uk](http://www.telegraph.co.uk)). It clearly shows that the population growth rate will be even sharper than what was predicted in 2002 demanding access to more freshwater. Also note, the freshwater consumption is increasing at the rate of 4-8 %/year. 2.5 times the population growth while the natural water resources remain constant across the world (Lior, 2006). Figure 1.2 demonstrates the estimation of the future total freshwater demand/consumption in Libya during the period 2006 – 2020. The results provide that the total water consumption increasing from 6294 million cubic meters in 2006 to 12473 million cubic meters in 2020 with an average annual rate of 4.97% (more than predicted by Lior, 2006). In addition, at the end of 2020 it is expected that the increases would be 98% of the total freshwater consumption in 2006 (Lawgali, 2008).

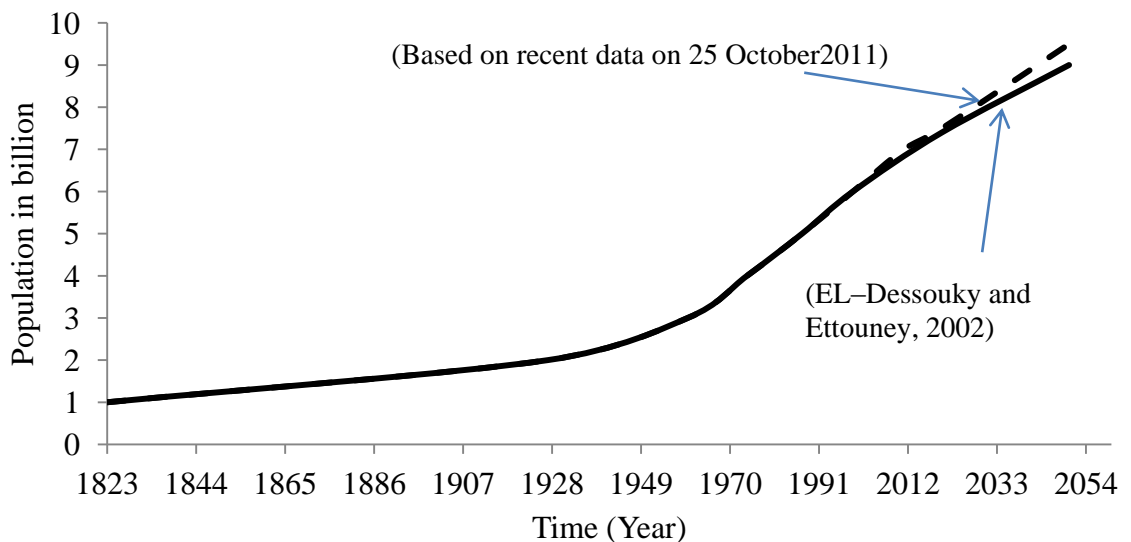


Figure 1.1 The variation in world population from 1823 to 2050 (Source for continuous line: EL–Dessouky and Ettouney, 2002; Source for dotted line: [www.telegraph.co.uk](http://www.telegraph.co.uk); 25 October 2011)

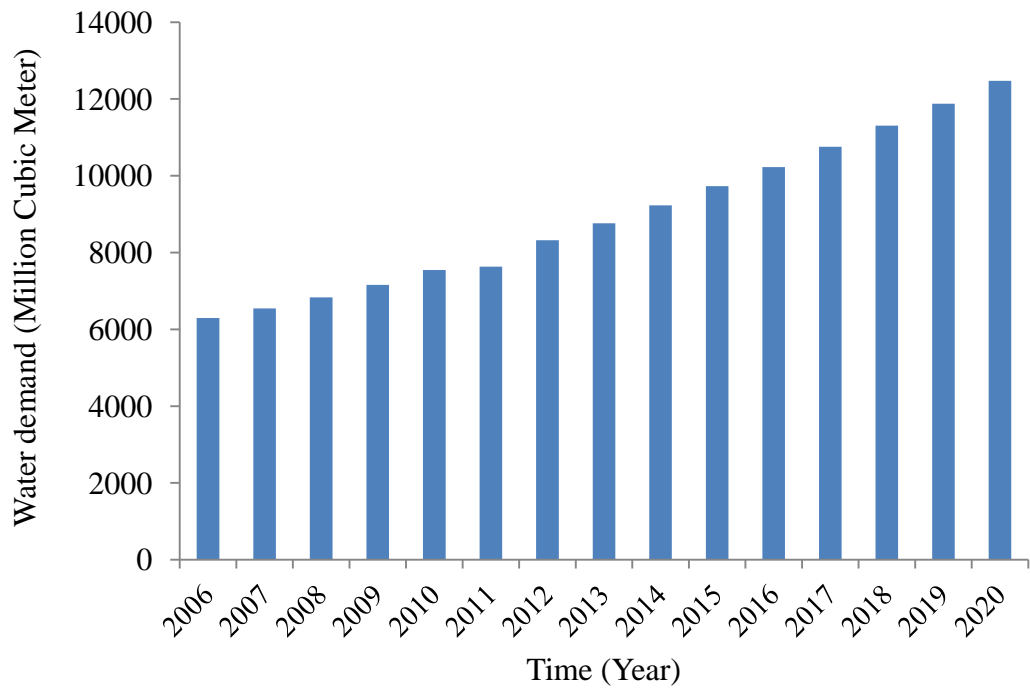


Figure 1.2 Freshwater consumption in Libya from 2006 to 2020 (Lawgali, 2008)

The conclusion that can be summarised from the above facts is that for life to continue on the earth preparation must be taken right now to face this challenge of supplying more freshwater for future generation. Seawater desalination has been proved to be the most suitable method to satisfy the world’s demand for fresh water in future (Tanvir and Mujtaba, 2008a). Desalination of seawater is fast becoming a major source of potable water for long-term human survival in many parts of the world. However, countries around the Mediterranean Sea, the Middle East and many other countries use desalinated seawater as a major water source (Gille, 2003). Of all seawater desalination processes, the multistage flash (MSF) desalination process is still a major source of freshwater around the world (Khawaji et al., 2008).

This chapter sets out the historical background of desalination, brief description of different desalination processes configurations and their importance and applications.

Next the scope, the aim and objectives of this research are summarised. Finally the layout of this thesis is outlined.

## **1.2 Desalination Market**

The main source of freshwater for domestic and industrial use is the desalination processes. The early desalination industry was based on thermal evaporation at the beginning of the last century. However, the operation was fundamentally modified in 1955. The numbers of desalination plant units are in operation total more than 17,348 units found in the world by the end 2002 and the total capacity of freshwater by 10350 desalination plants are about  $37.75 \times 10^6$  m<sup>3</sup>/day (Khawaji et al., 2008). However, Gulf countries account for more than half of the total world production (EL-Dessouky et al., 2004). The desalination industry becomes the main source of freshwater for domestic, industrial and agriculture use in Gulf countries. For seawater desalination MSF processes represent about 60% and 26.7% are membrane processes (Khawaji et al., 2008).

Desalinated water is used in almost half of the world, for example in North Africa, Saudi Arabia ranks first in total capacity (24.4% of total world capacity) followed by the United States second (15.5%), the United Arab Emirates (10.6%) and Kuwait (9.1%) (EL-Dessouky et al., 1995). Most of the Gulf States have been using multistage flash (MSF) distillation for nearly half a century and about half of the desalination market has been covered by MSF processes in recent years as indicated in Figure 1.3 (IDA, 2006).



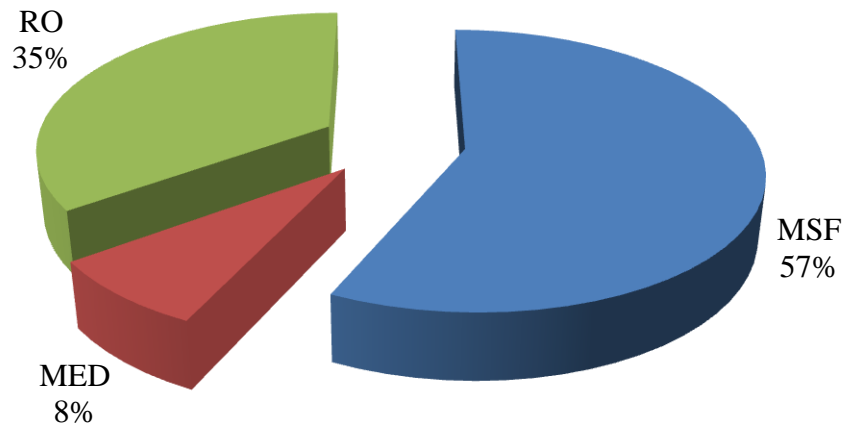


Figure 1.3 Market share of the main desalination process for desalination of seawater (IDA, 2006)

### 1.3 Classification of Desalination Processes

There are many methods, which have been developed to produce freshwater from saltwater, but few are commercially used. Figure 1.4 shows the major desalting processes widely used in the world which can be classified into the two most popular methods:

- Thermal Process
- Membrane Process

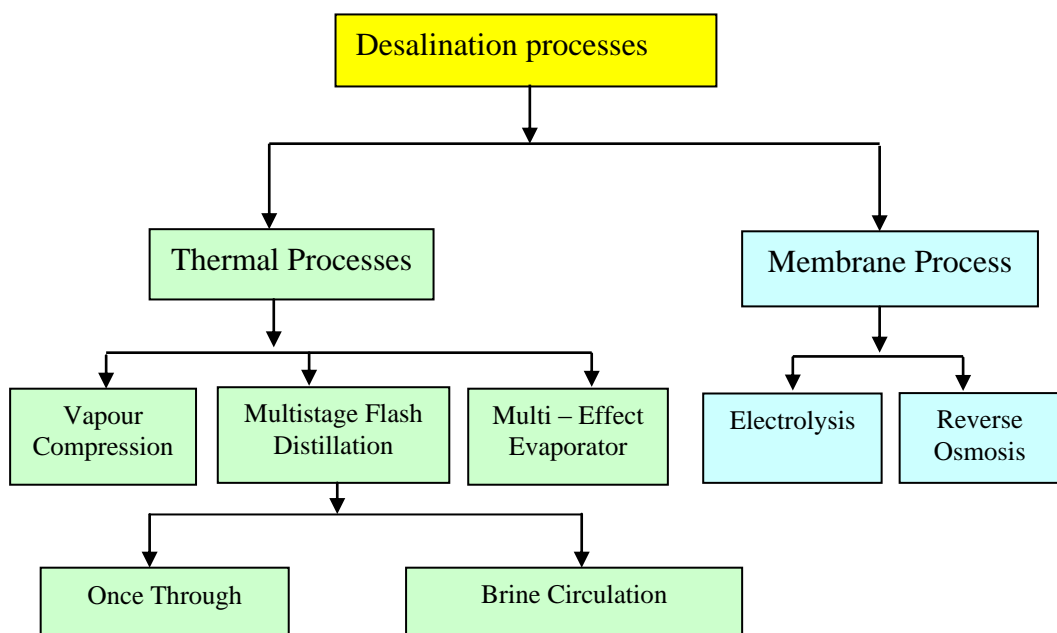


Figure 1.4 Classification of desalting processes

### **1.3.1 Thermal Processes**

Thermal process is the most widely used in desalination technology because of earlier applications and higher experience in process control. The Thermal process is based on heating the salt water, producing steam (water vapour) and then condensation of water vapour to form freshwater at the end.

Thermal processes are used in three commercially important desalination processes:-

- Thermal or mechanical vapour compression (TVC, MCV).
- Multistage Flash Distillation (MSF).
- Multi-Effect Evaporator (MEE).

MEE and MSF are the main ones in the thermal desalination field. Vapour compression distillation uses mechanical energy rather than thermal energy.

#### 1.3.1.1 Multistage Flash Distillation (MSF)

There are many desalination technologies finding their position in industrial application and this includes MSF process. However, this process has been in large-scale commercial use for several years because of high productivity, operability, flexibility and simple construction and control. In addition, it has high capacity output that give higher thermal efficiency and reliability, which leads to high performance and lower production costs (EL-Bairouty et al., 2005). The percentage of MSF installed capacity over the total seawater desalination installed capacity worldwide is over 60% (Khawaji et al., 2008). On the other hand, the MSF desalination process can produce high quality of freshwater, which is used for many applications such as the makeup water for boilers, some application related to electronic industry, pharmaceuticals etc. In addition, applications include chemical reactions, dairy and food washing and cleaning and cooling. Moreover, thermal desalination technology can successfully removes the Boron in drinking water to nearly zero concentration (Hilal et al., 2011). MSF commercial systems are divided into:

### A. Multi stage flash once through (MSF-OT)

The seawater passes throughout the process once through as shown in Figure 1.5. The MSF-OT configuration are similar to single stage flashing process with larger number of flashing stages, where the same flashing stages is repeated. In this process the seawater flows through the condenser tubes in the flash chambers from the last stage of the recovery section to the next. This results in energy recovery and increase the seawater temperature before it is heated to the top brine temperature in the brine heater. Then it flows into a flash chamber with high temperature at the bottom of these stages flows in the opposite direction. The brine partly flashes into steam upon entering the next stage and condenses on the condenser tubes. The condensed vapour accumulates and flows in the distillate tray across the stages.

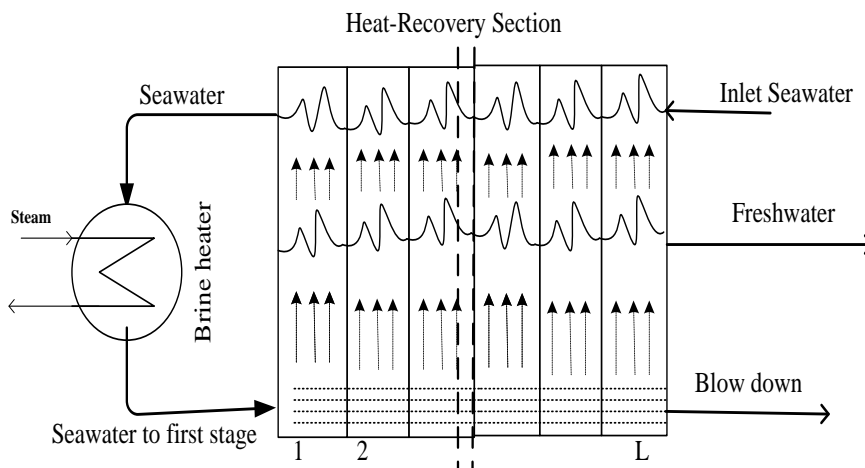


Figure 1.5 MSF-Once Through Multi Stage Flash

### B. Multi stage flash with brine circulation (MSF-BR)

Figure 1.6 shows the MSF process with brine circulation. In this process the brine exists from the last stage and is divided into a recycle stream and a blow downstream which is rejected to the sea. The recycle stream is mixed with the sea water feed (see further details of MSF process in Chapter 2). MSF-BR has received more attention due to its

added advantages over the MSF–OT, such as less water feed (seawater make-up) and simultaneously less chemical consumption (scale and foam) for pre-treatment of the plant and higher performance (EL-Dessouky, 2000).

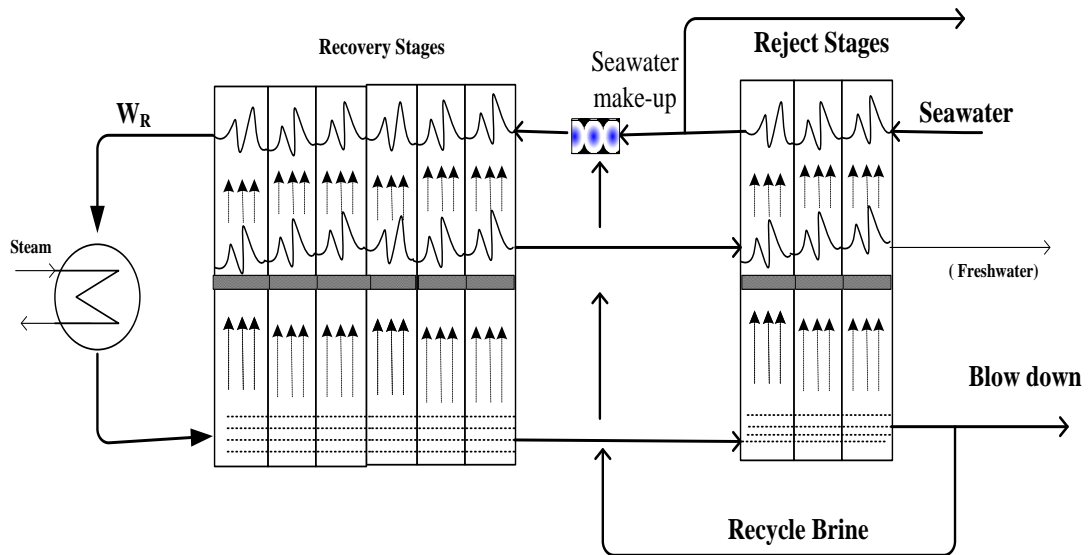


Figure 1.6 Multi Stage Flash with brine circulation (MSF–BR)

Some advantages of MSF process are:

- MSF produces high quality fresh water (less than 30 ppm TDS) (Mohsen and Al-Jayyousi, 1999).
- MSF process has a long history of commercial uses and a good amount of experience.
- A large capacity can be handled by MSF process.
- Strict plant control giving better operation and maintenance schemes.
- The MSF process can be combined with other desalination processes such as (RO process), to optimise the efficiency of the energy and to minimize the cost (Marian et al., 2005).

Some disadvantages of MSF process are:

- High capital and operating costs and requires a high level of technical knowledge.
- High concentration ratio (make-up to distillate ratio) so, the recovery ratio is low.
- High-energy requirement to boil the seawater.

### 1.3.1.2 Multi-Effect Evaporator (MEE) Process

MEE desalination was the first process used to produce freshwater from seawater. There are many configurations of evaporators presented in the literatures. The multiple effect evaporation system is widely used in the sugar and paper industries (EL-Dessouky and Ettouney, 2002). The Multiple-Effect Evaporation (MEE) process is shown in Figure 1.7. The process includes a series of feed water heat exchangers, and a series of flashing boxes, down condensers, and a venting system. The direction of heat flow and the flow direction of the brine and vapour are from left to right. The pressure in the flashing box decreases in the flow direction.

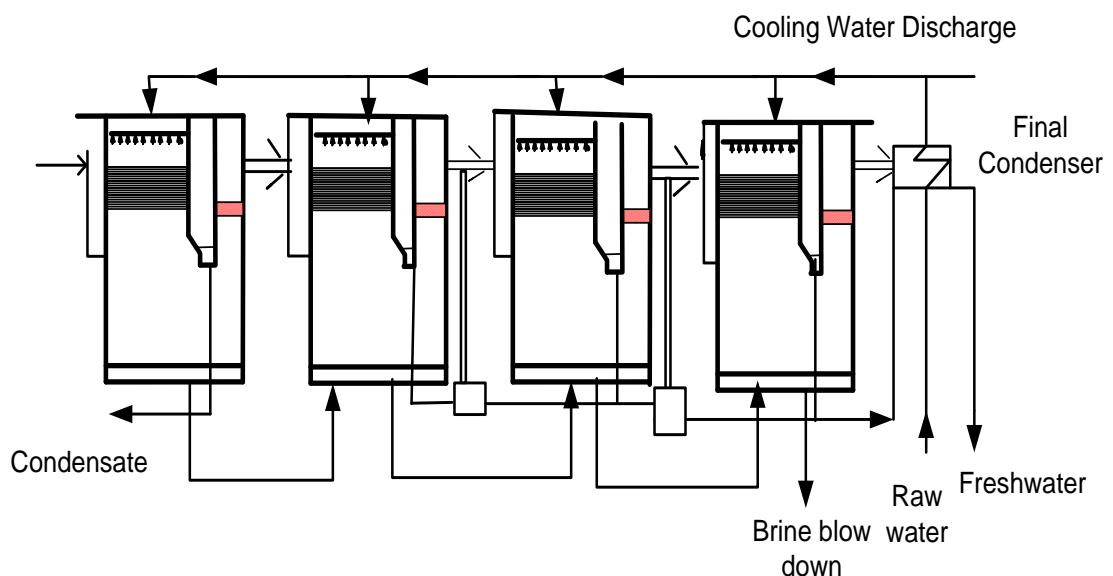


Figure 1.7 Multi-Effect Evaporator (MME) process

### 1.3.2 Membrane Process

The main membrane desalination process is Reverse Osmosis (RO). The principle of this process is to separate the pure water and salt solution through membranes. The pure water diffuses through the membranes while rejecting most of the dissolved salts. To reverse this osmosis (Figure 1.8) external pressure is to be used on a concentrated solution (seawater) to force pure water to flow through the semi porous membrane. Performance of reverse osmosis systems depends on the membranes characteristics, pre-treatment of the feed water and recycle stream (Sassi and Mujtaba, 2011).

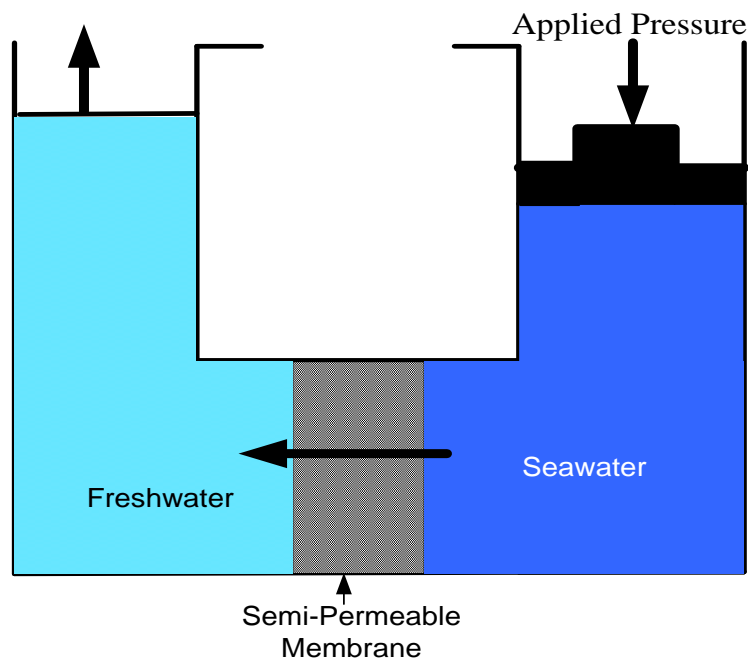


Figure 1.8 Reverse Osmosis process (RO)

### 1.4 Scope of this Research

This research is focused on simulation and optimisation of MSF desalination process with fixed/variable freshwater demand and fouling of brine heater and demister incorporating maintenance and scheduling/operation under variable demand and seawater temperature (day/night and throughout the year). The main issues in MSF desalination process are:

- Improving the productivity.
- Improving the performance.
- Minimising the utility cost (operating cost including energy).
- Optimising the design and operation of the system

Several studies developed the modelling, simulation and optimisation framework for MSF desalination process (steady state and dynamic) in terms of maximum performance, minimum operating cost and energy in the past. However, most of them considered steady state modelling studies (Beamer and Wilde, 1971; Hayakawa et al., 1973; Helal et al., 1986; Rosso et al., 1996; EL-Dessouky and Ettouney, 1997; Tanvir and Mujtaba, 2006a; Tanvir, 2007; Abdel-Jabbar et al. 2007. Few researches considered dynamic modelling studies such as (Glueck and Bradshaw, 1970; Delene and Ball, 1971; Rimawi et al., 1989; Husain et al., 1994; Mazzotti et al., 2000; Tanvir, 2007). As seen in the literature (Chapter 2) the effect of fouling of brine heater (a steady state or dynamic optimisation) on performance and operating cost of the MSF plant was very limited. However, in the past several modelling, simulation and optimisation studies of MSF process have been carried out using fixed fouling factor for the brine heater (Tanvir and Mujtaba, 2008a; Mussati et al., 2004; EL–Dessouky and Ettouney, 2002). In addition, all of these simulations (steady state or dynamic), did not include the study on the effect of demister separation efficiency and fouling (with variation of seawater temperature) on the freshwater purity in MSF desalination Process.

There are only few published works dealing with rigours mathematical optimisation and model based control on MSF desalination processes including Wade et al. (1999), Mussati et al. (2001), Mussati et al. (2005), Mussati et al. (2008), Tanvir and Mujtaba (2008a). However, the main focus of many of these studies was on optimal design and operation of MSF processes based on simplifying assumptions such as fixed seawater

temperature and freshwater demand during a day and year. In reality the demand (Alvisi et al., 2007) and also the seawater temperatures (Yasunaga et al., 2008) vary throughout the day and throughout the year.

In fact, to the author's best knowledge, no studies (except authors' own) have been reported to date on optimisation of MSF desalination process involving a variable demand/consumption of freshwater throughout the day and throughout the year, with varying seawater temperatures throughout the day and year.

With this in mind, this research is focused on the following:

- To understand the role of dynamic brine heater fouling with time and with varying seawater temperature on plant performance, top brine temperature, brine flow rate, amount of recycle and steam consumption for fixed freshwater demand under fixed steam temperature operation. Also to study the effect of brine heater fouling factor with seasonal variation of seawater temperatures on the utility cost. The monthly operation cost is selected to minimize, while optimising the operating parameters such as make up, brine recycle flow rate and steam temperature.
- To investigate the effect of variable freshwater demand (day/night throughout the day and year, with varying seawater temperatures without any shortage of freshwater access for users) on design and operation of MSF desalination process. The role of intermediate storage tank in meeting the variable demand and operation of the plant.
- To study the effect of separation efficiency of demister with seasonal variation of seawater temperatures on the final purity of freshwater for both cleaned and fouled demister. The variation of the purity of freshwater production when the plant operates with clean and fouled demister.



## 1.5 The Aim and the Objectives of This Work

The aim of this thesis is to find optimal (and flexible) design and operation (involving scheduling) of MSF desalination process under fouling to meet fixed or variable freshwater demand throughout the year via simulation and optimisation.

The specific objectives of this research are:

- To carry out literature survey on the modelling, simulation and optimisation of MSF desalination process (steady state and dynamic).
- To develop a steady state model of MSF based on the basic laws of mass balance, energy balance, and heat transfer equations with supporting correlations for physical properties calculations using gPROMS model builder 2.3.4 software. The model includes parameters such as the brine flow rate, freshwater flow rate, the temperature profiles for all stages, top brine temperature and steam flow rate.
- To validate the model against the data reported by Rosso et al. (1996), before it is used in further investigation in this work.
- To develop a time dependent fouling factor (to represent dynamic scaling effect) based on actual plant data, which allows calculation of fouling factor at different time (season of the year).
- To study the role of changing brine heater fouling factor with varying seawater temperatures on the plant performance for fixed freshwater demand, steam temperature and top brine temperature.
- To investigate the effect of brine heater fouling factor with seasonal variation of seawater temperatures during the year from January to December and its effect on the plant performance of MSF desalination process for fixed freshwater demand and fixed top brine temperature.

- To optimise operation of MSF desalination process with different top brine temperature and different anti-scalent dosages with changing brine heater fouling factor and varying seawater temperatures during a year. The optimising operating parameters such as steam temperature, make-up and brine recycle will be implemented to achieve the minimum monthly operating cost for a given configuration of the MSF process and with a fixed fresh water demand throughout the year.
- To develop Neural Network (NN) based correlation for estimating dynamic freshwater demand/consumption profiles at different times of the day and seasons. Also to develop a simple polynomial correlation which can be used for calculating dynamic seawater temperature profile during 24h. These correlations are embedded in the gPROMS based process model.
- To include an intermediate storage between the MSF process and the client and to link the steady state process model for the MSF process with the dynamic model for the storage tank. The model is then incorporated into the optimisation framework to find the optimal design and operation of the process and scheduling/operation to meet seasonal variable freshwater demand with varying seawater temperature throughout the day and the year.
- To minimise the total daily cost (including capital cost component of the process and the storage tank and the operating cost) of the process while optimising the design parameters such as total number of flash stages and some significant operating parameters such as recycle brine and seawater make up at discrete time interval for all seasons with varying freshwater demand/consumption and seawater temperature profiles during a particular day.
- Finally, to develop detailed modelling of the MSF demister for both clean and fouled conditions and, to study the effect of separation efficiency of demister on

the final purity of freshwater for both conditions with seasonal variation of seawater temperatures.

## **1.6 Thesis Organisation**

The layout of the thesis is presented below.

### Chapter 1: Introduction

The general background in desalination, water shortage problems around the world, desalination market and the need for water desalination are described in this chapter. Also it includes a brief summary of different water desalination processes followed by short description of two main types of MSF desalination process (MSF-OT and MSF-BC). Some advantages and disadvantages of using MSF desalination processes are also presented. The scope of the research is highlighted and the objectives of the thesis are described.

### Chapter 2: Literature Review

The general description of the main parameters affecting the performance of MSF desalination process is carried out. The role of effect of fouling factor, and corrosion on operation of MSF desalination process are highlighted. Also it includes a general overview of the neural network techniques and network based application in process engineering. Past work in the literature review relating to fouling and importance of simulation and optimization of MSF desalination process are also highlighted.

### Chapter 3: gPROMS: An Equation Oriented Tool for Modelling Simulation and Optimisation

The features of gPROMS software package which has been used for modelling simulation and optimisation is considered in this chapter. Also this chapter introduces overview, application and the advantages of the (gPROMS) software. The comparison

in terms of the benefit of using the gPROMS rather than other modelling packages is also highlighted.

#### Chapter 4: Modelling MSF Desalination Process

A detailed steady state mathematical MSF process models and physical property correlations from the literature are presented here with validation of results from the literature.

#### Chapter 5: Simulation of MSF Desalination Process: Impact of Brine Heater Fouling

This chapter includes different case studies, which are simulated using detailed steady state model of MSF desalination process, which are discussed here. The effect of brine heater fouling factor on the production of freshwater by MSF desalination process are also presented and analysed. The effect of changing brine heater fouling with varying seawater temperature on the MSF process performance to maintain the fixed freshwater demand is also investigated.

#### Chapter 6: Effect of Brine Heater Fouling on Optimal Design and Operation of MSF Desalination Process

Performance and economic optimisation of MSF desalination process is carried out for different top brine temperature, different anti-scalent dosages and fixed freshwater demand with varying seawater temperature during a year. Also optimal design and operation of MSF desalination process with monthly fixed freshwater demand, seawater temperature and fouling throughout the year.

#### Chapter 7: Meeting Variable Freshwater Demand by Flexible Design and Operation of MSF Desalination Process

Neural network based correlation for predicting dynamic freshwater demand/consumption profiles at different time of the day and season has been

developed validated with actual data from the literature. A detailed steady state MSF process model incorporating NN based correlation for predicting freshwater demand/consumption coupled with a dynamic model for the storage tank is presented in this chapter. Performance and economic optimizations are carried out for variable freshwater demand/consumption with changing seawater temperature throughout the day and year. Flexible scheduling and maintenance strategy of MSF desalination process is also discussed.

Chapter 8: Effect of Demister Separation Efficiency on the Freshwater Purity in MSF Desalination Process.

A detailed theoretical demister efficiency correlation and the distillate purity calculations for both clean and fouled conditions from the literature are presented in this chapter. The effect of demister performance on the purity of freshwater for different seawater temperature to maintain the fixed water demand and fixed TBT are presented and analysed in this chapter.

Chapter 9: Conclusion and Future Work

The final conclusion, which is reached during the study of this work and suggested future recommendations are presented.

# Chapter 2

## Literature Review

### 2.1 Introduction

This chapter describes the aspects of the main parameters affecting the performance of MSF desalination process. The general description of the role of fouling factor on the operation of MSF desalination process is also considered briefly here. Also it provides review in brief of the past work relating to fouling and the neural network techniques and network based application in process engineering. Further literature reviews on the importance of simulation, optimization of MSF desalination process and the numerical techniques for solving the optimization problems are outlined.

### 2.2 MSF Process Configuration

A typical MSF plant is shown in Figure 2.1. The process consists of essentially a steam source, water/steam circuit (brine heater), pumping units and flashing stages sections. The seawater is pumped through the condenser tubes from the end of the rejection section to the left of the section. Before the recovery section, seawater is partially discharged into the sea to balance the heat. The other part is treated with a mixture of anti-scaling such as polyphosphonates, sulphuric acid and chlorination compounds and is mixed with recycled brine and fed into the last stage of the recovery section and is preheated in the condenser units by exchanging heat with the distillate vapour. The preheated seawater is further heated in the brine heater and flows into the first flash chamber with the highest possible temperature (TBT) and low pressure. However, the brine partly flashes into vapour upon entering the next stage and condenses on the condenser tubes. The condensed vapour accumulates and flows in the distillate tray across the stages. The brine is divided into a blow downstream and a recycle stream,

which is combined with the make-up water and enters the heat recovery section (Hawaidi and Mujtaba, 2010).

Note, due to high temperature in the recovery stages and brine heater, seawater is treated with anti-scaling and assisted by sponge ball cleaning method to reduce scale formation. Acid cleaning is required after more than a year in operation (Wade, 2001).

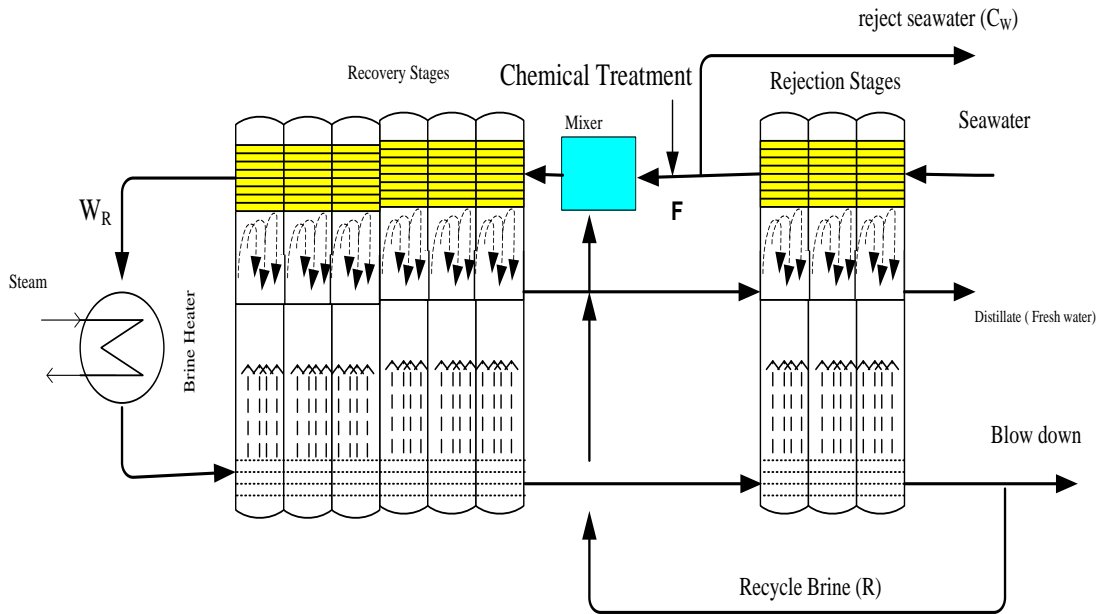


Figure 2.1 A typical MSF process (Hawaidi and Mujtaba, 2010)

Each stage of an MSF process (Figure 4.2) consists of

- The tube bundles of the condenser to condense the vapour in the stage.
- The demister to reject brine droplets.
- The distillate tray to collect the distillate water.
- Inlet/outlet brine orifices and a weir box to control flashing brine level.
- An extraction pipe leading to ejectors to remove non- condensable gases.
- A large brine pool.

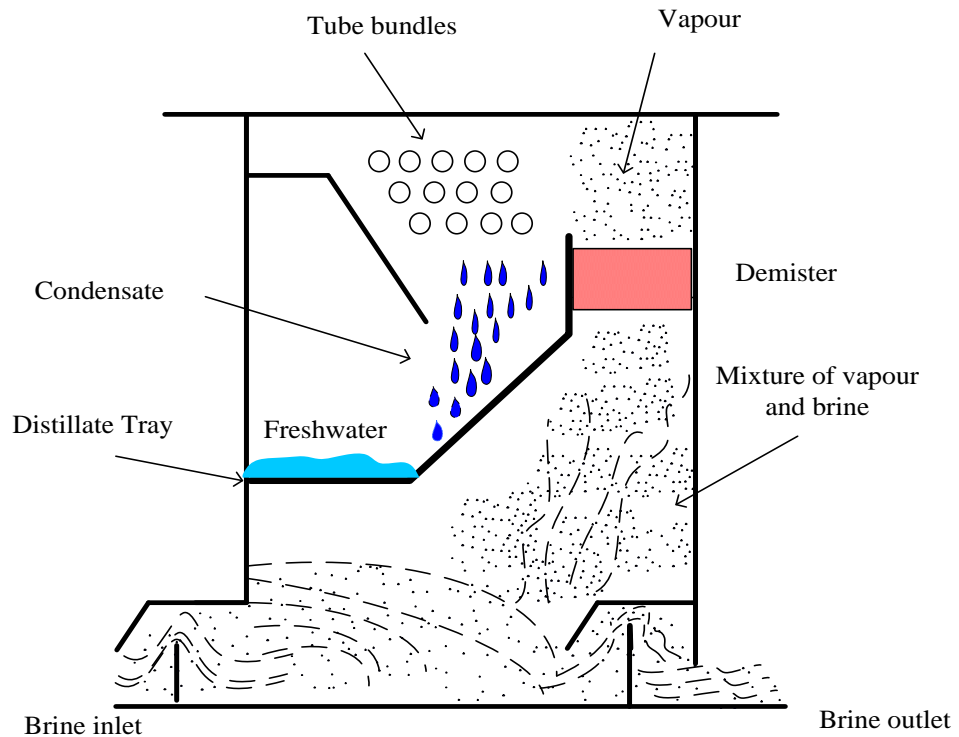


Figure 2.2 A typical flash stage

## 2.3 Parameters Affecting the Performance of MSF

### Top Brine Temperature (TBT)

TBT (the outlet brine heater temperature) plays an important part of all process parameters affecting the performance of an MSF process, distillate production and the levels of brine in each flash chamber. It is often constrained by a maximum value to produce more distillate but should not exceed it in order to reduce scaling and corrosion problems.

The choice of TBT depends upon a number of factors:-

- Surface area of the condenser
- Scale formation and corrosion control
- Brine recycle flow rate
- Performance ratio (defined as the ratio of freshwater flow rate to the heating steam)



The top brine temperature (TBT) is a design parameter that depends upon the type of the scale inhibitor added to the makeup (Nada, 2002). TBT is limited to 121°C for acid treatment, 90°C for polyphosphate treatment and about 110°C for high temperature additives. It is well known that the increase of TBT has the following advantages:-

- Less heat transfer surface area requirement due to greater temperature differential, higher overall heat transfer coefficients, and lower non-equilibrium temperature losses.
- Lower brine recycle to distillate ratio  $R/D_j$  and cooling water to distillate ratio  $W_{sw}/D_j$ , and consequently lower pumping energy.
- Less vacuum system duty and improved inter stage brine and distillate transfer.

These advantages with high TBT are countered by some disadvantages such as:-

- Higher cost of heating steam (higher steam temperature need).
- More problems associated with scale formation, corrosion problems and thermal expansion.
- Higher pressure design for evaporators and pumps.

#### Total Brine Recirculating Flow Rate ( $W_R$ )

This parameter has a direct effect on process performance such as the steam temperature and consumption. The operating range is constrained by the minimum and maximum allowable velocities (can be calculated by dividing  $W_R$  (kg/h) by density of brine ( $\text{kg/m}^3$ ) and tube cross-sectional area ( $\text{m}^2$ )) in the recovery condenser tube. The lower limit is dictated by heat transfer and flashing efficiency considerations and the higher limit by tube erosion damaged and higher pumping costs (El-Nashar, 1998).

### Seawater Feed Temperature

This parameter has a direct influence on the heat transfer in the reject section and also affects the temperature of bottom the brine (flashing brine temperature in the last stage), seawater make-up and recycled brine.

### Cooling Water Flow Rate in the Rejection Section ( $W_{sw}$ )

The cooling water flow rate has an effect on the bottom brine temperature due to its effect on the heat transfer coefficient in the rejection section. The operating range is constrained by the minimum and maximum allowable velocities (can be calculated by dividing  $W_{sw}$  (kg/h) by density of seawater ( $\text{kg/m}^3$ ) and tube cross-sectional area ( $\text{m}^2$ )) in the rejection condenser tubes.

### Ratio of Seawater Make-up ( $F$ ) to Freshwater ( $D_j$ )

The ratio of the brine blow-down to seawater flow rate is directly influenced by the ratio between the seawater make-up flow and the freshwater flow,  $F/D_j$ . A lower ratio means lower make up flow, which normally results in a reduction in the consumption of an anti-scaling chemical.

### Anti-scale Dosage Level

As a general rule, the required dosage of anti-scaling is strongly dependent on the top brine temperature (TBT) and seawater make-up flow rate. However, the dosage of anti-scalent has reviewed many times over the past years due to better anti-scale performance and consciousness of chemical consumption. For example, Saudi Arabia reduced dosing gradually from 4.5 - 12.5ppm (depending on top brine temperature 90 – 110°C) to 1-2ppm from 1981 to 2000 (Hamed et al., 2000).

### Steam Temperature

This temperature has a strong effect on the scaling formation of the brine heater and on the top brine temperature and should be carefully controlled.

## 2.4 Fouling Factor

Fouling of heat exchangers arises as results of one or more number of mechanisms and fouling processes can usually be classified in Figure 2.3.

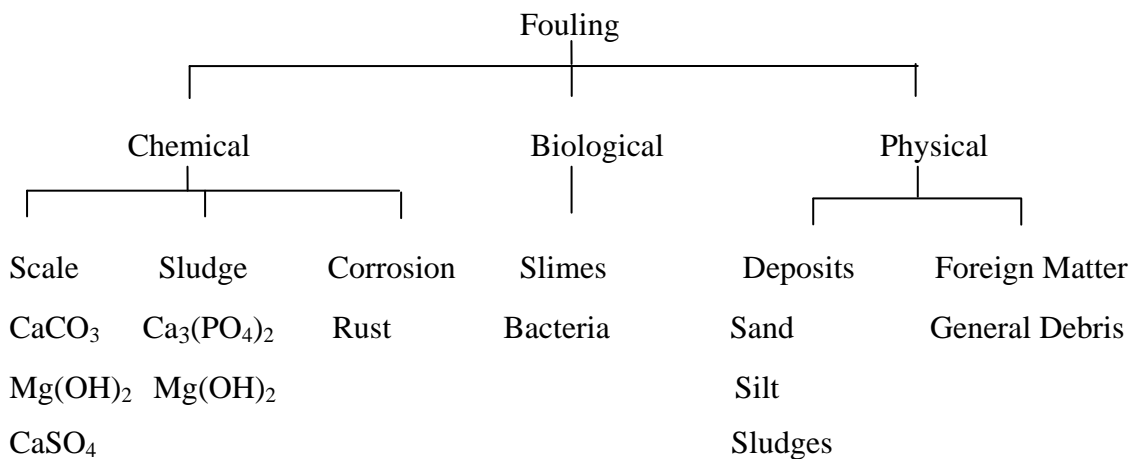


Figure 2.3 Fouling classifications (Finan, 1991)

The fouling factors are usually calculated as average values for groups of three or more stages, and are calculated based on the knowledge of measured temperatures and flow rates. Water formed deposits, commonly referred to as scale, can be defined as crystalline growth of an adherent layer (barrier) of sparingly soluble salts that can readily precipitate on a heat transfer surface in evaporative concentration operation.

The rate of fouling depends on many variables such as temperature, pH, concentration of bicarbonate ions, and rate of CO<sub>2</sub> release, concentration of Ca<sup>2+</sup> and Mg<sup>2+</sup> ions, and total dissolved solids (AL-Anezi and Hilal, 2007). Fouling can reduce the heat transfer process; reduce heat transfer efficiency by plugging the exchanger. In addition, fouling

can increase specific energy consumption and operating costs and causes frequent shut down of the evaporator for cleaning.

In seawater desalination plants, and particularly those using a thermal process such as the MSF, the phenomenon of fouling as scale formation is mainly caused by crystallization of calcium carbonate e.g.  $\text{CaCO}_3$  (alkaline scales) and at higher temperatures, magnesium hydroxide  $\text{Mg(OH)}_2$ . Non-alkaline scales e.g.  $\text{CaSO}_4$  are perhaps the most common scales found in multistage flash (MSF) (AL-Sofi, 1999). The most costly design and operating problems in seawater desalination continue to be due to scale formation. The design of the heat transfer area in a MSF plant constitutes about 30% of the total cost, and the fouling tendency requires about 20 to 25% of excess design allowance (Gill, 1999).

Increased energy and maintenance costs, as well as plant shutdowns, are some of the economic penalties resulting from scale deposition. For thermodynamic, technical, and economic reasons, maximum brine temperature should be as high as possible. Most of the MSF units usually operate at top brine temperatures (TBT) of 90 -120°C.

One of the main factors that affect the thermal efficiency of the MSF process is the outlet brine heater temperature (Top Brine Temperature). Even though operating a plant at the higher top brine temperature increases the efficiency, it increases the potential for scale formation and accelerated corrosion of metal surfaces (Aly and El-Fiqi, 2003). However, from practical experience the fouling formation rate was significantly increased inside the condensers and brine heater tubes and led to shutdown of the plant for cleaning when the plant operates at high top brine temperature. Figure 2.4 shows the cross sectional view of its brine heater when the plant operated for a period of time at  $\text{TBT} = 115^\circ\text{C}$ . Most of the scale formation was in the hot outlet area of two-pass flow

brine heater. More than half of the brine heater tubes' outlets were blocked by scale, but the inlet tubes of the heat exchanger were clean (El-Moudir et al., 2008).

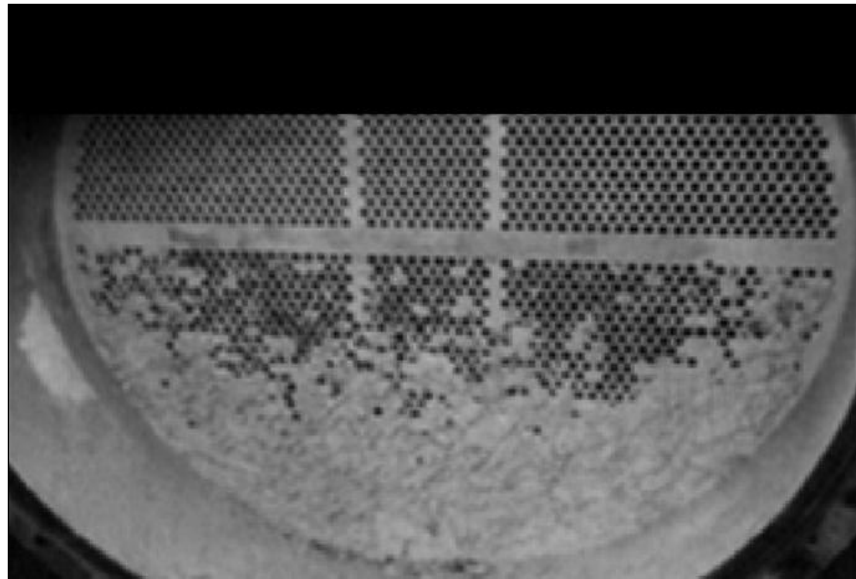


Figure 2.4 Fouling in brine heater after operation for a period of time at TBT = 115°C (El-Moudir et al., 2008)

#### 2.4.1 Prediction of Scaling Tendency

Many methods have been proposed to predict the formation of calcium carbonates. The more commonly used equations or indices are the Ryzner indices (RSI) and Langelier saturation (LSI). These are based upon comparison of the actual pH at which the water would be saturated  $pH_s$  (pH at which system would be saturated with calcium carbonate). The Ryzner and Langelier Index (RSI) are defined as:

$$RSI = 2pH - pH_s \quad (2.1)$$

$$LSI = pH - pH_s \quad (2.2)$$

Where the pH is the actual measured value in the water, and  $pH_s$  is the saturation pH of calcium carbonate in water.

Interpretation of LSI and RSI values are listed in Table 2.1.

Table 2.1 Prediction of water characteristics by LSI and RSI

LSI	RSI	Tendency of water
2	<4	Heavy scale formation, not aggressive
0.5	5 to 6	Slightly scale forming and mildly aggressive
0.0	6 to 6.5	Balanced but pitting corrosion possible
-0.5	6.5 to 7	No scaling and slightly aggressive
-2.0	>8	Under saturated, very aggressive

The indices in Table 2.1 indicate only the tendency for calcium carbonate to deposit, not the rate or capacity for deposition. Also, these values do not take into account the tendency for calcium carbonate to supersaturate, its rate of formation.

#### 2.4.2 Factors Affecting the Rate of Scale Formation

From practical experience there are three variables can have significantly greater impact on the scale formation than others. Temperatures, brine velocity and concentration of scale such as CaCO<sub>3</sub> and Mg(OH)<sub>2</sub> are the most important determining factors in the build up of deposits on heat exchanger surfaces.

##### 2.4.2.1 Temperature

The normal solubility of salts increase with temperature, calcium carbonate has inverse solubility characteristics, i.e. as temperature increases the solubility of calcium carbonate decreases. The hotter water will enhance the precipitation of calcium carbonate and increase fouling rates.



The reaction above is moving to the right with increasing temperature, increasing CO<sub>3</sub><sup>2-</sup> concentration and increasing the likelihood of precipitation of calcium carbonate and

fouling (Miller, 1952). Figure 2.5 shows the general behaviour of  $\text{CaCO}_3$  solubility as a function of temperature.

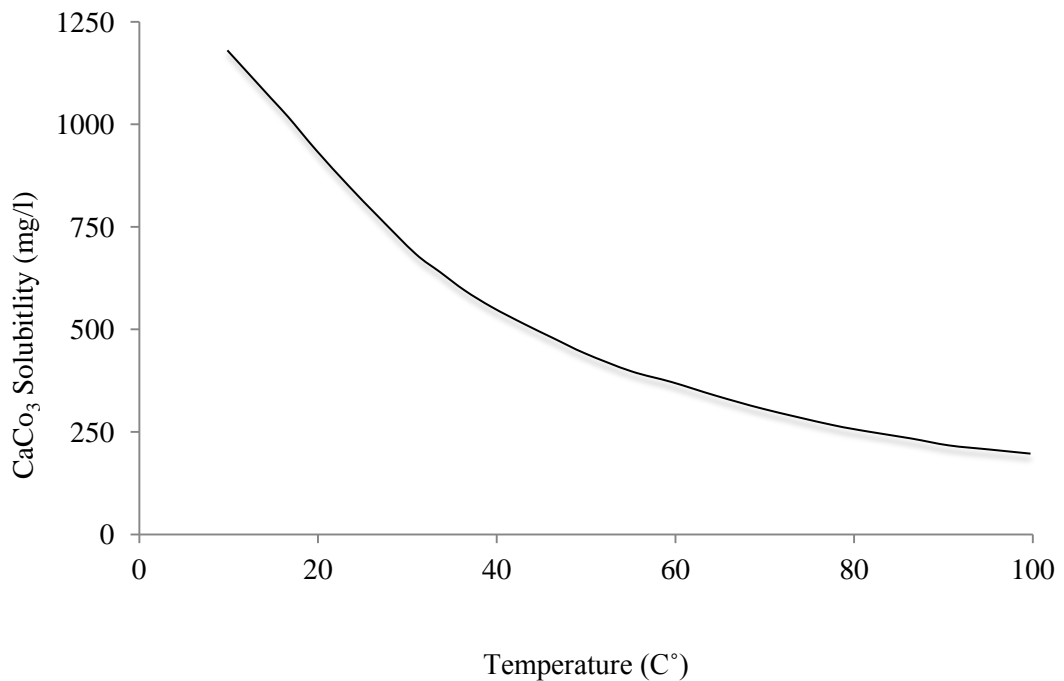


Figure 2.5 solubility of  $\text{CaCO}_3$  in pure water at 1 bar  $\text{CO}_2$  partial pressure (Miller, 1952)

#### 2.4.2.2 Flow Velocity

With increasing brine velocity in the condenser tubes the boundary layer of fluid viscosity at the solid/liquid interface becomes thinner and the resistance to diffusion of scale forming ions and the transport of particulate material from the bulk is reduced. However, as velocity increases the shear force generated at solid/liquid interface increase and the tendency for any deposit formed to be swept away is increased.

#### 2.4.2.3 Concentration of scale

The concentration of scale forming species in the seawater will determine the rate of mass transfer and hence the rate of fouling. However, higher concentration of scale

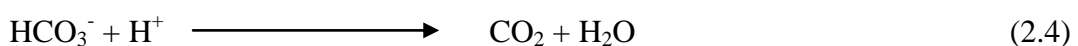
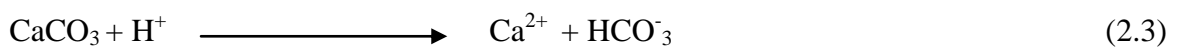
forming species will lead to higher fouling rates particularly for salts such as calcium carbonate with high temperature.

### 2.4.3 Scale Control Additives

The areas where scale and sludge formation commonly occur in MSF desalination plant are brine heater, tube bundles of the condenser, demister, flash chamber brine stages, inlet / outlet brine orifices, water boxes and tube sheets (AL-Sofi et al., 1987; Shams EL-Din and Rizk, 1994). Common inhibition of scale formation in MSF plants is achieved by one of the following control methods:

#### 2.4.3.1 Acid dosing

Scale control involves pH adjustment, the desired level being based on the Langelier or Ryzner index (Table 2.1). Precipitation becomes more likely as the scale concentration of brine is increased but can be controlled by acidification of make-up seawater. With this method, the acid reacts with the carbonate present in brine and thereby increases CaCO<sub>3</sub> solubility and evolves CO<sub>2</sub> out of solution.



Different acids can be used, for example sulphuric acid H<sub>2</sub>SO<sub>4</sub> or hydrochloric acid HCL, but H<sub>2</sub>SO<sub>4</sub> is preferred because of cost. On the other hand, acid should be added in high concentrations of about 100-200 ppm, H<sub>2</sub>SO<sub>4</sub> is normally used (Shams EL Din and Makkawi, 1998).

#### 2.4.3.2 Anti scaling

The second approach for scale prevention is the use of anti-scale agents. The Figure 2.6 below summarised the process of nucleation of calcium carbonate, whether



homogeneous or heterogeneous, and crystallisation which is the precursor to deposition without adding anti-scaling.

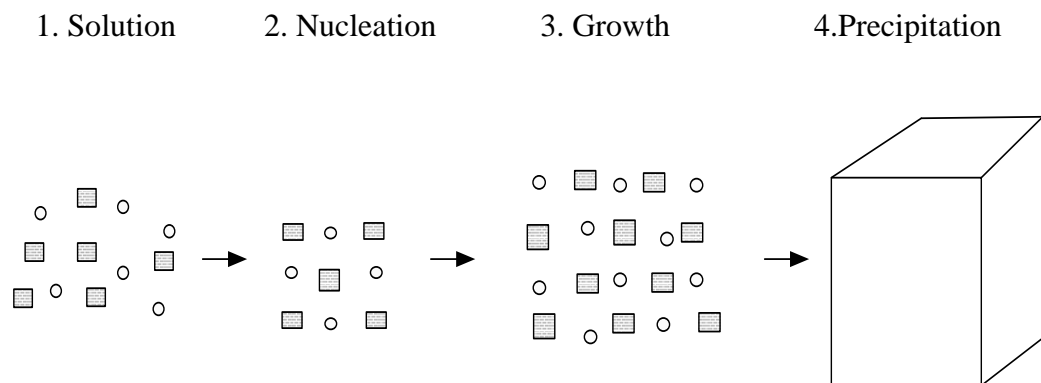


Figure 2.6 The process of nucleation of calcium carbonate and crystallisation without anti-scaling (Finan, 1991)

1. Calcium and carbonate ions in the solution phase at normal temperature
2. Under the right conditions of temperature and concentration, nucleation occurs to give an embryonic crystal of less than the critical size required for precipitation.
3. The crystal nucleus continues to grow and:
4. Precipitation.

This processes let to produce crystal growth which is regular giving increased to hard deposit which is not easily removed from the surface. When small amounts of scale inhibitor such as phosphate, polyphosphate, polyacrylic acid, polymaleic acid etc, (a few ppm) are added into seawater, they can reduce scale formation. However, the required dosage of anti-scaling is dependent on the top brine temperature (TBT). The anti-scalent inhibits the crystallization of calcium carbonate crystallites by suppressing crystal growth ‘the threshold effect’ and ‘crystal distortion’ as shown in Figure 2.7 below.

Anti-scalent does not react with scale but interacts in different physical-chemical ways. Anti-scalent is absorbed into the calcium carbonate crystal structure, limiting the growth of  $\text{CaCO}_3$  and ultimately limiting scale formation. It retards  $\text{CaCO}_3$  scale by maintaining

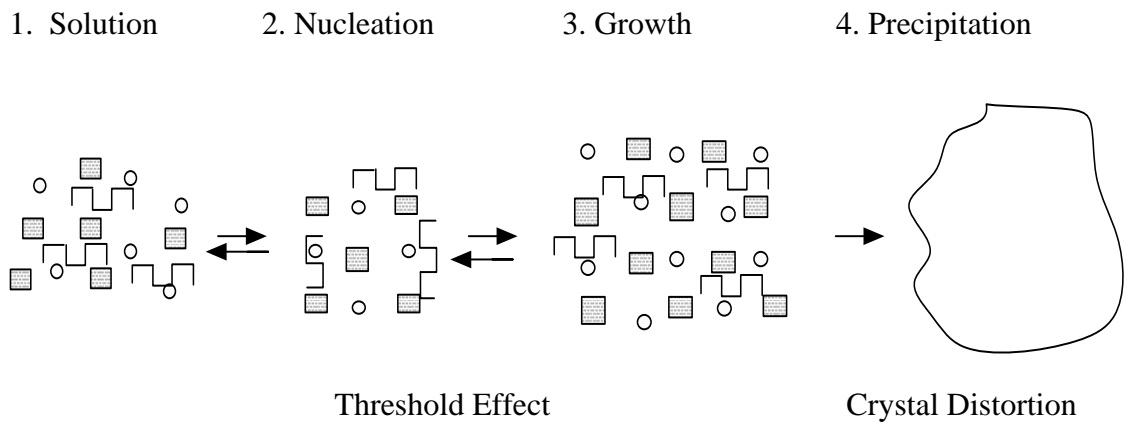


Figure 2.7 General action mode of anti-scalent (Finan, 1991)

small particles of distorted crystalline material in suspension. However, treatment with scale inhibitor should be supported by mechanical cleaning such as sponge balls to keep the internal tube surface clean and free of deposits (AL-Deffeeri, 2007).

The toxicity of all anti-scalents and acids to aquatic life is very low. In contrast, phosphonates are stable substances with low biodegradation rates, which results in relatively long residence time in coastal waters. As these substances reduce scale formation by dispersing complex calcium and magnesium ions in the desalination plant, they could also influence natural processes of these and other divalent metals in the marine environment (Lattemann and Hopner, 2008).

#### 2.4.4 Review of Some Previous Work on Fouling Problems in MSF process

Many researchers have studied the fouling problems in MSF desalination process. Most of these researches are experimental work. Cooper et al. (1983) carried out certain aspects of the development of fouling in MSF plants, which cannot be applied as a linear behaviour. They introduced the concept of a deposition-removal model and discussed some properties of the model when applied to MSF plants. EL-Dessouky and Khalifa (1985) investigated the effect of increasing the fouling factor of brine heater tubes on the heat transfer coefficient, performance ratio and ratio of seawater to the distillate of once through multi stage desalination plant. They pointed out that scale

formation can restrict the flow rate of water by decreasing the overall heat transfer coefficient and increases pumping loads and leads to lower thermal performance.

Al-Bakeri and El Hares (1993) studied the on-line condenser tube cleaning system and some of the difficulties encountered during operation. They optimised the parameters such as number of operating balls per tube, number of cycles per day, overall permitted working life of balls, etc. They used experimental results from the Umm Al Nar desalination plants. Al-Ahmad and Aleem (1994) studied various models and mechanisms of fouling factor behaviour in desalination plants. They successfully applied the asymptotic fouling model of Kern and Seaton to correlate the actual fouling data and the interaction between scale formation and corrosion problems in desalination plants. Al-Sofi (1999) discussed the effect of anti-scaling and causes of its deterioration and he studied the operational aspects with very brief reference to design causes of scale and sludge formation and also ball-cleaning requirements were considered.

Hamed et al. (2007) considered the effect of interruption of anti-scalent dosing or ball cleaning during MSF plant operation on brine heater performance at top brine temperature of 90°C. They investigated the impact of sudden or gradual interruption of anti-scaling dosing without cleaning balls circulation for two different types of anti scalent. AL-Anezi and Hilal (2007) studied and reviewed the solubility of CO<sub>2</sub> in saline solutions under real conditions in the MSF evaporators such as low pressures and high temperatures. They concluded that the gas solubility can be calculated by considering the ionic strength and the salting-out parameter. And also the MSF desalination process fouling occurs as a consequence of CO<sub>2</sub> release and alkaline scale formation in seawater distillers. Moreover, the rate of scale formation of calcium carbonate and magnesium hydroxide in seawater is a complicated function of many variables such as temperature, pH, concentration of bicarbonate ions, and rate of CO<sub>2</sub> release, concentration of Ca<sup>2+</sup>

and  $Mg^{2+}$  ions, and total dissolved solids. On the other hand AL-Rawajfeh (2008) implemented the simulation of the adsorption-crystallisation of  $CO_2 - CaCO_3$  in both of MSF once through and MSF with brine recycle. He observed that the  $CO_2$  release rates increase with increasing TBT and  $CaCO_3$  deposition and thus the fouling factor is increased.

## **2.5 Corrosion in MSF Desalination Plants**

The corrosion processes and fouling of heat transfer equipment should be understood if long-term reliability is to be achieved. Corrosion can be defined in a very practical sense as the deterioration of metal caused by the reaction with its surrounding environment. Most of the corrosion problems, which occur in industry, are due to presence of water. It may be present in large amounts, or in small quantities, but it is necessary to the corrosion process. However, the addition of acid to the seawater make-up for cleaning or scale prevention should be carefully controlled; otherwise the condenser tubes and the de-aerator are prone to serious corrosion attack (Shams EL Din and Makkawi, 1998). About 41 % of the corrosion failures in MSF plants are pitting and crevice corrosion (Malik and Kutty, 1992) and, about 21% of the failures in MSF plants are due to erosion corrosion (Malik and Kutty, 1992).

Good design of an MSF desalination plant requires that materials used in their construction and in the manufacturing of the plants must be carefully selected, based on their behaviour in the working environment in relation to the plant's availability and maintainability, and cost effectiveness

## **2.6 Application of Neural Networks in Process Engineering**

This section briefly reviews the applications of NN in process engineering. NN has been widely used extensively in chemical engineering such as in process modelling, model based control, dynamic modelling, fault detection, parameter estimation process, on line

process optimisation, process control and analysis, oil and gas exploration etc. However, the neural network is also used in chemistry for determining molecular structure by comparing the data obtained by spectroscopic analyses and determining the complex relationship between the controlled and manipulated variable comparing the data obtained from the monitoring of the process and the fault revealing (Zupan and Gasteiger, 1999; Mujtaba et al., 2006)

Krothapally and Palanki (1997) developed a neural network strategy for batch process optimisation. Bomberger et al. (2001) proposed using radial basis function (RBF) neural networks stirred tank reactor. Eikens et al. (2001a) demonstrated the use of self-organising map neural networks to predict the different physiological states in a yeast fermentation process. Aziz et al. (2001) implemented a Generic Model Control (GMC) for controlling reactor temperature by manipulating the temperature of the heating jacket, using neural networks to calculate the heat released in an exothermic batch reactor system. Zeybeck et al. (2004) applied neural networks to implement adaptive heuristic criticism control to improve the temperature control of free radical solution polymerisation of styrene.

Tanvir and Mujtaba (2006b) developed three NN based correlations for estimating temperature elevation (TE) of MSF desalination process for given seawater salinity and boiling point temperature (BPT). The results were compared with experimental data. Al-bri and Hilal (2008) demonstrated the use of back propagation artificial neural network (BPNN) to predict membrane performance and fouling. They compared different architectures to determine the best performance to use in data prediction. BPNN simulation results were validated against the experimental data. However, the results were very close and the difference between them was lower than 5%. Ekpo and Mujtaba (2008) proposed the optimal reactor temperature process for the batch free

radical polymerisation of styrene and methyl methacrylate were used as set points for the design and implementation of different advanced non-linear controllers. Aminian (2010) used a radial basis function (RBF) neural network model to predicate temperature elevation (TE) in multi-stage flash (MSF) desalination processes over a wide range of operating condition. The results showed that the RBF neural network has high accuracy in predicting TE for seawater in MSF desalination process better than the empirical correlations. Said et al. (2011) proposed correlations for predicting the first dissociation constant (K1) and second dissociation constant (K2) of carbonic acid in seawater as function of temperature and salinity. The correlations were implemented with MSF desalination process model for performance evaluation.

### **2.6.1 Neural Network Architecture**

A neural network provides of a number of layers; input layer, hiding layer and output layer. Furthermore, the architecture of NN consists of number of neurons; transfer functions, weights and biases. A signal layered neural network has only a single layer of connection weights. Multilayered network has several layers of hidden and neurons between the input and output units. The multilayered NN are more able to solve complex functions increases than single layered network. However, multilayered networks are quite powerful, making them more suitable for use in this work (see Chapter 7).

Signals flow in the feed forward direction from the input units to the output units incorporates feedback in its operation are widely used in process engineering due to its simplicity and available mathematical algorithms to perform its function. A sample of multilayered (three layered) feed forward network is shown in Figure 2.8.

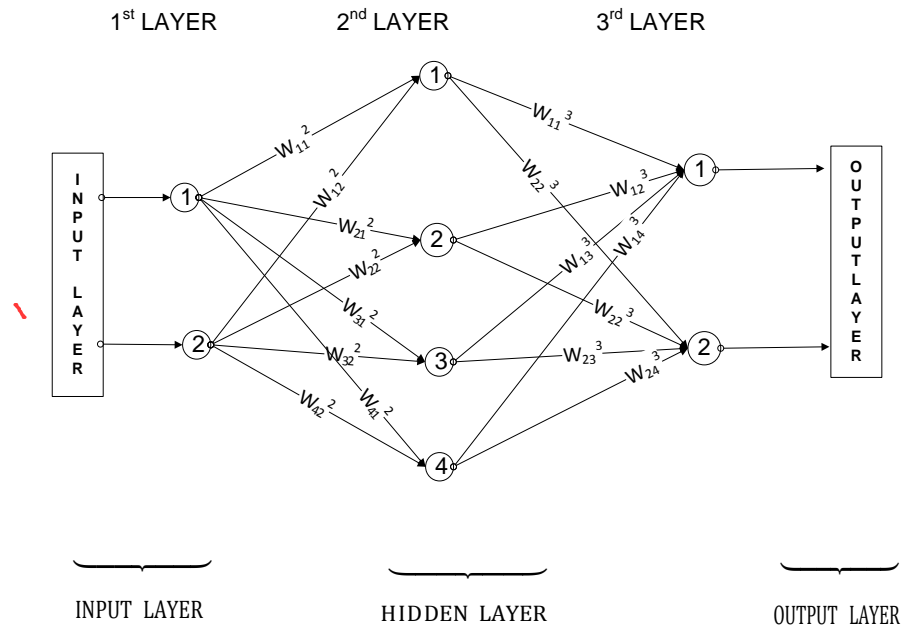


Figure 2.8 A Multilayered feed forward Neural network

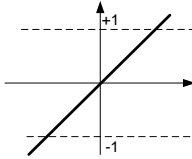
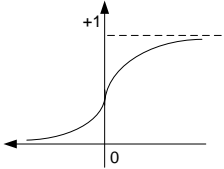
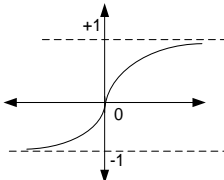
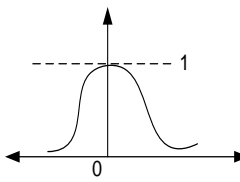
Transfer functions may be linear or nonlinear functions chosen to satisfy a specification of the problem that is used to determine node's output using a mathematical operation on the total activation of the node. The most commonly used functions are shown in the Table 2.2.

### 2.6.2 Neural network based physical properties

The neural network (NN) in MSF desalination process has been used to estimate physical properties such as temperature elevation TE (Tanvir and Mujtaba, 2006b; Aminian, 2010).

The linear and nonlinear relationship between input and output of a system can be built up cost effectively by NNs. In this work, NNs are used to develop correlation for estimating freshwater demand/consumption for given time (in terms h) and season. The eventual objective is to this correlation to calculate variable of freshwater demand/consumption during a day and year and implemented with MSF process modelling and optimisation framework (see Chapter 7).

Table 2.2 Commonly used transfer function (Hagan et al., 1996)

Name of the Transfer function	Mathematical function	Icon
Linear	$f(x) = 1$	 <p>pure line</p>
Sigmoid transfer function	$f(x) = \frac{1}{1 + e^{-x}}$ $[0 \leq f(x) \leq 1]$	 <p>sigmoid</p>
Hyperbolic transfer function	$f(x) = \tanh(x) = \frac{e^x - e^{-x}}{e^x + e^{-x}}$ $[-1 \leq f(x) \leq 1]$	 <p>hyperbolic</p>
Gaussian transfer function	$f(x) = \exp\left(\frac{-x^2}{2}\right)$ $[0 \leq f(x) \leq 1]$	 <p>gaussian</p>

## 2.7 Modelling and Simulation of MSF Desalination Process

Detailed steady state and dynamic models are thought to simulate process performance correctly and help to determine design and operating characteristics.

### 2.7.1 Steady State Modelling

The detailed steady state models include mass and energy balance and the operation of the equipment are determined by nonlinear equations. Many models have been



developed to analyse the MSF water desalination process over the years. Most of these models are developed from the basic mass, energy balance and heat transfer equations.

Coleman (1971) developed a simple stage-to-stage model with constant physical properties, specific heat capacity, heat transfer coefficient in condensers and simplified TE (boiling point elevation) correlation for stage temperature range (112-168 °C) with seawater temperature 38°C and steam temperature 268°C. Constant heat transfer coefficient in condensers and no fouling/scale model equations reformulated for easy sequential or iterative solution. The steady state modelling, with more detail, was carried out by Omar (1983) and Ettouney et al. (2002) to evaluate stage variations in the amount of flashed off vapour, thermodynamic losses, heat transfer coefficient. Helal et al. (1986) and Rosso et al. (1996) applied a steady state simulation of multistage flash. The model was used to analyse the operating and design variable to identify plant behaviour. The brine flow rate, freshwater and the temperature profiles for all stages were calculated by the model. Also the effect of changing top brine temperature on the performance of plant was presented.

Handury, (1995) studied the effect of scale formation on the performance of Multi-Effective (ME) desalination plants. However, he observed that the fouling increases the performance ratio decreases slowly. EL-Dessouky et al. (1998) studied the mathematical model and considered short cut techniques to estimate performance ratio of the MSF process. Aly and EL-Fiqi (2003) described the steady state mathematical model of both MSF and ME processes. The model considered the variation of the physical properties of seawater with seawater temperature, salt concentration and the geometry of stages. They investigated the effect of increasing fouling at constant plant performance on the production rate and overall heat transfer coefficient in recovery and rejection sections.

Tanvir and Mujtaba (2006a) carried out the multi stage flash (MSF) desalination processes model incorporating mass, energy balance and physical property correlation. They reported the sensitivity of operating parameters such as changing the seawater temperature and steam temperature in brine heater on the plant's performance, the total amount of fresh water, top brine temperature (TBT) and final bottom brine temperature (BBT) of the MSF process. Abdel-Jabber et al. (2007) developed the detailed steady state model which is used to predict design and operating characteristics of the plant. The stage dimension, tube bundle length and the demister length were included in the plant design. Moreover, the operating features include temperature profiles and the flow rate.

### **2.7.2 Dynamic Modelling**

MSF model also includes system dynamic. Most of these models have similar features and utilize the parameter analysis. Glueck and Bradshaw (1970) and Hayakawa et al. (1973) applied empirical correlation to determine the evaporation rates. Furuki et al. (1985) developed an automatic control system for the MSF process using a dynamic model. Rimawi et al. (1989) developed the dynamic model for once through MSF plant. The model was solved using a combination of the method of lines and Gears solver of the IMSL library. Falcetta and Sciubba (1999) described a novel method for the simulation of the MSF desalination process and optimized system controllers. Husain et al. (1994) used a commercial software SPEEDUP package to study dynamic simulation of MSF plants. The study was carried out under various operating conditions. The model was very detailed and the simulation results as well. Aly and Marwan (1995) devolved the transients of the system profiles by using the Newton's method and solved the MSF dynamic using a stage by stage calculation. Thomas et al. (1998) investigated the simulation of MSF process as dynamic based on the set of equations, and the dynamic model was used to simulate the effect of step changes in stream flow to the

brine heater. In addition, Mazzotti et al. (2000) developed a dynamic mathematical model to analyse the role of the operating and design variables in the MSF process performance. Moreover, Tanvir (2007) developed dynamic simulation and optimization of MSF process using gPROMS. He used the model to simulate the operation of MSF with varying seawater temperature and steam temperature and also used the dynamic optimization to optimize steam temperature profile, subject to maximizing plant performance.

### **2.7.3 Numerical Methods and Computational Tools Employed for Simulation of MSF process**

There were many methods which were used to solve the MSF process model equation such as Sequential Iterative Method (Glueck and Bradshaw, 1970; Hayakawa et al., 1973), Tri diagonal Matrix (TDM) method (Helal et al., 1986; Husain et al., 1994), Equation Oriented Solvers in commercial software (Husain et al., 1993, 1994), combination of Newton-Raphson and Runge-Kutta method (Aly and Marwan, 1995).

Rimawi et al. (1989) used a combination of the method of lines and Gears solver of the IMSL library. Husain et al. (1994) used a commercial software SPEEDUP package to study dynamic simulation. Falcetta and Sciubba (1999) used CAMEL modular simulator to solve the steady state and dynamic model. Mazzotti et al. (2000) used the commercial software (LSODA routine) to solve the MSF dynamic model. Tanvir and Mujtaba (2006a) and Tanvir (2007) developed steady state and dynamic simulation and optimization of MSF process by using gPROMS builder. Figure 2.9 shows the typical modelling for simulation and optimisation used numerical solvers by gPROMS software.

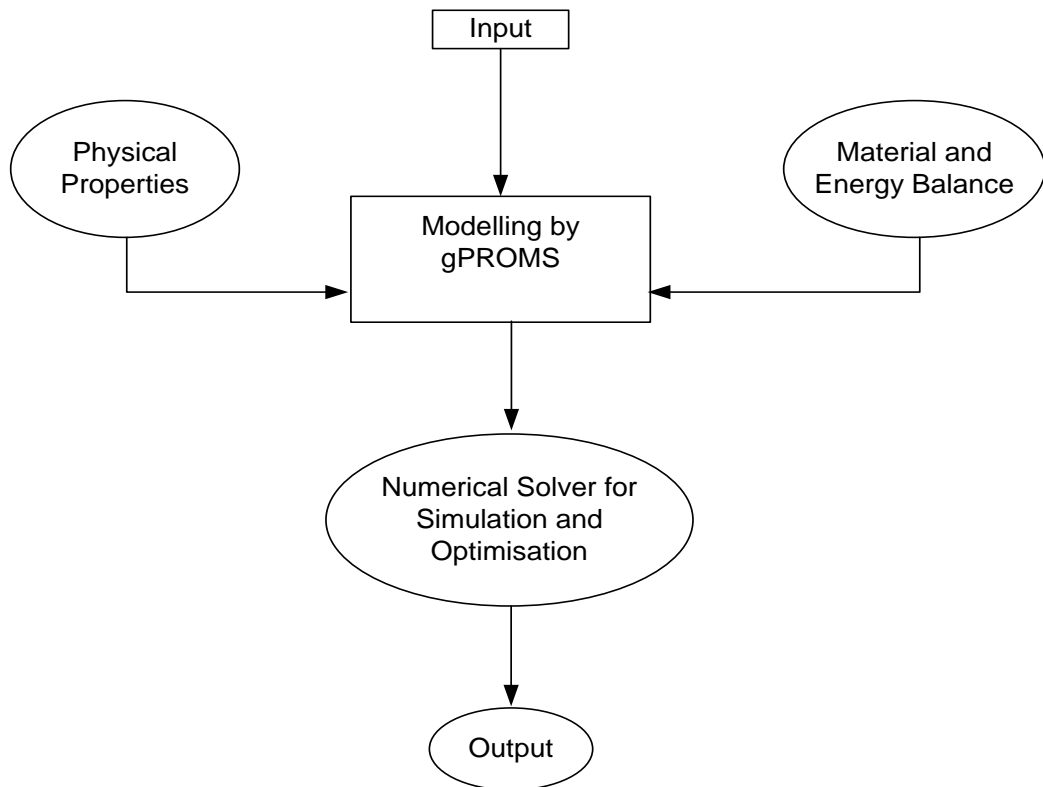


Figure 2.9 Typical simulation and optimisation Architecture

#### 2.7.4 Summary

As seen in the literature the modelling and simulation (steady state or dynamic) of the MSF has become an interesting area for many researches in the past. However, study of the effect of scaling/fouling (such as in brine heater and demister) on the production of freshwater by MSF desalination process are rarely found in literature.

### 2.8 Optimization of MSF Desalination Process

There are some works related to optimization of MSF desalination process. Clelland and Stewart (1966) described the optimization of the design parameters of the unit size based on large scale MSF and how the design can be incorporated in a double purpose power/water system to produce fresh water. Mandil and Ghafour (1970) used short-cut model based analytical optimization ‘minimization by setting first derivative to zero’. The modal equations was constant physical properties (not as a function of temperature

and concentration), constant heat transfer coefficients and stage temperature. Coleman (1971) developed a mathematical economic model of a single MSF desalination system and used dynamic programming based cost optimization within a simple stage-to-stage model. The effects of salinity, specific heat and boiling point elevation on flow rates, heat transfer surface areas, flashing temperatures, and the number of stages were studied.

Wade et al. (1999) applied desalination options with sensitivity analysis to power cost variations and they evaluated energy consumption for five schemes of MSF with four different power plants. They concluded that the MSF with brine recalculation is the least expensive with low energy costs. Mussati et al. (2001) presented a rigorous model for MSF process based on Nonlinear Programming (NLP) optimization with a detailed model.

Mussati et al. (2004) considered finding the optimal process design and operating conditions for given water demand. A very simple model was considered to account for the flash chamber geometric design, number stages, number of tubes in the brine heater, boiling point elevation etc.

Mussati et al. (2005) focused on the minimization of total cost, while optimization of a superstructure of alternative configurations of Dual Purpose Desalination Plants (DPP). They used the resulting MINLP mathematical model for synthesis. Tanvir and Mujtaba (2008a) carried out hybrid modelling and MINLP based optimization of design and operation parameters of MSF desalination process within gPROMS. The sensitivity analysis of the cost parameters were studied for one set water demand and seawater temperature variation. In addition, Mussati et al. (2008) presented a new mathematical model for the superstructure of alternative configurations of DPP considered by Mussati et al. (2005). The new formulation was based on the generalized disjunctive

programming (GDP) of Grossmann (2002) and was applied for the synthesis as well as for analyzing different alternatives configurations.

### 2.8.1 Optimization Framework

The main target of any optimization problem is to find the best (optimal) solution from among the lot by use of efficient and cost effective methods. Some benefits of optimization would include minimizing the cost of operations or maximizing the profit and better utilization of men and machines. Two types of optimization problems are often used:

Linear optimization: - objective function, constraints are linear.

Nonlinear optimization: - objective function model equation and constraints call for nonlinear programming (NLP) optimization techniques or combination of linear and nonlinear systems (Mujtaba, 2004).

Generally, three items have to be defined in any optimization problem.

- An objective function (e.g. profit function, cost function, etc) often called the economic model.
- Equality constraints (e.g. model equations).
- Inequality constraint (e.g. lower and uppers bounds of operating variables, such as flow rate, top brine temperature, steam temperature in MSF desalination process).

In general NLP based optimization has been described mathematically as:

Min or Max

J

X

Subject to equality and inequality constraint

$$f(x) = 0 \tag{2.6}$$

$$h(x) = 0 \quad (2.7)$$

$$g(x) \leq 0 \quad (2.8)$$

Where  $J$  is a nonlinear objective function,  $f(x)$  represents the model in compact form, whilst ensuring that the model operates within the limits imposed by equality  $h(x)$  and inequality  $g(x)$  constraints,  $x$  is the set of decision variables to be optimised. Figure 2.10 illustrates a typical computational sequence for NLP problem for the optimization problem.

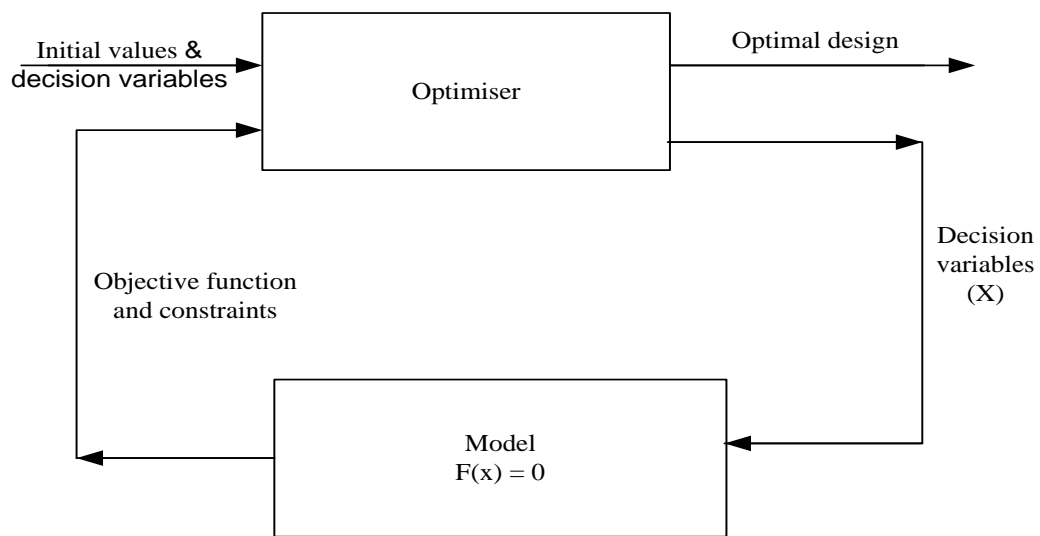


Figure 2.10 Pictorial representation of the NLP optimization framework

In general, as shown in Figure 2.10, the optimizer summons the model with a set of values of decision variable  $X$ . The model simulates the process with these variables and then calculates the objective function ( $J$ ) and constraints ( $g$  and  $h$ ). This information is employed by the optimizer to determine a new set of decision variables. This process is repeated until the optimization criteria pertaining to the optimization algorithms are satisfied.

Often an optimisation problem deals with integer decision variables. For example, the number of stages in MSF process is an integer variable. If the integer parameter is to be

optimised (design optimisation in the case of MSF process) the optimisation problem will lead to Mixed Integer Nonlinear Programming (MINLP) problems (Tanvir and Mujtaba, 2008a).

An MINLP problem can be written mathematically in the following general form:

$$\text{Minimize} \quad z = f(x, y) + c^T y \quad (2.9)$$

$$\text{Subject to} \quad h(x) = 0 \quad (2.10)$$

$$g(x) + My \leq 0 \quad (2.11)$$

$$x \in X \quad (2.12)$$

$$y \in Y \quad (2.13)$$

Where  $x$  is the vector of continuous variables,  $y$  is the vector of integer (usually binary) variables;  $M$  is a matrix of the binary variables. Tanvir and Mujtaba (2008a) described the solution techniques of such MINLP problems.

## 2.10 Conclusion

In this chapter,

- A description of MSF desalination process and the main factors that affected the performance of MSF such as top brine temperature, seawater temperature, and brine recycling, etc. are highlighted. Special attention is given to the role of fouling factor, corrosion problems on operation of the MSF desalination process.
- Neural network based correlations are considered.
- The aspects of modelling simulation and optimisation of MSF desalination process (steady state or dynamic) considered by many researchers (Beamer and Wilde, 1971; Hayakawa et al., 1973; Helal et al., 1986; Rosso et al., 1996; EL-Dessouky and Ettouney, 1997; Tanvir and Mujtaba, 2006a; Abdel-Jaddar et al.,



2007; Glueck and Bradshaw, 1970; Delene and Ball, 1971; Rimawi et al., 1989; Husain et al., 1994; Mazzotti et al., 2000; Aly and Marwan, 1995; Tanvir, 2007) are discussed. The overall heat transfer coefficient is based on a constant fouling factor in all the process models used in these studies. In reality, the fouling factor is a function of time (Hamed et al., 1999, 2000). However, the accurate calculation of the overall heat transfer coefficient (which is also a function fouling factor) is of substantial importance in MSF processes. On the other hand, scaling changes the heat transfer co-efficient of heat exchangers and thus leads to dynamic adjustment of operating parameters if certain freshwater demand is to be met.

- Most of the recent works including Mussati et al., 2005; Tanvir and Mujtaba, 2008a on optimization of MSF desalination process using MINLP technique is discussed. However, their works were constrained to finding optimal design and operation based on fixed freshwater demand and fixed seawater temperature during 24 h a day. However, in reality the seawater temperature is subject to variation during 24 h a day and throughout the year (Yasunaga et al., 2008). Also the fresh water consumption/demand vary throughout the day and throughout the year (Alvisi et al., 2007). These variations will affect the rate of production of freshwater using MSF process throughout the day and throughout the year.

With the investigations carried out in the past (and as summarised above) this work focuses on the following:

- Impact of brine heater fouling on the performance of MSF process with fixed seawater temperature, steam temperature and steam consumption are studied.

- Sensitivity of brine heater fouling on the performance of MSF process with varying seawater temperature, fixed freshwater demand, steam temperature and top brine temperature are analysed.
- A time dependent fouling factor (to represent dynamic scaling effect) is developed and a series of operation snapshots are taken (using steady state model) at discrete time intervals.
- For fixed freshwater demand throughout the year and with seasonal variation of seawater temperature and brine heater fouling factor, the total monthly operation cost of MSF desalination is minimized while the operation parameters are optimized.
- An NN based correlation is developed to estimate dynamic freshwater demand/consumption profile at different time of the day and year.
- A steady state process model for the MSF process coupled with a dynamic model for the storage tank is developed to meet variable freshwater demand/consumption with varying seawater temperatures
- The optimal design and operation of multistage flash (MSF) desalination processes based on variable demands of freshwater with changing seawater temperature throughout the day and throughout the year are considered with a view to generate flexible scheduling.
- Effect of separation efficiency of clean and fouled demisters performance on production of freshwater by MSF desalination process are analysed.

## Chapter 3

### **gPROMS: An Equation Oriented Tool for Modelling**

#### **Simulation and Optimisation**

##### **3.1 Introductions**

gPROMS is a **g**eneral **P**ROcess **M**odelling **S**ystem model builder with proven capabilities for the simulation for dynamics and steady state, optimization, experiment design and parameter estimation of any process (Oh and Pantelides, 1996; Gosling, 2005). However, it can be employed for any process that can be described by a mathematical model and can be exported to most of the modelling and solution engines in packages, for example, HYSYS, Matlab and Simulink by using package components. Moreover, it has a built- in interface to MS EXCEL that allows the user to automatically test the statistical results.

In this work, gPROMS (version 2.3.4 model builder) has been used to mimic the state of MSF desalination process and provided a general overview on the main features of this simulator.

##### **3.2 The Features of gPROMS**

gPROMS uses high-level language to describe a complex process based on the equation- oriented technology. In addition, it has built-in a numerical solver for process simulation and optimization problems. Moreover, modelling by gPROMS software has several activities such as process flow sheeting, laboratory experimental design, simultaneous optimization and design of optimal procedure.

Here the MSF desalination configuration processes considered in the course of this thesis are modelled and optimised using the software package “general PROcess

Modelling System'' (gPROMS) developed by Process Systems Enterprise Ltd., London.

gPROMS means has been used for a wide range of applications in petrochemical, food pharmaceuticals, especially chemicals and automation. Moreover, it uses for any process that can be illustrated by a set of mathematical equations. gPROMS can be used for (PSE, 2004):

- Dynamic simulation.
- Steady state simulation.
- Dynamic optimisation.
- Steady-state optimisation.
- Steady-state parameter estimation.
- Dynamic parameter estimation.

gPROMS has a number of advanced features including the ability to use data from multiple steady-state and dynamic experiments and to estimate an unlimited number of parameters. In addition, it provides the user complete flexibility in that they can specify different variance models for different variables in different experiments. Furthermore, it has a connected to MS Excel that allows the user to automatically test the statistical significance of results, generate plots overlaying model data and experimental data, plot confidence ellipsoids.

gPROMS has many advantages that make it an attractive tool for solving dynamic and steady state modelling problems. Some of its numerous advantages include; clear and concise language, unparalleled modelling power and the ability to model process discontinuities and operating conditions among many others (gPROMS Introductory User Guide, 2005).

### **3.3 The Advantages of gPROMS**

There are many advantages that make gPROMS an important tool for solving steady state and dynamic modelling problems:-

- It can handle a huge number of algebraic and differential equations, and over 100,000 equations can be simulated (gPROMS, 2004).
- gPROMS can be used for the same model for different simulation and optimization activity.
- gPROMS has powerful custom modelling capabilities. This allows the user to develop a competitive advantage by representing your own processes rather than using an off the shelf black – box models to a high degree of accuracy.
- It can be readily integrated with most of the automation software, MS Office and with other standard tools such as HSYSYS, Matalb, Simulink etc.
- It is a clear and concise language, unparalleled modelling power and with the ability to model process discontinuities and operating conditions among many others.
- It can be used specific processes-rather than using black-box models; this is because it has powerful modeling capabilities.
- gPROMS has an active editor for easy constriction and maintenance.

### **3.4 Model Development using gPROMS**

The gPROMS model builder has a number of entries, among them are important:

- Variable Types
- Stream Types
- Tasks
- Processes
- Optimisation

- Parameter estimation
- Experimental design

In this work just four of the sections are used. These are; Variable types section is to specify the types and range of the variables, which are used in the Model. Models, where the process model (physical properties, equipment unit equation and set of differential and algebraic equations) are written in model section file in gPROMS which consists of the following parts: parameter, where constant values should be provided before simulation, VARIABLE section is used to declare the variables of a MODEL, and EQUATION section is used to declare the equations that determine the time trajectories of the variables already declared in the VARIABLE section. Processes (contain specification for simulating the MSF desalination process).

As a result of the many advantages pointed out above, and many others not outlined here, gPROMS was selected as the software of choice for the modelling and optimisation of the MSF desalination process configurations which were carried out in the course of this thesis.

### **3.5 gPROMS Entities**

Here, the gPROMS model builder is chosen due to:

- Time saving for developing the model because the solution algorithm needs to be specified rather than to be written.
- It can be run using the same model for different simulation and optimisation.
- gPROMS has an intellectual editors for easy creation and repairs

#### **3.5.1 Model Entity**

MODEL is defined as the modelling of chemical, physical and biological plant behaviour. Generally, any gPROMS MODEL is described in the following:

- Three types of constant (REAL, INTEGER, LOGICAL) that clarify the system. They are declared in the PARAMETER section. These values should be provided before simulation start.
- Variables and corresponding variable type of the model that may or may not vary with time are declared in the VARIABLE section. Variables type can be clarified as density, enthalpy, temperature, etc.
- A set of equations involving the differential, algebraic are declared in the EQUATION section.

Model equations for MSF desalination process which are mentioned in Chapter 4 are modelled within gPROMS model builder and shown in Figure 3.1.

```

67 AC,AC2,C1,C2,C3,C4,C5,CDM,CIM,Amntanc,Asteam, Achem,Aelec AS AC
68 AA AS AA
69
70 EQUATION
71 #####
72 # BRINE HEATER CALCULATION
73 #####
74 TA=TBj0*1.8+32;
75 CPh=(1-CR*(0.011311-1.146*TA/100000))* (1.0011833-6.1666652*TA/100000+1.3999989*TA^2/10000000+1.3
76 DENSITYh=16.01846*(62.707172+49.364088*(CR/100)-0.43955304*TA/100-0.032554667*(CR/100)*TA-0.46076
77 LATENTHEATH=( 2501.897149 - 2.407064037* TSTEM + 1.192217E-3 *TSTEM^2
78 - 1.5863E-5 *TSTEM^3)*.2388;
79 velocityh=6909.914/denstyh;
80 Uh =4.8857/(((velocityh*IDh)^0.2))/((160+1.92*(TBj0*1.8+32))*velocityh))+ (0.1024768/100-0.7473
81 ALFAh=EXP(((Uh*AREAh)/(WR*CPh)));
82 TFJ(1)=(Tstem*(1-alfah)+alfah*TBj0);
83 MS=((WR*CPh*(TBj0-TFJ(1)))/(LATENTHEATH));
84 QH=WR*CPH*(TBj0-TFJ(1));
85 #####
86 #RECOVERY SECTION CALCULATION
87 #####

```

Figure 3.1 Screenshot of the Model Entity for The MSF Process gPROMS Mode

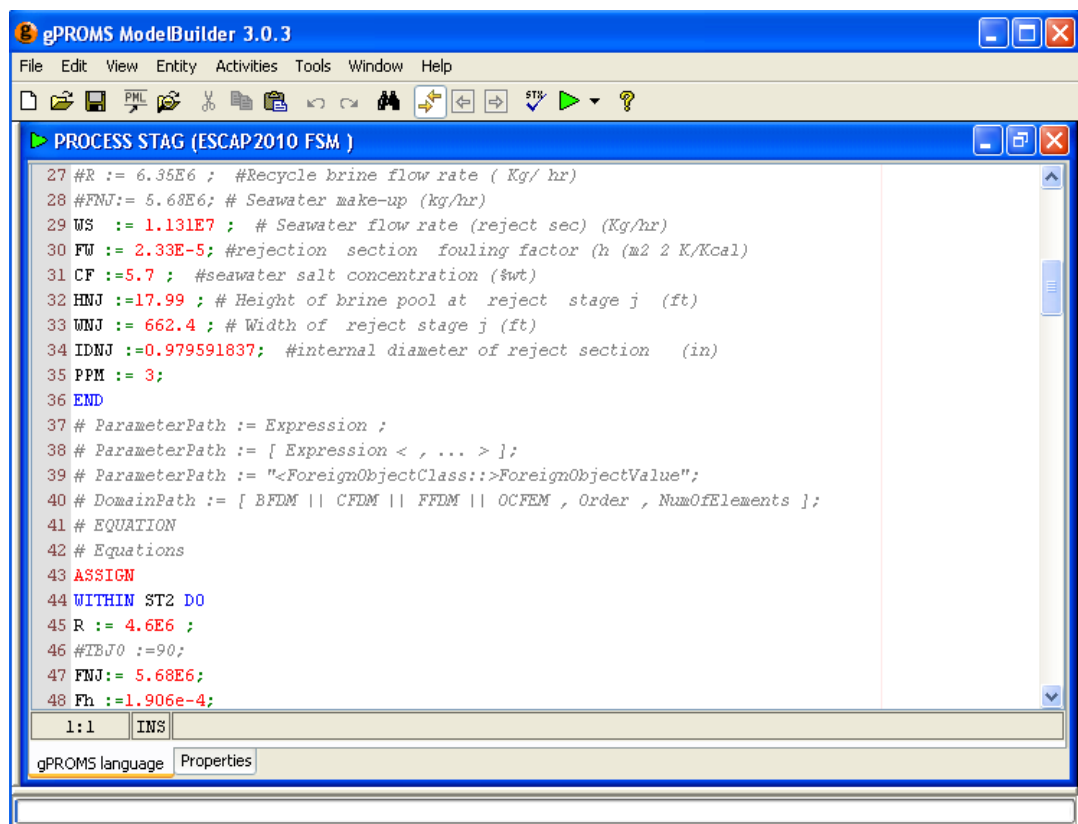
### 3.5.2 Task/Process Entity

The Task/Process (contains specification for simulating the MSF desalination process).

Processes section, the process is analyzed by the composition of different levels of models in hierarchical order. The main process sections used to carry out simulation studies in this work are

- UNIT
- SET
- ASSIGN
- SOLUTIONPARAMETERS
- SCHEDULE.

The Snapshot of entity PROCESS for steady state simulation involving the MSF desalination process is shown in Figure 3.2



```
gPROMS ModelBuilder 3.0.3
File Edit View Entity Activities Tools Window Help
PROCESS STAG (ESCAP2010 FSM )
27 #R := 6.35E6 ; #Recycle brine flow rate ( Kg/ hr)
28 #FNJ:= 5.68E6; # Seawater make-up (kg/hr)
29 WS := 1.131E7 ; # Seawater flow rate (reject sec) (Kg/hr)
30 FW := 2.33E-5; #rejection section fouling factor (h (m2 2 K/Kcal)
31 CF :=5.7 ; #seawater salt concentration (%wt)
32 HNJ :=17.99 ; # Height of brine pool at reject stage j (ft)
33 WNJ := 662.4 ; # Width of reject stage j (ft)
34 IDNJ :=0.979591837; #internal diameter of reject section (in)
35 PPM := 3;
36 END
37 # ParameterPath := Expression ;
38 # ParameterPath := [ Expression < , ... > ];
39 # ParameterPath := "<ForeignObjectClass::>ForeignObjectValue";
40 # DomainPath := [ BFDM || CFDM || FFDM || OCFEM , Order , NumOfElements ];
41 # EQUATION
42 # Equations
43 ASSIGN
44 WITHIN ST2 DO
45 R := 4.6E6 ;
46 #TBJ0 :=90;
47 FNJ:= 5.68E6;
48 Fh :=1.906e-4;
```

Figure 3.2 Screenshot Showing The gPROMS Process Entity.



### 3.6 Simulation in gPROMS

gPROMS provides of the mathematical solvers for simulation, optimisation and parameter estimation, these fall in several categories (gPROMS Introductory User Guide, 2004):

- *Mathematical solvers for linear algebraic equations:*

Two important mathematical solvers, namely MA28 and MA48 solve sets of linear algebraic equations in gPROMS,.

- *Solvers for sets of nonlinear algebraic equations:*

There are three important mathematical solvers to solve sets of nonlinear algebraic equations in gPROMS are:

- ✓ **BDNLSOL** is nonlinear solver with reversible symmetric discontinuities.
- ✓ **NLSOL** solves the nonlinear algebraic equations with and without block decomposition.
- ✓ **SPARSE**: is sophisticated performance of a Newton-type method without block decomposition.

- *Solvers for mixed sets of nonlinear algebraic and differential equations:*

There are two standard mathematical solvers, namely DASOLV and SRADAU, solving mixed sets of differential and algebraic equations in gPROMS. In addition, these solvers are able to handle the partial derivatives.

- *Solvers for optimisation problems.*

There is a general numerical solver manager available in gPROMS for solving dynamic and steady state optimisation problem called DOSOLV.

Mathematical solvers for optimisation are specified in the SOLUTION PARAMETERS section of a PROCESS entity through the syntax:

SOLUTIONPARAMETERS

DOSolver: = "CVP\_SS";

## SOLUTIONPARAMETERS

DOSolver: = "CVP\_MS";

PIECEWISE CONSTANT, PIECEWISE LINEAR and TIME INTERVAL should be ASSIGNED in the gPROMS PROCESS entity.

### 3.7 Optimisation Entity

Optimization section: the optimization entry has three additional tabs to solve any optimization problem: [general, controls and constraints]. The objective function to be minimized or maximized and at the same time satisfying any imposed constraints.

Some other important parameters specified in the optimisation section are (user of Guide gPROMS, 2004):

- The objective function to be minimised or maximised.
- Endpoint equality constraints and inequality constraints
- The time horizon and its limits for the process
- The number of intervals.
- The control values and their limits in different control interval.

The mathematical statement of the optimization problem can be summarized in Figure 3.3.

### 3.8 Control Variable Profiles in gPROMS

The dynamic optimisation problem needs to be specific relating to the type of the variation of the control variables over time that is prepared to consider. gPROMS provides of two types of the control variable profiles in the dynamic optimisation are:

- Piecewise-constant controls.
- Piecewise-linear controls.

Figure (3.4) shows the Piecewise-constant controls which is used to carry out optimisation studies in this work.

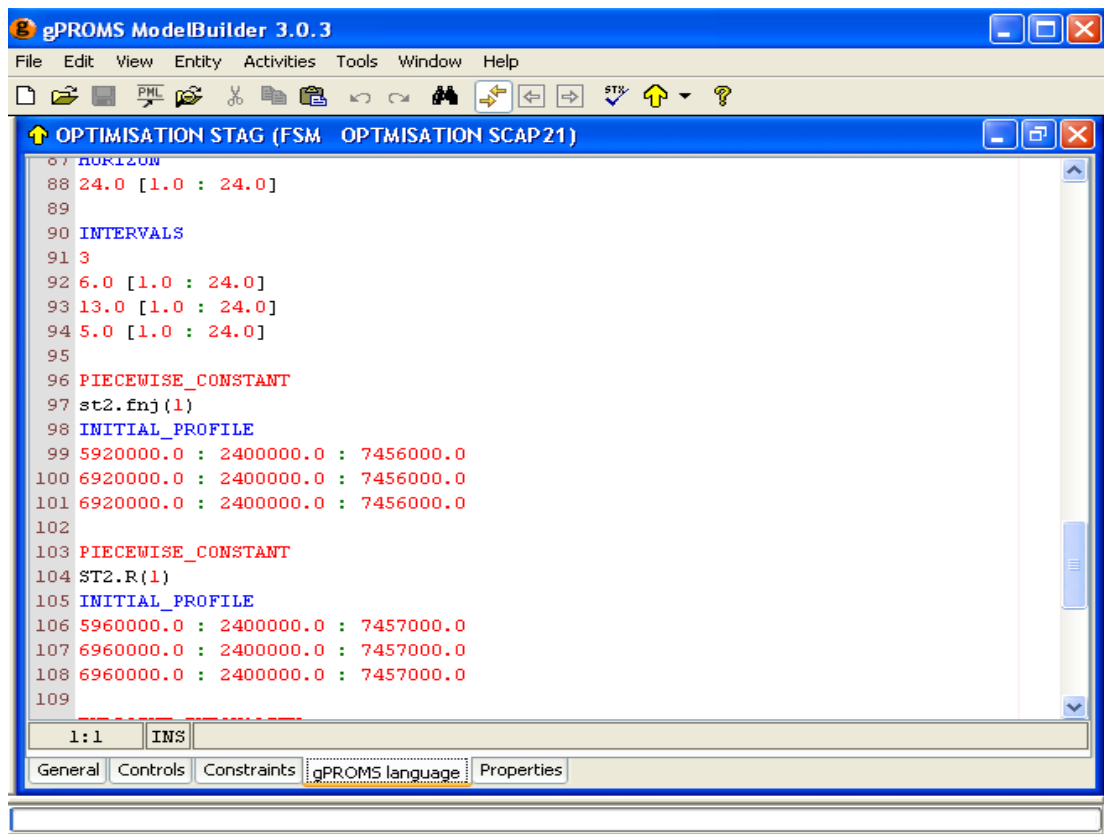


Figure 3.3 Screenshot Showing The gPROMS Optimisation Entity

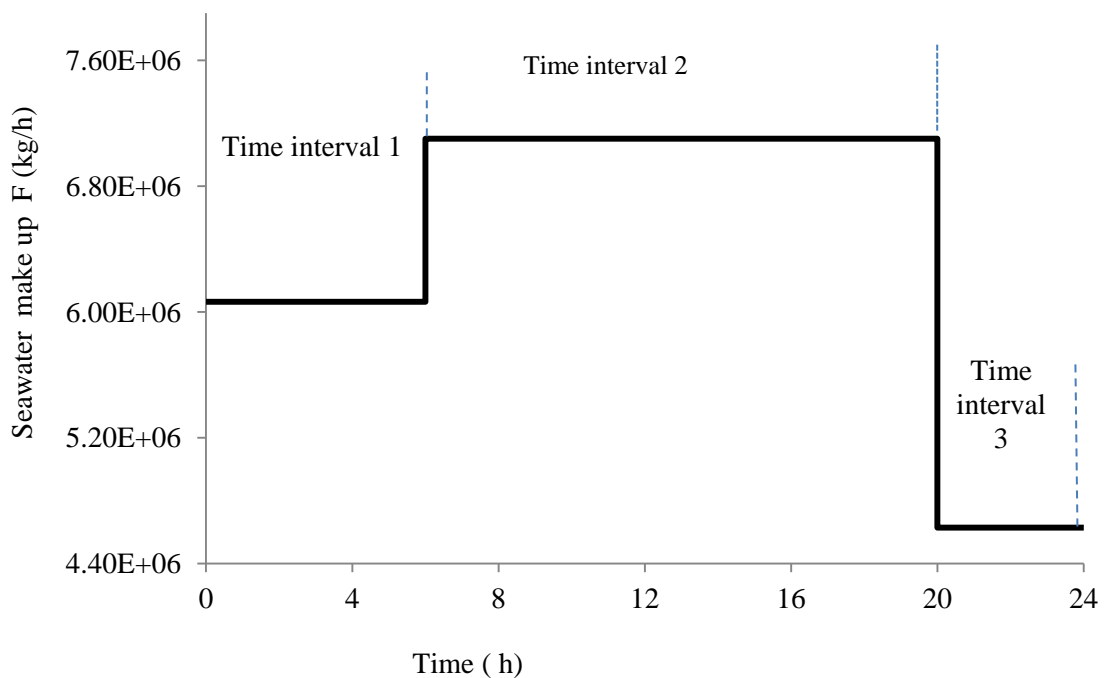


Figure 3.4 Piecewise Constant seawater make up  $F$  (kg/h)

### **3.9 Comparison of gPROMS with Other Commercial Software**

There are number of commercial software packages available for developing model process simulations, optimisations, and optimal control such as Hysis and AspenPlus. Each of these commercial packages is developed with different characteristics; it looks all of them give a wide range of application flexibility. However, it would be useful to highlight some of the research in public area which was comparing different commercial software.

Tijl (2005) has conducted comparison between the performances of Aspen Custom Modeller (ACM) with the performance of gPROMS, to optimise the Sec-Butyl Alcohol (SBA) stripper as case study. For both softwares the SBA model was built to perform parameter estimation and assesses their capabilities and CAPE-OPEN was utilised to use some thermodynamic and physical properties of the components in both software (ASC and gPROMS). The conclusion of the study has found the parameter estimation capabilities of gPROMS were better than ACM. Choi et al. (2007) presented an optimal condition of the Simulated Moving Bed (SMB) for the complete separation of bupivacaine. gPROMS and Aspen Chromatography package were used for simulation of the SMB process. They conclude that the gPROMS software more closely matched experimental data than those obtained by the Aspen Chromatography package.

### **3.10 Conclusion**

This chapter includes brief general overview of the importance of using gPROMS model builder software package for modelling, simulation and optimization and a brief discussion of the features in gPROMS that have been used for this work.

The gPROMS software has an additional functionality compared to software packages such as ACM software, which is Sequential Experiment Design (SED) (gPROMS, 2004). This would allow the user to sequentially design future experiments such that the

experimental data used obtain better accuracy of previously estimated parameters (Tijl, 2005).

Due to many advantages and applications summarized above, and many others not outlined here, gPROMS was selected as the software for the modelling steady state and dynamic optimisation of an MSF desalination process carried out in the course of this thesis.

Further information can be found in Oh and Pantelides (1996), Tanvir and Mujtaba (2008a) and at [www.psenterprise.com](http://www.psenterprise.com).

# Chapter 4

## Modelling MSF Desalination Process

### 4.1 Introduction

Mathematical modelling in engineering is concerned with the use of mathematical equations to predict the actual process behaviour. There are many advantages of using the model and simulation (described by set of mathematical equations) rather than using experimental work or real plant operations. Some of these are summarized as follows:-

- Use of a model saves time.
- It is cheaper than using a real process.
- Computer simulation and optimization saves money in design and operation.
- It is safer and the results are much less fatal if something goes wrong with the investigation.

There are mainly two types of chemical process models: a steady state and dynamic model. In the steady state model no change in process variables with time is considered, but the dynamic model depends on time.

In this work, a steady state model of MSF is developed based on the basic laws of mass balance, energy balance, and heat transfer equations with supporting correlations for brine densities, boiling temperatures, brine and vapour enthalpies, and heat transfer coefficient. In addition, the temperature losses due to boiling point elevation, non-equilibrium allowance and temperature losses in the demisters are represented. Most of these equations are nonlinear due to the dependency of physical properties of the streams on temperature and salinity. The model includes parameters such as the brine flow rate, freshwater flow rate, the temperature profiles for all stages, top brine

temperature and steam flow rate. gPROMS model builder 2.3.4 software is used for model development and simulation. The model is validated against the simulation results reported by Rosso et al. (1996).

## **4.2 Steady State Model of MSF Process**

### **4.2.1 Process Description**

Figure 4.1 shows the schematics of an MSF desalination Process. The process consists of essentially a steam source, water/steam circuit (brine heater), flashing stages sections and pumping units. As shown, the process is divided into two main sections, recovery stages and rejection stages. The feed seawater ( $W_{sw}$ ) passes through the heat rejection section (condenser tubes) to cool the distillate and to get the lowest possible temperature of brine before it is discharged back to the sea. In the last stage of rejection, the seawater is divided into the rejection stream ( $C_w$ ), which is rejected to the sea to balance the heat and a make-up stream ( $F$ ) which is then combined with the recycle stream ( $R$ ). The combined stream ( $W_R$ ) enters the tubes of the recovery section to raise its temperature from the stages, and then passes through the brine heater to reach its highest temperature, the 'top brine temperature (TBT)' approximately equal to the saturation temperature of the brine at the system pressure. At this point, the feed ( $B_0$ ) enters the first heat recovery stage through an orifice and partly flashes into vapour upon entering the next stage. The vapour passes through a demister to reject any brine droplet and condenses on the cool outside of tube bundle of the heat exchanger and then drips into a distillate tray. The distillate from each stage is collected in a distillate tray to form the final freshwater product ( $D_j$ ). The concentrated brine is divided into two streams as blow down ( $B_D$ ) which is rejected to the sea and a recycle stream ( $R$ ) which returns to mix with the make-up ( $F$ ) as mentioned above.

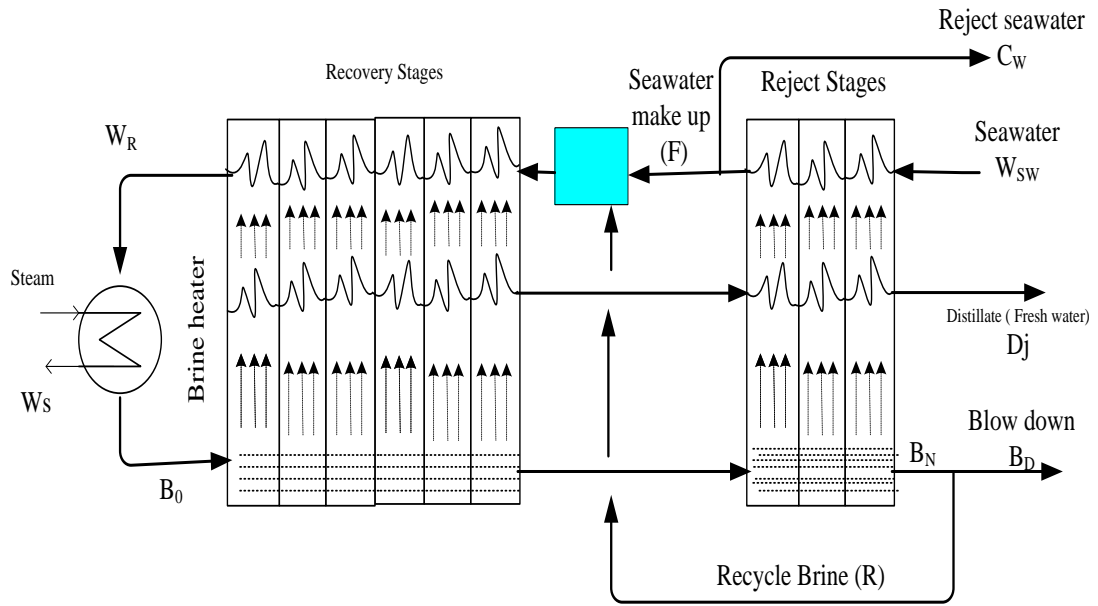


Figure 4.1 Typical MSF Process (Hawaidi and Mujtaba, 2011)

#### 4.2.2 Model Equations

The model equations are constituted of a set of mass and energy balances which are given in the following (all symbols are defined in the list of symbols).

The assumptions used to develop the mathematical model include the following:-

- Steady state operation.
- Heat losses to the surroundings are negligible.
- Heat transfer areas in each flashing stage in the heat recovery and rejection section are equal.
- The heat capacities, specific enthalpy and physical properties for feed seawater, brine, and distillate product are functions of temperature and composition.
- The fouling resistance is constant for recovery and rejection section.
- Thermodynamic losses include the boiling point elevation ( $TE_j$ ), the non-equilibrium allowance ( $\delta_j$ ) and demister losses ( $\Delta_j$ ).



- The distillate product is salt free.
- Heat of mixing is negligible.
- No sub cooling of condensate leaving the brine heater.

#### 4.2.2.1 Stage Model

Referring to Figure 4.2, the following equations can be written for stage number  $j$  at steady state

Mass balance in the flash chamber:

$$B_{j-1} = B_j + D_j \quad (4.1)$$

Stage salt balance:

$$X_{Bj} B_j = X_{Bj-1} B_{j-1} \quad (4.2)$$

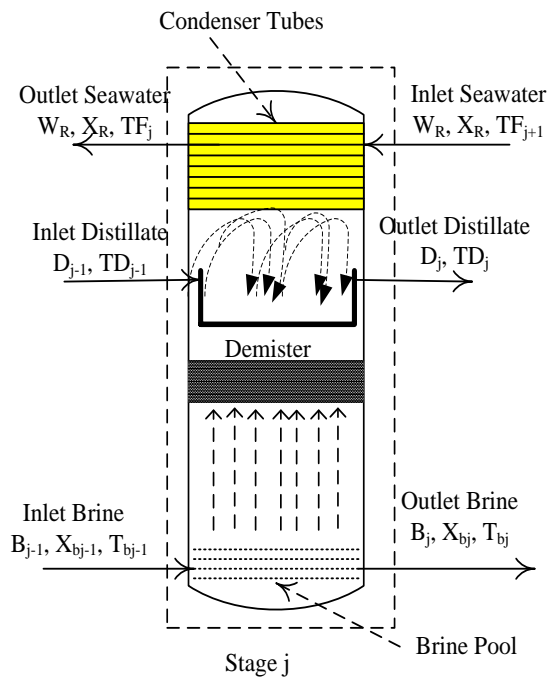


Figure 4.2 A general stage in a MSF plant

Mass balance for distillate tray:

$$\sum_{k=1}^j D_k = \sum_{k=1}^{j-1} D_k + D_j \quad (4.3)$$

Enthalpy balance on flash brine:

$$\frac{B_j}{B_{j-1}} = \frac{(h_{Bj-1} - h_{vj})}{(h_{Bj} - h_{vj})} \quad (4.4)$$

$$h_{vj} = f(T_{vj}) \quad (4.5)$$

$$h_{Bj} = f(T_{Bj}, X_{Bj}) \quad (4.6)$$

Overall energy balance on stage :

$$W_R \text{cp}_j (T_{Fj} - T_{Fj+1}) = \sum_{k=1}^{j-1} D_k \text{cp}_{Dj-1} (T_{Dj-1} - T^*) - \sum_{k=1}^j D_k \text{cp}_{Dj} (T_{Dj} - T^*) \\ + B_{j-1} \text{cp}_{Bj-1} (T_{Bj-1} - T^*) - B_j \text{cp}_{Bj} (T_{Bj} - T^*) \quad (4.7)$$

Heat transfer equation (Condenser):

$$W_R \text{cp}_j (T_{Fj} - T_{Fj+1}) = U_j A_j \text{LMTD}_j \quad (4.8)$$

The logarithmic mean temperature difference in the recovery and rejection stage:

$$\text{LMTD}_j = \frac{(T_{Fj} - T_{Fj+1})}{\ln[(T_{Dj} - T_{Fj+1}) / (T_{Dj} - T_{Fj})]} \quad (4.9)$$

Where  $U_j$  is calculated in terms of  $W_R$ ,  $T_{Fj}$ ,  $T_{Fj+1}$ ,  $T_{Dj}$ , ID, OD and  $F_j$

$$\text{cp}_j = f(T_{Fj+1}, T_{Fj}, X_R) \quad (4.10)$$

$$\text{CP}_{Bj} = f(T_{Bj}, X_{Bj}) \quad (4.11)$$

$$\text{CP}_{Dj} = f(T_{Dj}) \quad (4.12)$$

Distillate and flashing brine temperature correlation:

$$T_{Bj} = T_{Dj} + TE_j + \Delta_j + \delta_j \quad (4.13)$$

Distillate flashed steam temperature correlation:

$$T_{Vj} = T_{Dj} + \Delta_j \quad (4.14)$$

$$\Delta_j = f(T_{Dj}) \quad (4.15)$$

$$TE_j = f(T_{Bj}, X_{Bj}) \quad (4.16)$$

$$\delta_j = f(T_{Bj}, H_j, W_j) \quad (4.17)$$

#### 4.2.2.2 Brine heater model

Brine heater performance (Figure 4.3) can be described by the following equations:

Mass and salt balance (brine):

$$B_0 = W_R \quad (4.18)$$

$$X_{B0} = X_R \quad (4.19)$$

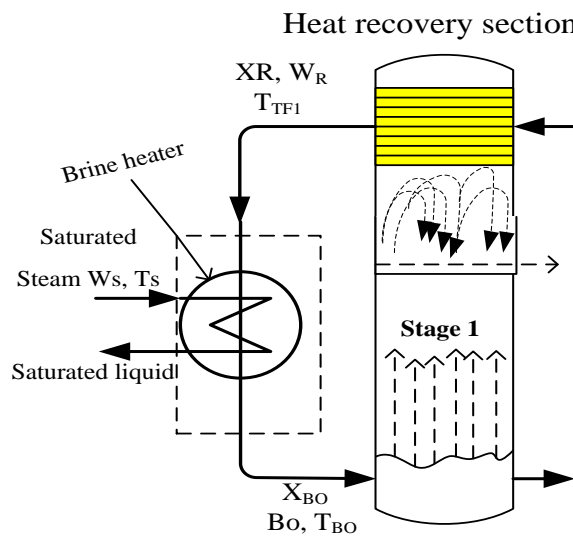


Figure 4.3 Typical brine heater

Overall enthalpy balance:

$$B_0 C_{pj} (T_{B0} - T_{F1}) = W_s \lambda_s \quad (4.20)$$

$$\lambda_s = f(T_s) \quad (4.21)$$

Heat transfer equation in the brine heater evaporator:

$$W_R C_{p_j} (T_{B0} - T_{F1}) = U_H A_H \text{LMTD} \quad (4.22)$$

The logarithmic mean temperature difference in brine heater:

$$\text{LMTD} = \frac{(T_{B0} - T_{F1})}{\ln[(T_s - T_{F1}) / (T_s - T_{B0})]} \quad (4.23)$$

Where  $U_H$  is calculated in terms of  $W_R$ ,  $T_{Fj}$ ,  $T_{B0}$ ,  $T_s$ , ID, OD and BHF

Plant performance:

$$\text{GOR} = \frac{D_N}{W_s} \quad (4.24)$$

#### 4.2.2.3 Mixer and Splitters Model

This model takes into account the MSF plant configuration and the model proposed by Rosso et al. (1996).

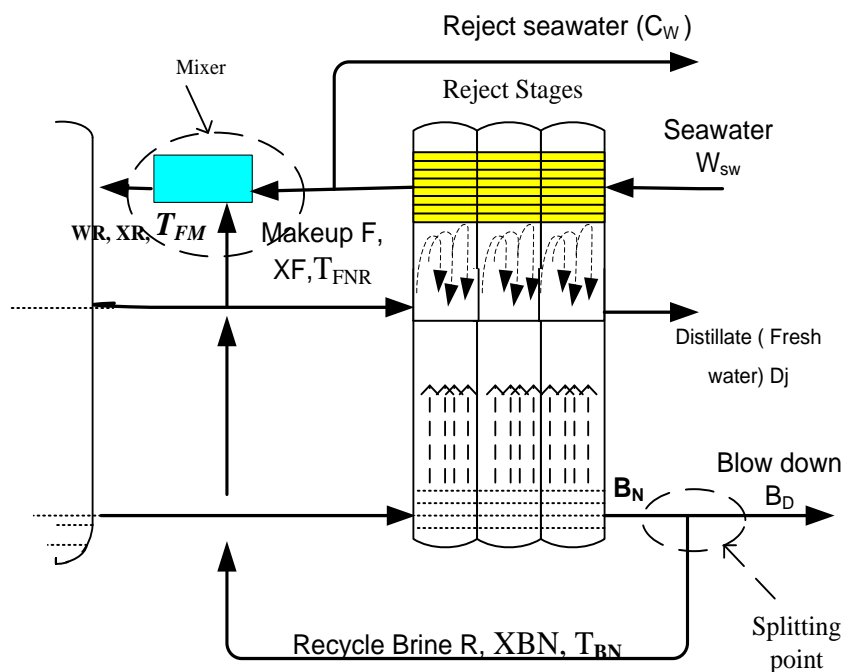


Figure 4.4 mixing and splitting points in the MSF desalination unit

Mass balance on mixer:

$$W_R = R + F \quad (4.25)$$

$$R X_{BN} + F X_F = W_R X_R \quad (4.26)$$

Enthalpy balance on mixer:

$$W_R h_m = R h_R + F h_F \quad (4.27)$$

$$h_M = f(T_{FM}, X_R) \quad (4.28)$$

$$h_F = f(T_{FNR}, X_F) \quad (4.29)$$

$$h_R = f(T_{BN}, X_{BN}) \quad (4.30)$$

Mass balance on seawater splitter:

$$B_D = B_N - R \quad (4.31)$$

$$C_W = W_{sw} - F \quad (4.32)$$

Physic-chemical properties correlations used to solve the MSF model are included in this section.

### Density

The expression for the brine density  $\rho_j$  given here is valid for the range 0-26 % concentrations and 40 – 300 F (4.4 – 148.8 °C) temperature.

$$\begin{aligned} \rho_j = & 16.0184 (62.7071 + 49.3640 X_{Bj} - 0.4395 \times 10^{-2} T_{Bj} - 0.3255 X_{Bj} T_{Bj} \\ & + 0.4607 \times 10^{-4} T_{Bj}^2 + 0.6324 \times 10^{-4} X_{Bj} T_{Bj}^2) \end{aligned} \quad (4.33)$$

### Specific volume of saturated water vapour, $v$ in $m^3/kg$

$$v = (4.605 (T_s + 273.15) / 1000 P_j - 0.02) \quad (4.34)$$

### Heat Capacity

Specific heat capacity of pure water ( $CP_{Dj}$ ):

$$CP_{Dj} = 1.001 - 6.1666 \times 10^{-5} T_{Dj} + 1.399 \times 10^{-7} T_{Dj}^2 + 1.333 \times 10^{-9} T_{Dj}^3 \quad (4.35)$$

Specific heat capacity of brine water ( $CP_{Dj}$ )

$$CP_{Bj} = \left[ 1 - X_{Bj} \left( 0.0113 - 1.146 \times 10^{-5} T_{Bj} \right) \right] CP_{Dj} \quad (4.36)$$

### Enthalpy and Latent Heat

Specific enthalpy ( $h_{Bj}$ ) of seawater/brine:

$$\begin{aligned} h_{Bj} = & 4.186 - 5.381 \times 10^{-3} X_{Bj} + 6.26 \times 10^{-6} X_{Bj}^2 T_{Bj} - \\ & (3.055 \times 10^{-5} + 2.774 \times 10^{-6} X_{Bj} - 4.318 \times 10^{-8} X_{Bj}^2) \\ & \left( \frac{T_{Bj}^2}{2} \right) + (8.844 \times 10^{-7} + 6.527 \times 10^{-8} X_{Bj} - 4.003 \times 10^{-10} X_{Bj}^2) / \left( \frac{T_{Bj}^3}{3} \right) \end{aligned} \quad (4.37)$$

Latent heat of condensation of steam as function of steam temperature ( $\lambda_s$ )

$$\lambda_s = (2499.5698 - 2.20486 T_s - 2.304 \times 10^{-3} T_s^2) \times 0.2388 \quad (4.38)$$

### Boiling Point Elevation

The temperature elevation (TE) due to salinity which is taken from EL-Dessouky and Ettouney (2002). Rosso et al. (1996) used TE correlation from Stoughton and Lietzl (1967) and is accurate within salinity range of 3.45 to 20 % and temperature 30 to 250°C. The TE correlation used by EL-Dessouky and Ettouney (2002) is accurate within salinity range 1 to 16% and temperature 10 to 180°C. Since the salinity and temperature range of this work fall within these limits this correlation is used in this work.

Boiling point elevation as function of temperature and salt concentration:

$$\begin{aligned} T_{Ej} = & ((8.325 \times 10^{-2}) + (1.883 \times 10^{-4}) T_{Bj} + (4.02 \times 10^{-6}) T_{Bj}^2) X_{Bj} \\ & + (-7.625 \times 10^{-4} + 9.02 \times 10^{-5} T_{Bj}) + 5.2 \times 10^{-7} T_{Bj}^2 X_{Bj}^2 \\ & + (1.522 \times 10^{-4} - (3 \times 10^{-6}) T_{Bj} - (3 \times 10^{-8}) T_{Bj}^2) X_{Bj}^3 \end{aligned} \quad (4.39)$$

### Non – Equilibrium Allowance ( $\delta$ )

Burns and Roe correlation (Rosso et al., 1996) reported the following correlation for the Non – equilibration allowance ( $\delta$ ), expressed as temperature loss ( $^{\circ}\text{C}$ ):

$$\delta_j = 195.556 H_j^{1.1} (\omega_j \times 10^{-3})^{0.5} \Delta T_{Bj}^{-0.25} T_{Dj}^{-2.5} \quad (4.40)$$

### Demister and Other Losses

Temperature loss due to the pressure drop in the demister and condenser tubes ( $\Delta_j$ )

(Rosso et al., 1996).

$$\Delta_j = e^{\frac{(1.885 - 0.02063 T_{Dj})}{1.8}} \quad (4.41)$$

### Overall Heat Transfer Coefficient ( $U$ )

The Griffin and Keller equation calculates the heat transfer coefficient both the brine and vapour side (Rosso et al., 1996).

$$U = \frac{4.8857}{(y + Z + 4.8857 F_j)} \quad (4.42)$$

Where,

$$Z = 0.102 \times 10^{-2} - 0.747 \times 10^{-5} T_{Dj} + 0.997 \times 10^{-7} T_{Dj}^2 - 0.430 \times 10^{-9} T_{Dj}^3 + 0.620 \times 10^{-12} T_{Dj}^4 \quad (4.43)$$

$$y = \frac{[V_{Bj} ID]^{0.2}}{[(160 + 1.92 T_{Bj}) V_{Bj}]} \quad (4.44)$$

Note,  $T^* = 0^{\circ}\text{C}$ .

### Stage Pressure ( $P_j$ )

The relationship for the evaluation of the stage pressure (Helal et al., 1986)

$$\ln \frac{P_c}{P_j} = \frac{X}{T_s} \left( \frac{a + b X + C X^3}{(1 + d X)} \right) \quad (4.45)$$

Where  $a = 3.24378$ ,  $b = 5.86826 \times 10^{-3}$ ,  $c = 1.170237 \times 10^{-8}$ ,  $d = 2.187846 \times 10^{-3}$ ,  $X = T_c - T_s$ ,  $P_c = 218.167$  atm and  $T_c = 647.27$  K

### 4.3 Model Validation

The case study reported by Rosso et al. (1996) (which was based on industrial data) is used here for model validation. The configuration investigated in this work includes 13 stages in heat recovery section and 3 stages in the heat rejection section (Figure 4.1). The model equations and physical property correlations constitute a set of nonlinear algebraic equations which are described above.

The specifications and constant parameters used by Rosso et al. (1996) and this work are shown in Table 4.1. The summary of the simulation results by Rosso et al. (1996) shown in Table 4.2 and this work shown in Table 4.3. Both models calculate the brine flow rate, freshwater and the temperature profiles for all stages, top brine temperature and steam flow rate as shown in Figure 4.5. A comparison of the results in Tables 4.2, 4.3 and Figure 4.5 show that there is an excellent agreement between them. Slight differences in the results are due to the use of different correlation for temperature elevation due to salinity. For instance Rosso et al. (1996) used TE correlation from Stoughton and Lietzke (1967) while this work used TE correlation used by EL-Dessouky and Ettouney (2002).

Table 4.1 Constant parameters and input data

	$A_j/A_H$	$ID_j/ID_H$	$OD_j/OD_H$	$f_j/f_{bh}$	$w_j/L_H$	$H_j$
Brine heater	3530	0.022	0.0244	0.159	12.2	--
Recovery stage	3995	0.022	0.0244	0.120	12.2	0.457
Rejection stage	3530	0.0239	0.0254	0.020	10.7	0.457
$W_{sw}$	$T_s$	$T_{sw}$	$X_{sw}$	$R$	$C_w$	
$1.131 \times 10^7$ kg/h	97°C	35°C	5.7 wt %	$6.35 \times 10^6$ kg/h	$5.62 \times 10^6$ kg/h	



Table 4.2 Summary of the simulation results by (Rosso et al., 1996)

Flow rates and concentrations

Seawater make-up (F)	5680000 kg/h
Blow down	4745902 kg/h
Cooling brine flow rate	$1.2030 \times 10^7$ kg/h
Seawater flow rate (reject section)	$1.1300 \times 10^7$ kg/h
Steam flow rate	134898.1 kg/h
Cooling brine salt concentration	6.292183 % wt
GOR (gained output ratio)	6.9244

Stage	B <sub>j</sub> (kg/h)	D <sub>j</sub>	XB <sub>j</sub> %	TF <sub>j</sub>	TD <sub>j</sub> (°C)	TB <sub>j</sub> (°C)	U <sub>j</sub> (kcal/hm <sup>2</sup> k)
0	1.203E+07		6.2922			89.74	2040.9
1	1.197E+07	5.940E+04	6.3234	83.33	85.75	86.89	2250.0
2	1.191E+07	1.187E+05	6.3549	80.41	82.87	84.01	2246.4
3	1.185E+07	1.784E+05	6.3869	77.44	79.95	81.08	2243.0
4	1.179E+07	2.385E+05	6.4195	74.43	76.97	78.11	2239.9
5	1.173E+07	2.989E+05	6.4525	71.37	73.94	75.09	2236.9
6	1.167E+07	3.595E+05	6.486	68.28	70.88	72.04	2234.2
7	1.161E+07	4.201E+05	6.5198	65.16	67.78	68.95	2231.7
8	1.155E+07	4.806E+05	6.554	62.01	64.65	65.84	2229.2
9	1.149E+07	5.410E+05	6.5885	58.84	61.49	62.7	2226.2
10	1.143E+07	6.010E+05	6.6231	55.65	58.32	59.55	2224.0
11	1.137E+07	6.606E+05	6.6578	52.46	55.13	56.39	2221.0
12	1.131E+07	7.197E+05	6.6925	49.27	51.93	53.24	2217.6
13	1.125E+07	7.780E+05	6.7272	46.09	48.74	50.09	2213.6
14	1.120E+07	8.296E+05	6.7582	44.06	45.87	47.28	2917.3
15	1.115E+07	8.816E+05	6.7897	41.1	42.95	44.42	2905.9
16	1.110E+07	9.341E+05	6.8219	38.07	39.98	41.51	2892.3

Table 4.3 Summary of the simulation results by using model in gPROMS

Flow rates and concentrations

Seawater make-up (F)	5680000 kg/h
Blow down	4742649 kg/h
Cooling brine flow rate	1.2030×10 <sup>7</sup> kg/h
Seawater flow rate (reject section)	1.1300 ×10 <sup>7</sup> kg/h
Steam flow rate	136085.64kg/h
Cooling brine salt concentration	6.294654 % wt
GOR (gained output ratio)	6.8879

Stage	B <sub>j</sub> (kg/h)	D <sub>j</sub>	XB <sub>j</sub> %	TF <sub>j</sub>	TD <sub>j</sub> (°C)	TB <sub>j</sub> (°C)	U <sub>j</sub> (kcal/hm <sup>2</sup> k)
0	1.203E+07		6.2946			89.71	2048.9
1	1.197E+07	58915	6.3256	83.25	85.68	86.86	2257.0
2	1.191E+07	118424	6.3572	80.29	82.77	83.97	2253.5
3	1.185E+07	178423	6.3894	77.29	79.81	81.03	2250.3
4	1.179E+07	238804	6.4221	74.26	76.80	78.05	2247.3
5	1.173E+07	299461	6.4553	71.18	73.75	75.03	2244.5
6	1.167E+07	360281	6.4889	68.08	70.67	71.98	2242.0
7	1.161E+07	421154	6.5230	64.95	67.56	68.91	2239.6
8	1.155E+07	481963	6.5573	61.80	64.42	65.81	2237.4
9	1.149E+07	542594	6.5919	58.64	61.26	62.71	2235.1
10	1.143E+07	602926	6.6267	55.46	58.10	59.59	2232.6
11	1.137E+07	662838	6.6617	52.29	54.92	56.48	2229.9
12	1.131E+07	722202	6.6966	49.11	51.74	53.37	2226.7
13	1.125E+07	778670	6.7302	45.95	48.69	50.39	2222.5
14	1.120E+07	830688	6.7615	44.09	45.84	47.62	2988.4
15	1.115E+07	883639	6.7936	41.13	42.92	44.79	2978.6
16	1.109E+07	937351	6.8265	38.09	39.94	41.90	2966.4

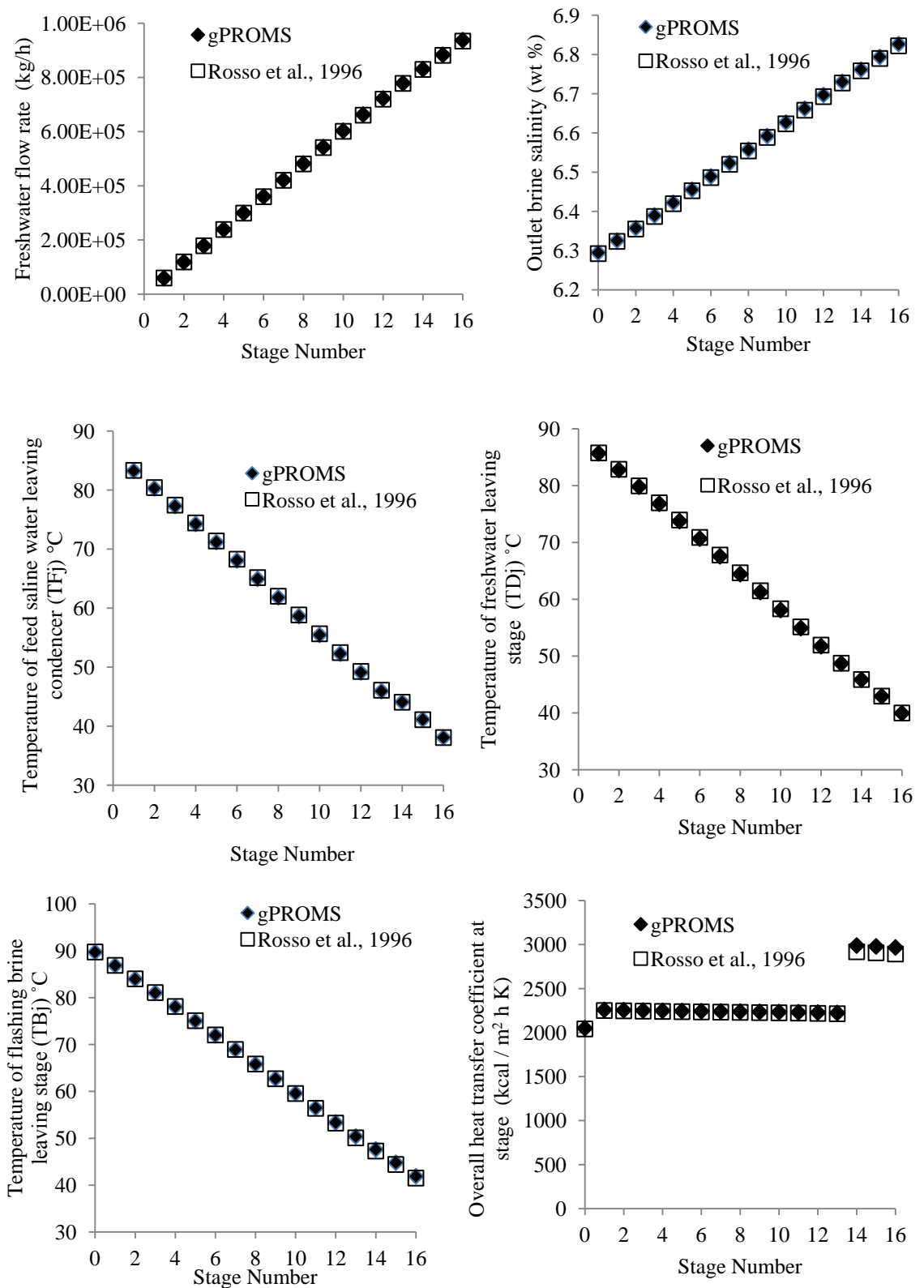


Figure 4.5 Comparison of gPROMS results and Rosso et al., 1996 results for stage profiles of flow rate, salinity, temperature and overall heat transfer coefficient

## **4.4 Conclusion**

This chapter discusses the process modelling and simulation of MSF desalination process. The model is essentially a set of algebraic equations that describe a steady state mathematical model of MSF process based on mass balance, energy balance, heat transfer equations and supported by correlation for brine densities, boiling temperatures, brine and vapour enthalpies, and heat transfer coefficient. In addition, the temperature losses due to boiling point elevation, non-equilibrium allowance and temperature losses in the demisters. All physical properties correlation, which are functions of temperature and salinity are taken from literature.

Here gPROMS tool has been used to model and simulate the MSF process. The model is validated against the simulation results reported by published results before it is used for further investigations. The results show that there is an excellent agreement between them. Therefore, the rigorous models presented in this chapter for MSF desalination process will be used in Chapters 5, 6, 7 and 8. Different types of MSF simulation and optimisation problems which will be used the course of this work.

# Chapter Five

## Simulation of MSF Desalination Process: Impact of Brine

### Heater Fouling

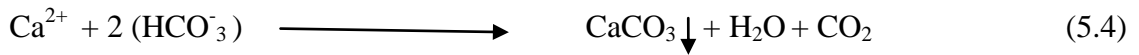
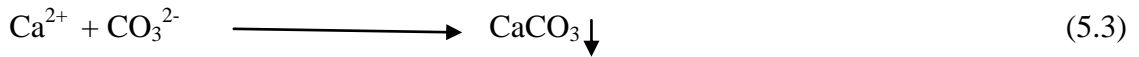
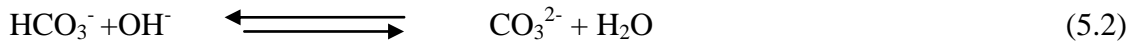
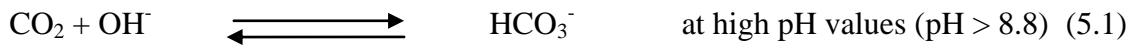
#### 5.1 Introduction

Fouling factor (a measure of scale formation) is one of the many important parameters that affect the operation of MSF processes. Scaling changes the heat transfer coefficient of heat exchangers and thus leads to dynamic adjustment of operating parameters if certain freshwater demand is to be met. In the past several modelling, simulation and optimisation studies of MSF have been carried out using a fixed fouling factor. Based on actual plant data, a simple linear dynamic fouling factor profile is developed which allows calculation of fouling factor at different time (season of the year).

Here, the model presented earlier is used to study the role of a changing brine heater fouling factor with varying seawater temperatures and its effect on the plant performance for fixed water demand, for a given steam and top brine temperature. For fixed water demand and TBT, this work also studies the effect of brine heater fouling factor with seasonal variation of seawater temperature on the performance of MSF desalination process. January is considered to be the starting time (when the fouling factor is minimum) of the process after yearly overhauling.

#### 5.2 Understanding Scaling and Fouling Factor

Calcium carbonate is perhaps the most common scale found in water systems. However, as the temperature increases the solubility of calcium carbonate decreases. Calcium carbonate scale is formed by the combination of calcium ion with either carbonate or bicarbonate ions as follows:



The CO<sub>2</sub> release rates increase with increasing TBT and CaCO<sub>3</sub> deposition and thus the fouling factor is increased. CaCO<sub>3</sub> deposition rates 76.9 – 123.0 gm/ton of distillate at 90 – 110 °C correspond to fouling factor of 0.64 – 1.0 m<sup>2</sup>K/kw (0.000745 to 0.00118 hm<sup>2</sup>K/kcal) respectively (AL-Rawajfeh, 2008). Note, these fouling factor values are very high compared to that used (fouling factor = 0.000186 hm<sup>2</sup> K/kcal, = 0.159 m<sup>2</sup>K/kw) in Rosso et al. (1996) who used anti scaling at seawater temperature =35°C and TBT=90°C.

### 5.3 Seawater Temperature Profile throughout the Year

Figure 5.1 shows the monthly average seawater temperature values in Kuwait throughout the year according to data from Abdel-Jawad and Tabtabaei (1999). It was reported that the seawater temperature can drop as low as 15 °C in January and the high temperature in August is about 35°C.

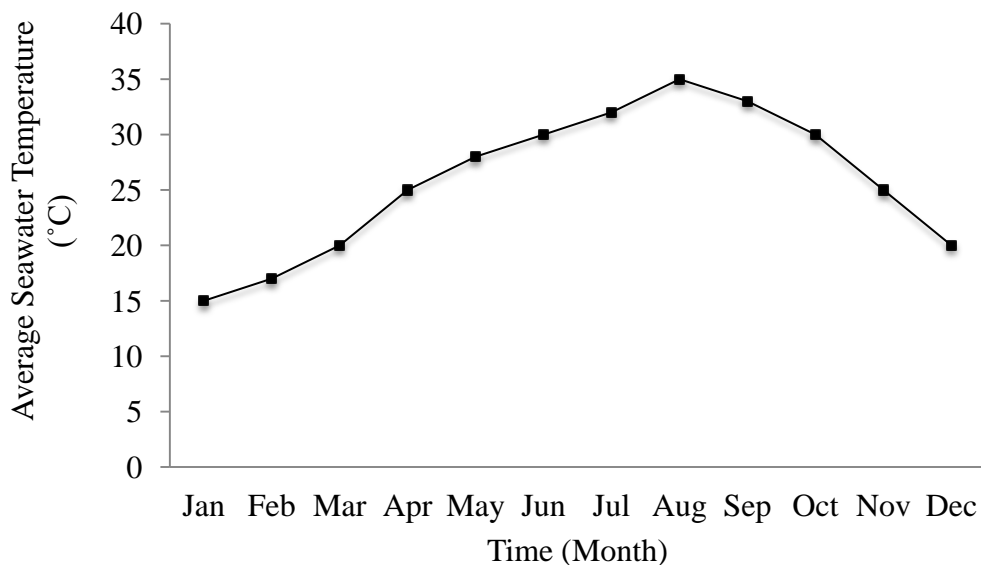


Figure 5.1 Monthly average seawater temperature during the year in Kuwait

## 5.4 Estimation of Dynamic Brine Heater Fouling Profile

Figure 5.2 shows the variation of actual fouling factor ( $\text{m}^2\text{K/kw}$ ) with time (h) of the brine heater section (Hamed et al., 1999, 2000). Using regression analysis, the following linear relationship is obtained (also shown in Figure 5.2). Note, high dosing is required for high TBT to keep the fouling factor at the same level of low dosing and low TBT case.

$$f_{bh} = 2.001 \times 10^{-5} t + 0.0506 \quad (5.5)$$

The constant 0.0506 in Equation (5.5) represents the initial fouling of the brine heater section ( $f_{bh}$ ,  $\text{m}^2\text{K/kw}$ ) at  $t = 0$  (say January, at the beginning of the operation after the plant overhauling). In this work, the trend of brine heater fouling  $f_{bh}$  profile is assumed to be valid for the whole year (i.e. 8000 hours).

Note, the actual fouling data in Figure 5.2 could have been fitted with a polynomial which could be used within the time horizon 0–2000 h. Beyond 2000 h a polynomial based expression predicts abnormally high value of fouling.

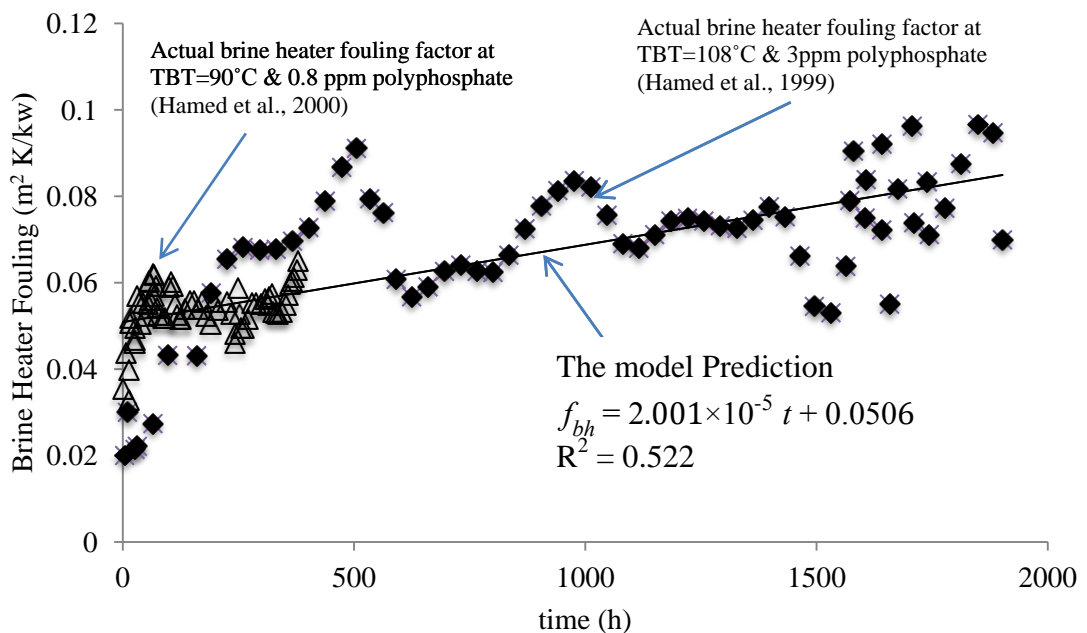


Figure 5.2 Brine Heater Fouling  $f_{bh}$  Profile

## 5.5 Effect of Brine Heater Fouling on the Performance of MSF Process

With the model (validated presented in Chapter 4), a series of simulations have been carried out to study the sensitivity of Brine Heater Fouling ( $f_{bh}$ ) on the performance of MSF processes. In this section, four studies are carried out as shown below.

- For a fixed seawater temperature and fixed steam temperature and consumption, the effects of changing of  $f_{bh}$  on top brine temperature, freshwater demand, brine recycle (R) and performance (GOR) are considered. Also the impact of brine heater fouling factor on the temperature profiles of feed brine and freshwater through all the stages (stage-by-stage) are studied.
- For fixed seawater temperature, Top Brine Temperature (TBT) and freshwater demand, the role of changing of brine heater fouling factor (with and without anti-scaling) on steam consumption and steam temperature are investigated.
- The impact of brine heater fouling factor with varying seawater temperatures on the Top Brine Temperature (TBT), steam consumption, brine recycle (R) and plant performance for fixed freshwater demand and steam temperature are discussed.
- For a fixed freshwater demand and TBT, the role of a changing brine heater fouling factor with seasonal variation of seawater temperatures throughout the year on performance operation parameters such as, brine recycle, steam temperature and consumption of MSF process are presented here.

Note, the configuration investigated and seawater make-up flow rate (F) for all cases in this section refers to the case study reported by Rosso et al. (1996) (Chapter 4). The rejection section consists of three stages and the number of stages in the recovery section is 13. The specifications and constant parameters (except for  $f_{bh}$  & R), which are used in this section, are shown in Table 4.1.



### 5.5.1 Fixed Seawater Temperature, Steam Temperature and Steam Consumption Rate

A series of simulations have been carried out to study the sensitivity of brine heater fouling factor on the performance of MSF desalination process (defined by Equation 4.24 in Chapter 4) for fixed steam temperature ( $T_s = 97^\circ\text{C}$ ), fixed steam consumption ( $W_s = 135000 \text{ kg/h}$ ) and fixed seawater temperature ( $T_{sw} = 35^\circ\text{C}$ ). The brine heater fouling factor  $f_{bh}$  is assumed to vary between 0.0 and  $3.5 \times 10^{-4} \text{ h m}^2 \text{ K/kcal}$  (0.0 - 0.30114  $\text{m}^2\text{K/kw}$ ). The other input data, which are fixed for all cases, are shown in Table 4.1.

Figure 5.3 illustrates the effect of  $f_{bh}$  on TBT and freshwater production rate ( $D_N$ ). It is clear from the Figure that TBT is strongly dependent of the  $f_{bh}$  i.e. as the fouling factor increases the TBT decreases and consequently the freshwater production rate decreases.

The sensitivity of  $f_{bh}$  on recycle brine flow rate (R) is shown in Figure 5.4. It can be seen that for a given steam temperature and consumption, as the  $f_{bh}$  increases the plant has to be operated at higher brine recycle flow rate (R).

Figures 5.5-5.7 represent the effect of the  $f_{bh}$  on temperature profiles of feed, brine and freshwater through all the stages (stage-by-stage). These figures demonstrate that the temperatures ( $T_{Fj}$ ,  $T_{Bj}$ , and  $T_{Dj}$ ) are dependent on  $f_{bh}$ . As  $f_{bh}$  increases, the temperatures decrease. As TBT ( $=T_{Bj0}$ ) is different for different  $f_{bh}$ , each  $T_{Bj}$  profiles are different with wider gap in temperature at the beginning but converging to a single value at the last stage due to the fixed seawater temperature for all cases. This is also true for  $T_{Fj}$  and  $T_{Dj}$  profiles.

Figure 5.8 illustrates the effect of increasing  $f_{bh}$  on plant performance (GOR) with fixed steam temperature and steam consumption rate. Increase in  $f_{bh}$  reduces the overall heat

transfer coefficient and the TBT leading to a reduction in the freshwater production and increasing in the brine recycle (as shown in Figures 5.3 and 5.4) accompanied by a reduction in the performance as shown in Figure 5.8. The production rate decreases by about 5.5%, and therefore the brine recycle flow rate increases by 7% and the performance ratio decreases by 5.5% as the  $f_{bh}$  increases from  $1.84 \times 10^{-4}$  to  $3.5 \times 10^{-4}$   $\text{h m}^2\text{K/kcal}$  (about 90% increase). This will therefore increase the operating cost. Attention should be paid to the brine heater fouling factor since this plays a critical role in the calculation of heat transfer.

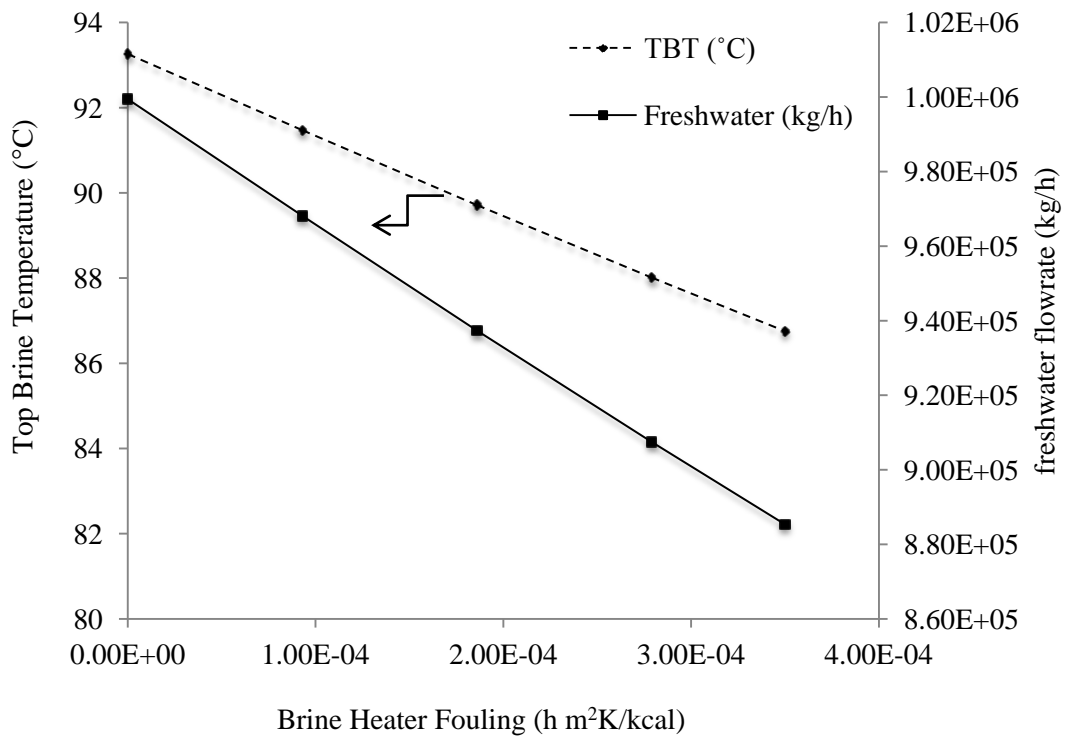


Figure 5.3 Effect of brine heater fouling factor on freshwater flow rate and TBT at fixed steam temperature and fixed steam consumption

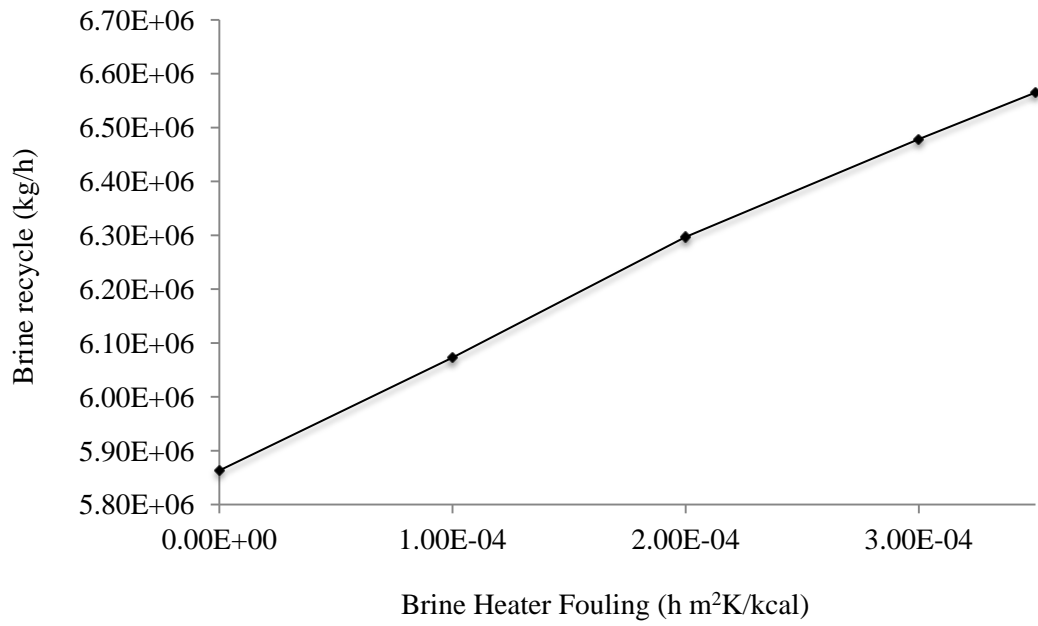


Figure 5.4 Effect of brine heater fouling factor on brine recycle flow rate at fixed steam temperature and fixed steam consumption

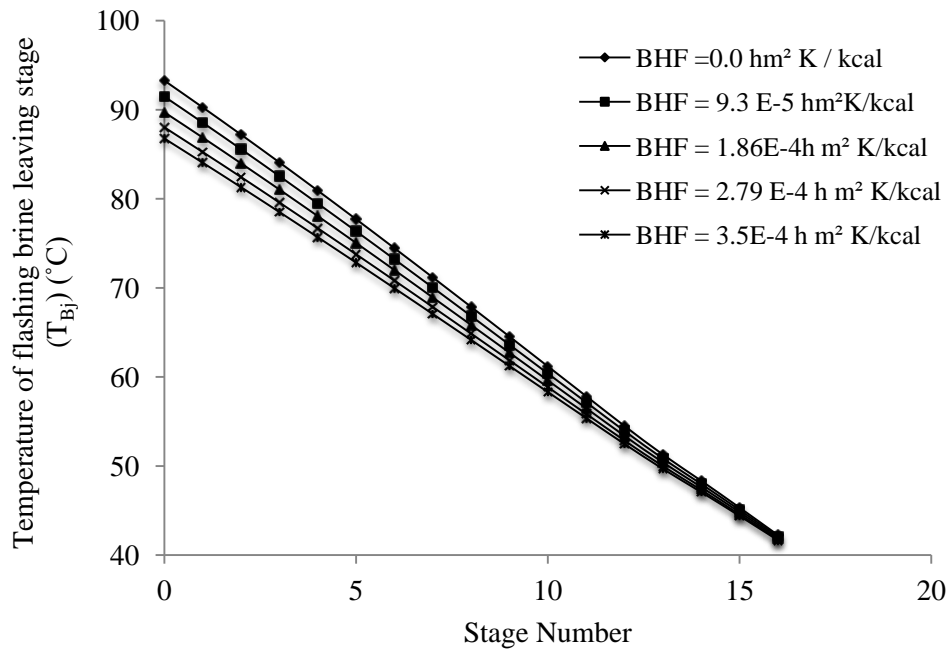


Figure 5.5 Temperature variation of brine through stages

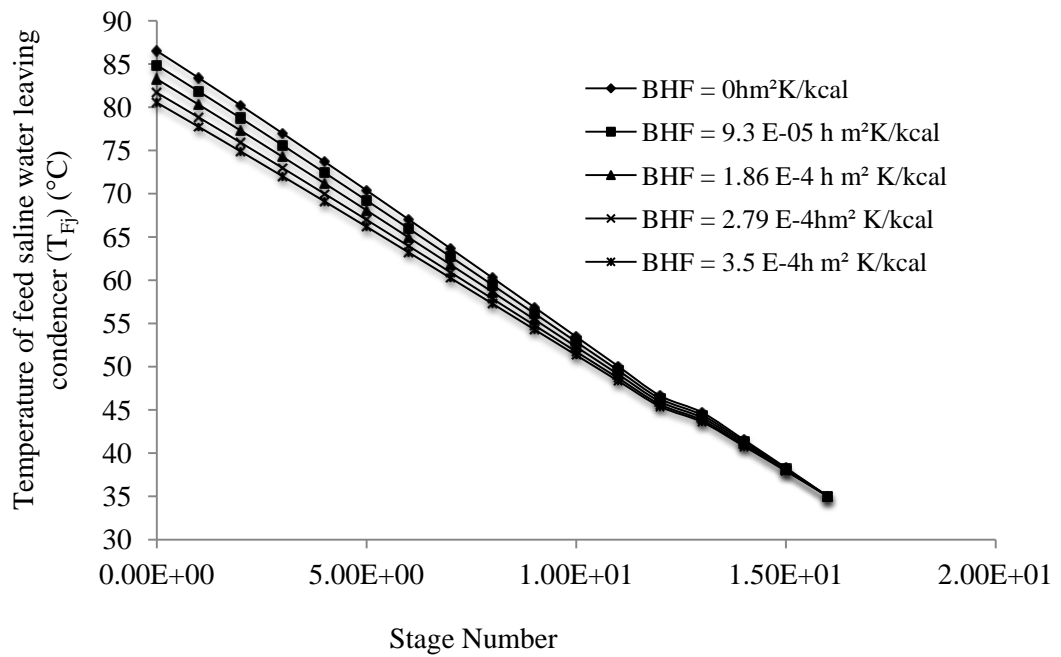


Figure 5.6 Temperature variation of feed saline water through condenser

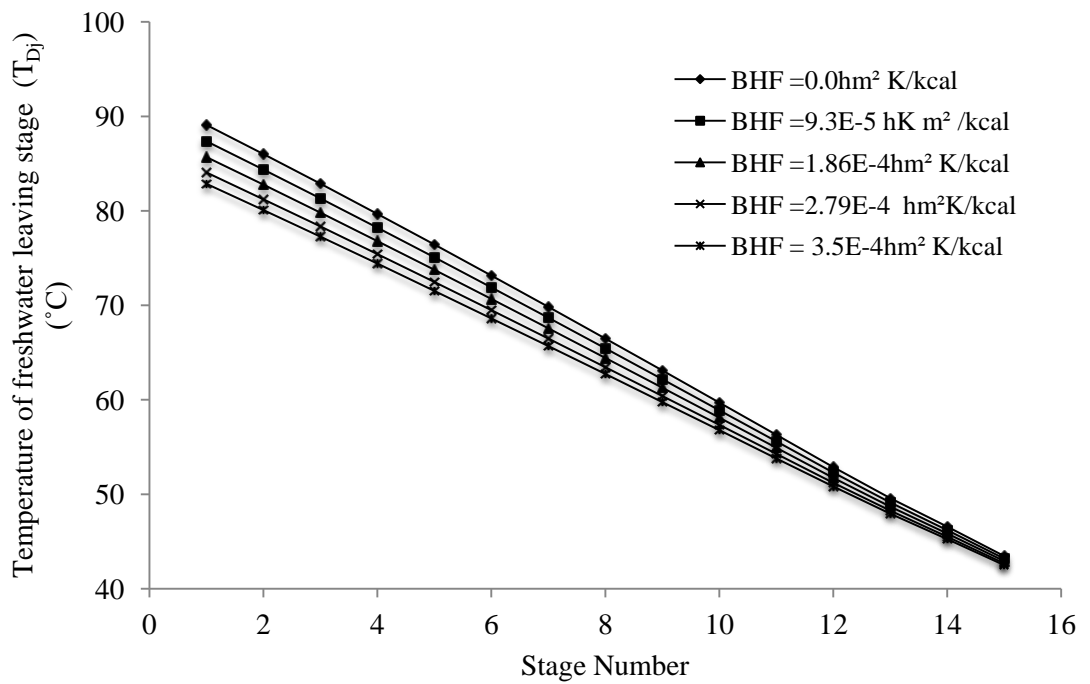


Figure 5.7 Temperature variation of freshwater through stages

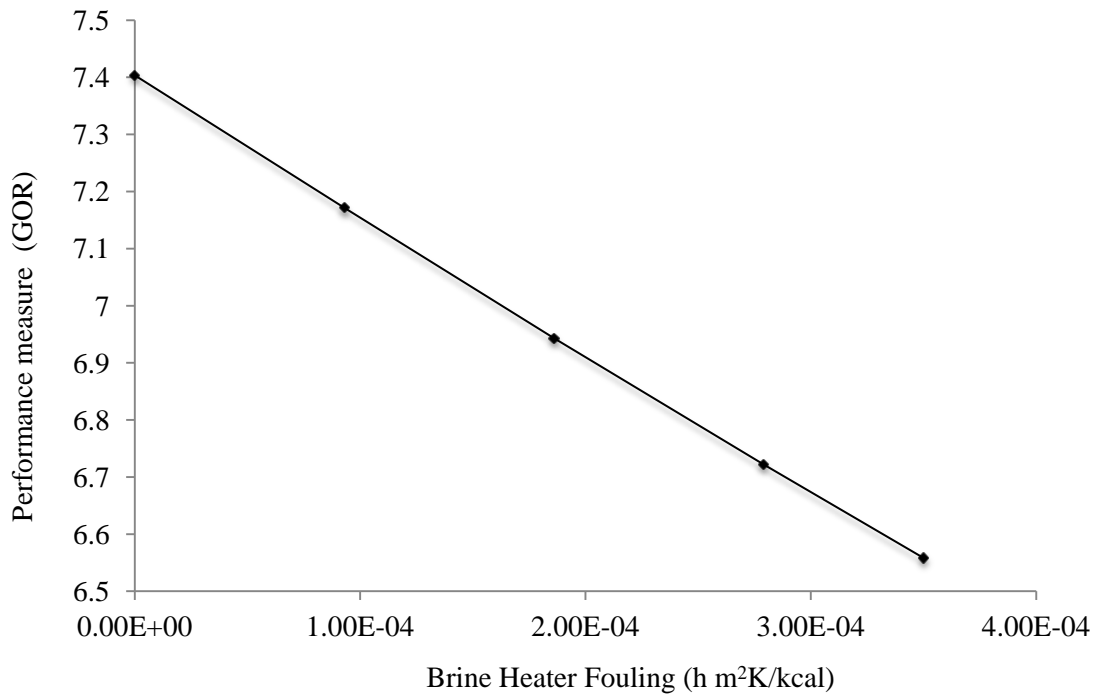


Figure 5.8 Effect of brine heater fouling on plant performance (GOR)

### 5.5.2 Fixed Seawater Temperature, Top Brine Temperature (TBT) and Fresh Water Demand

For the purpose of better understanding of the effect of CaCO<sub>3</sub> deposit (without the use of anti-scalant) further simulation is carried out to study of sensitivity of  $f_{bh}$  on the performance of the MSF process with fixed seawater temperature ( $T_{sw} = 35^{\circ}\text{C}$ ), fresh water demand ( $D_N = 9.43 \times 10^5 \text{ kg/h}$ ), TBT =  $90^{\circ}\text{C}$  and brine recycle ( $R = 6.36 \times 10^6 \text{ kg/h}$ ).

Figure 5.9 shows the effect of  $f_{bh}$  on the steam temperature ( $T_s$ ) and steam flow rate ( $W_s$ ), while the  $f_{bh}$  increases from  $1.84 \times 10^{-4}$  (Rosso et al., 1996) to  $7.53 \times 10^{-4} \text{ h m}^2 \text{ K/kcal}$  (AL-Rawajfeh, 2008). About 1.5% increase in steam consumption and corresponding increase in steam temperature by 12% are noted. According to Equation (4.24) the performance ratio decreases also by 1.75 %.

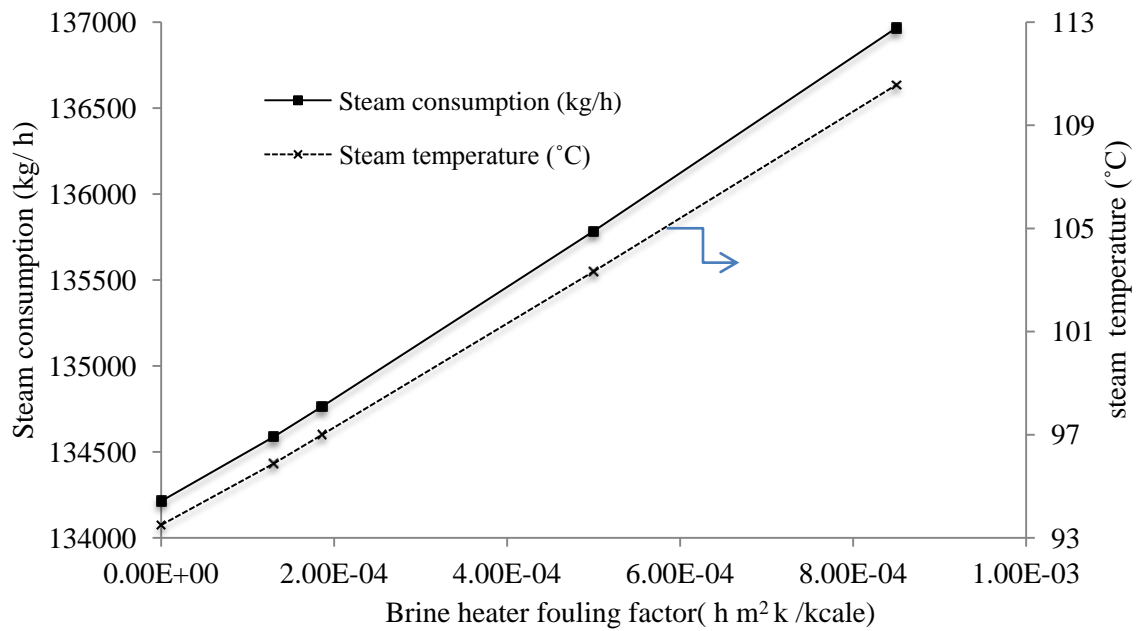


Figure 5.9 Effect of brine heater fouling factor on steam consumption and steam temperature

### 5.5.3 Variable Seawater Temperature, Fixed Freshwater Demand and Fixed Steam Temperature

The brine heater fouling is assumed to vary between 0.0 and  $3.53 \times 10^{-4}$   $\text{hm}^2\text{K/kcal}$  (0 – 0.3  $\text{m}^2\text{K/kw}$ ) and the seawater temperature from 20 and 35°C (Abdel-Jawad and AL-Tabtabeal, 1999). The sensitivity of brine heater fouling ( $f_{bh}$ ) on the performance of the MSF processes with fixed steam temperature ( $T_s = 97^\circ\text{C}$ ) and fixed freshwater demand ( $D_N = 9.45 \times 10^5$  kg/h) are shown in Figures 5.10 – 5.15.

Figure 5.10 represents the effect of  $f_{bh}$  on TBT with changing seawater temperatures from winter to summer season. For a given  $f_{bh}$ , TBT decreases as seawater temperature increases. However, interestingly it can be noted that the plant can operate a lower TBT

at higher brine heater fouling producing the same amount of freshwater by adjusting parameters such as brine recycle discussed below. For a given seawater temperature, TBT decreases as  $f_{bh}$  increases for fixed steam temperature.

Figure 5.11 illustrates the effect of  $f_{bh}$  on steam consumption. It is clear from the figure that the steam consumption increases as the fouling factor and the seawater temperature increase. This is required to maintain the freshwater production at the desired level. Also note, higher TBT requires a lower amount of steam at any seawater temperature (Figures 5.10 and 5.11). It is interesting to reflect that when seawater temperature is fixed, steam temperature needs to increase together with steam consumption (Figure 5.9) with increasing  $f_{bh}$ . However, when seawater temperature increases, steam consumption needs to be increased with increasing  $f_{bh}$  but steam temperature can be kept constant (Figure 5.11).

Figure 5.12 demonstrates that the amount of brine recycling  $R$  increases with increased brine heater fouling and seawater temperature.

Figure 5.13 and 5.14 show the effect of changing of brine heater fouling factor on temperature of feed brine inlet to brine heater ( $T_{Fj}$ ) and total feed of brine ( $W_R$ ) in the recovery section for a given seawater temperature. At any seawater temperature (say 35 °C). It can be seen that with increasing  $f_{bh}$ , total feed of brine ( $W_R$ ) will increase,  $T_{Fj}$  will decrease. Therefore the plant has to be operated at higher steam consumption (Figure 5.11) to raise the feed temperature to the required TBT (Figure 5.10) with fixed freshwater demand.

Comparison of Figures 5.10 – 5.14 reveal that at any seawater temperature, increase of  $f_{bh}$  (i) decreases TBT, (ii) increases steam consumption and (iii) increases brine

recycling (iv) decreases  $T_{Fj}$  (iiv) increases  $W_R$  to maintain the freshwater production at the desired level.

Figure 5.15 shows the effect of increasing brine heater fouling factor on the performance ratio. Here, the reduction in the TBT results in increases in the steam flow rate as shown in Figures 5.11 and 5.15, accompanied by a reduction in the performance. For example at seawater temperature  $35^\circ\text{C}$  the amount of steam increases by 14%, and the performance ratio decreases by 9% as the brine heater fouling changes from  $1.86 \times 10^{-4} \text{ m}^2\text{hK/kcal}$  to maximum value. Furthermore, the brine recycle rate will increase at about 15%, and TBT decreases by  $4.15^\circ\text{C}$ .

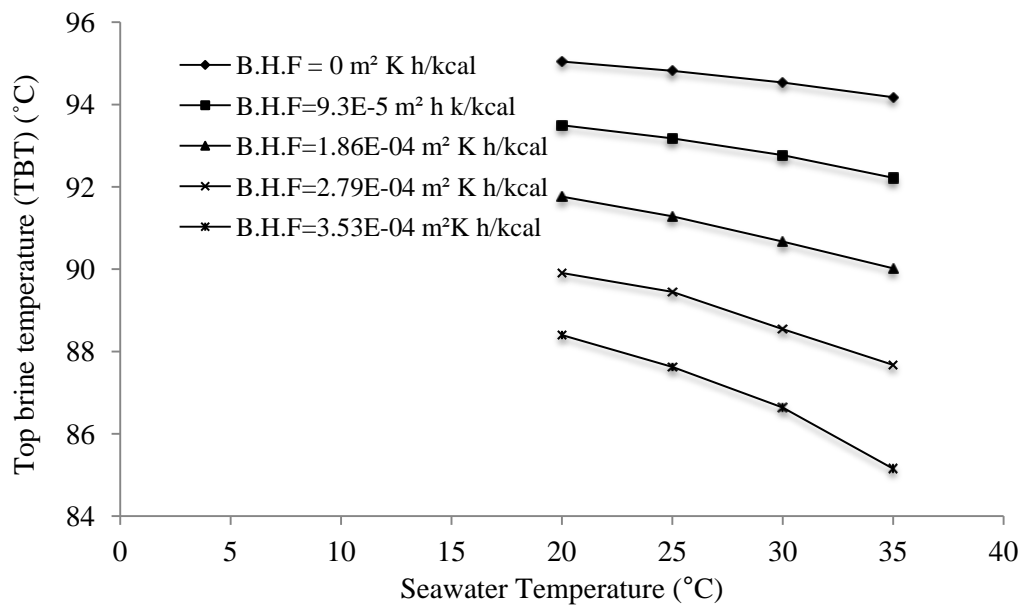


Figure 5.10 Effect of the brine heater fouling on TBT



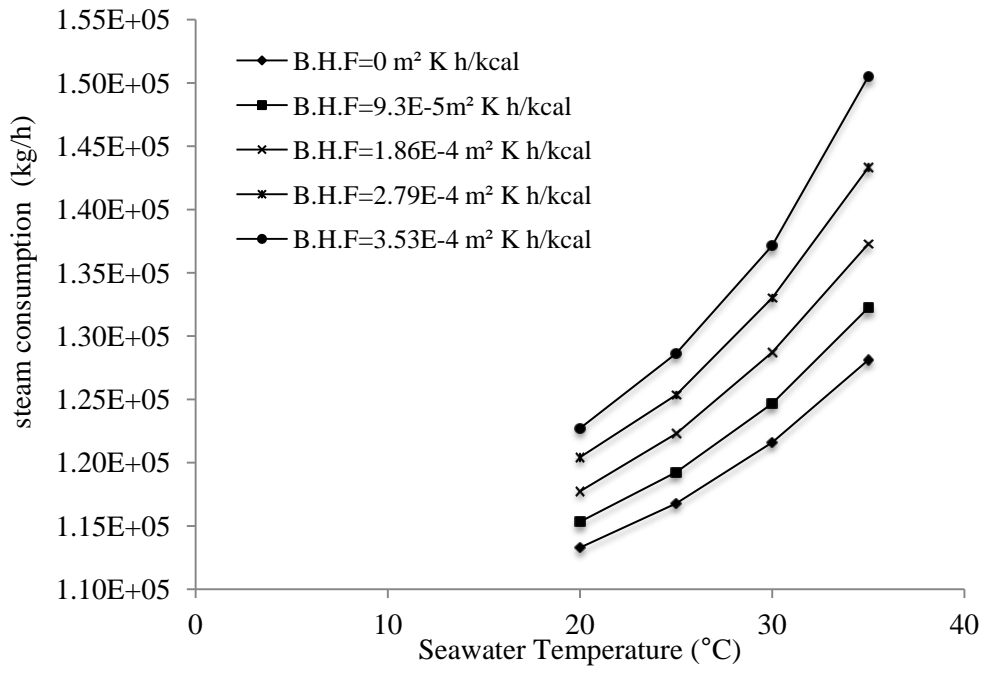


Figure 5.11 Effect of brine heater fouling on steam flow rate

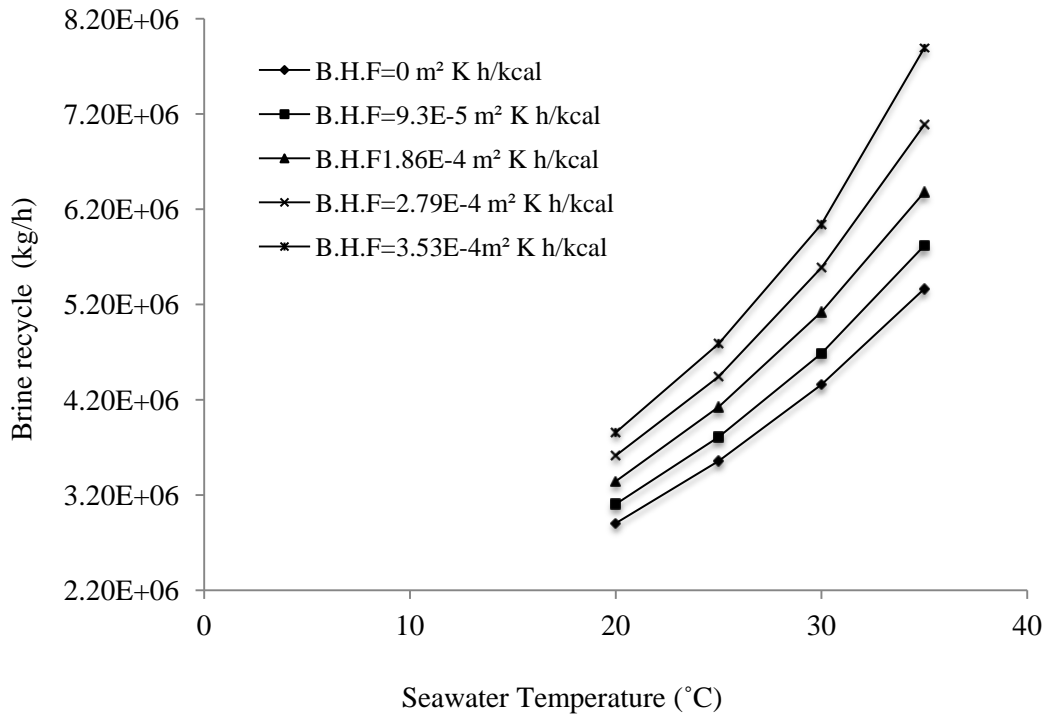


Figure 5.12 Effect of brine heater fouling on brine recycle flow rate

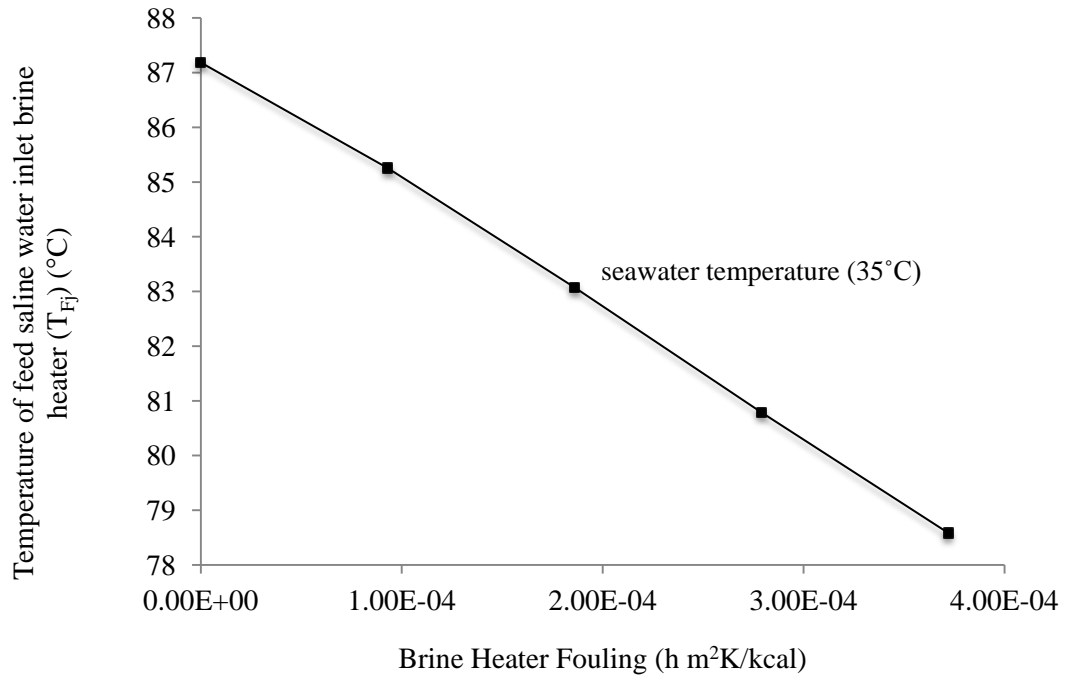


Figure 5.13 Effect of brine heater fouling on temperature of feed saline water inlet brine heater

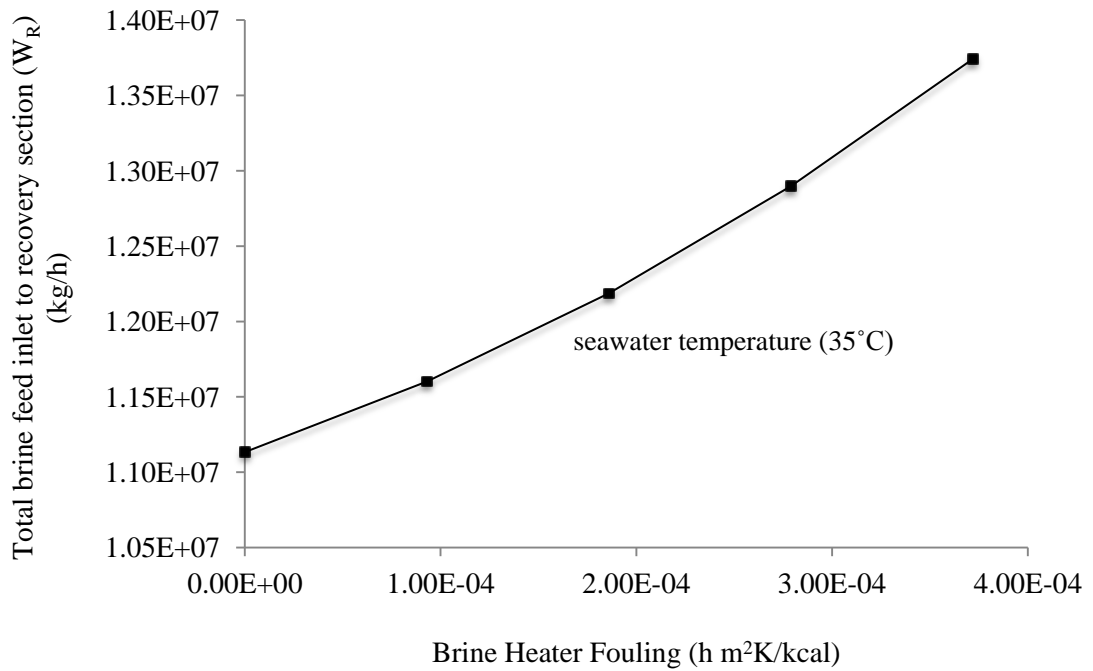


Figure 5.14 Effect of brine heater fouling on total brine feed inlet to recovery section

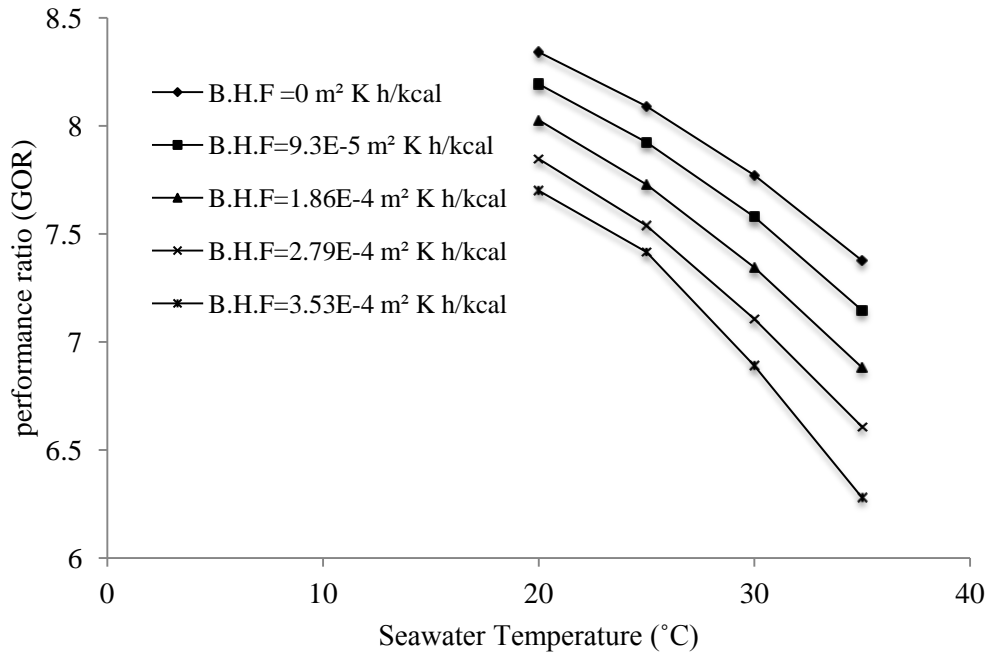


Figure 5.15 Effect of brine heater fouling on performance

#### 5.5.4 Fixed TBT and Fixed Freshwater Demand throughout the Year

The effect of changing the brine heater fouling factor with time throughout the year on the performance of MSF desalination process with fixed freshwater demand ( $D_N = 945000$  kg/h), top brine temperature (TBT =  $90^\circ\text{C}$ ) and reject seawater ( $C_W = 5.62 \times 10^6$  kg/h) is studied here. The average seawater temperature variation during the year from January to December was taken from (Abdel-Jawad and AL-Tabtabaei, 1999) as shown in Figure 5.1. The increasing of the fouling factor in the brine heater  $f_{bh}$  with time (t, h) is calculated using equation (5.5).

Figure 5.16 represents the variation of steam temperature during the year. The results clearly show that the steam temperature is strongly affected with brine heater fouling factor to reach the required top brine temperature (TBT= $90^\circ\text{C}$ ) and fresh water ( $D_N = 9.45 \times 10^5$  kg/h) rather than seawater temperature. Even though the seawater temperature

decreases at the end of year, the highest steam temperature required is noted in December.

The variation of steam flow rate, and brine recycling through the year are shown in Figures 5.17, 5.18, respectively. In this case, at fixed top brine temperature and fixed freshwater demand, both of them are dependent on seawater temperature rather than brine heater fouling factor. It is seen that both steam flow rate and brine recycle flow rate are increased with increased seawater temperature and then they decrease as the seawater temperature decreases, even the fouling factor is increased. However, the maximum flow rates for both are in August at maximum seawater temperature of about 35°C. The effect of  $f_{bh}$  and seawater temperature on the performance ratio (GOR) is shown in Figure 5.19. It is seen that performance depends on seawater temperature, as it increases performance is decreased with the increase in seawater temperature.

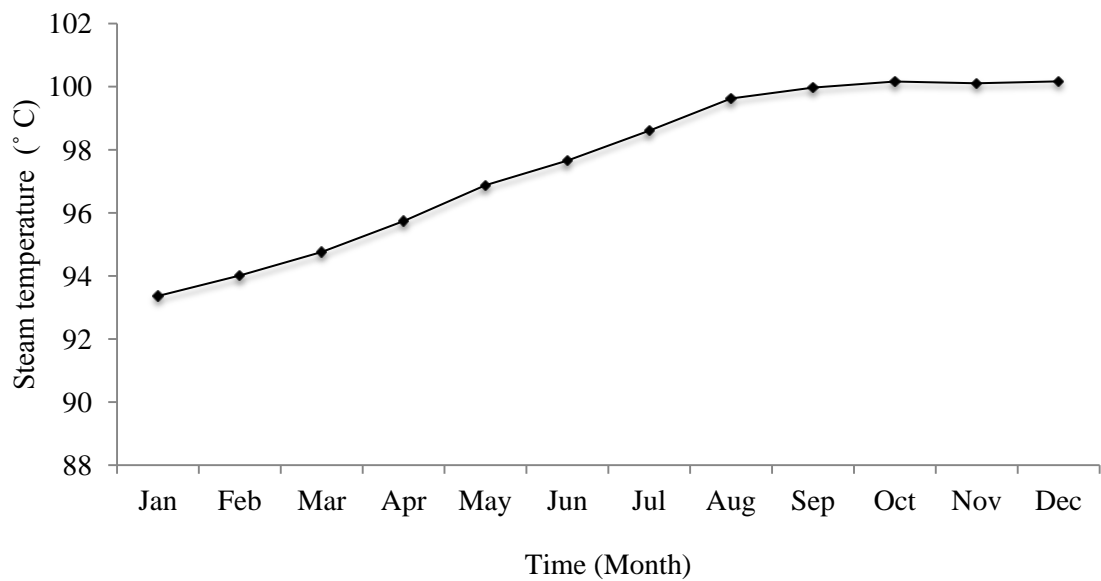


Figure 5.16 Variation of steam temperature throughout the year

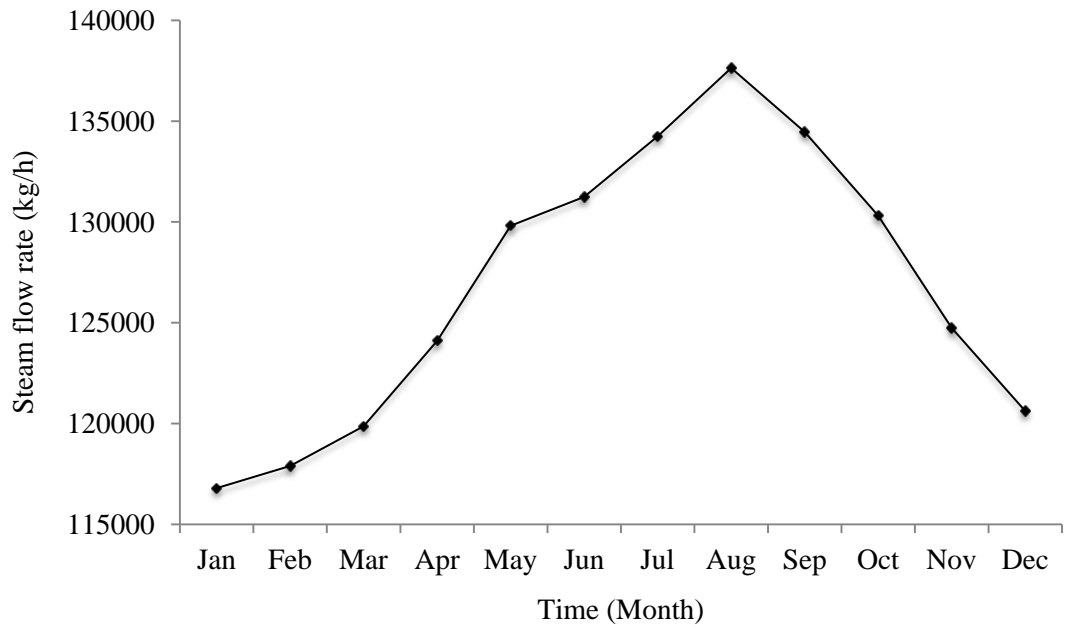


Figure 5.17 Variation of steam flow rate throughout the year

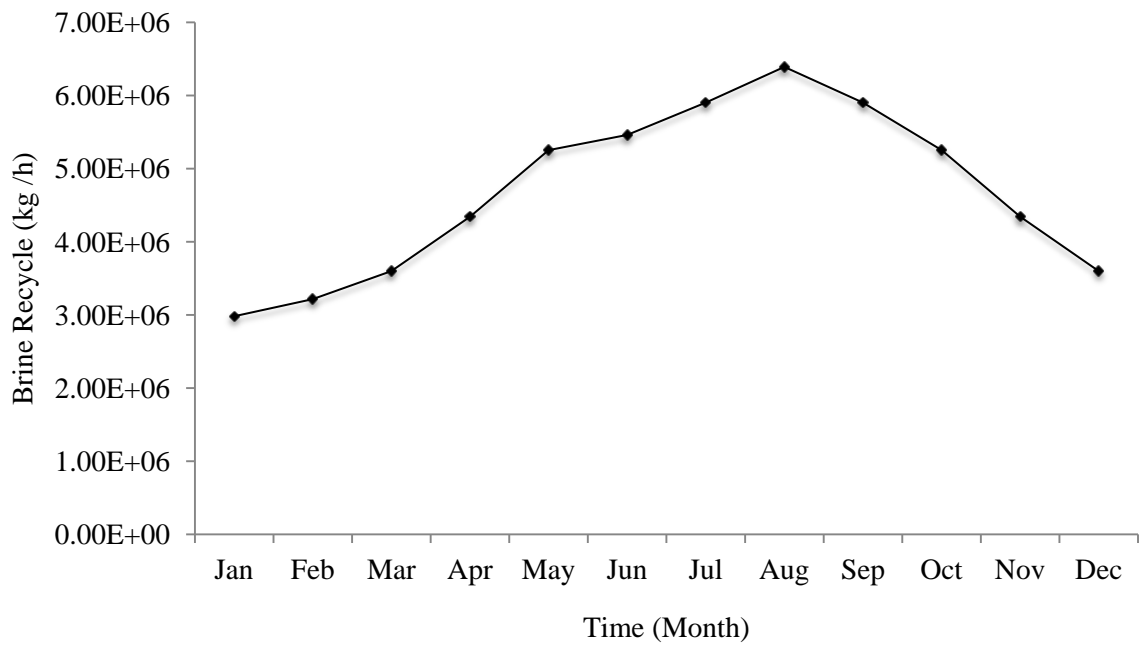


Figure 5.18 Variation of brine recycle throughout the year

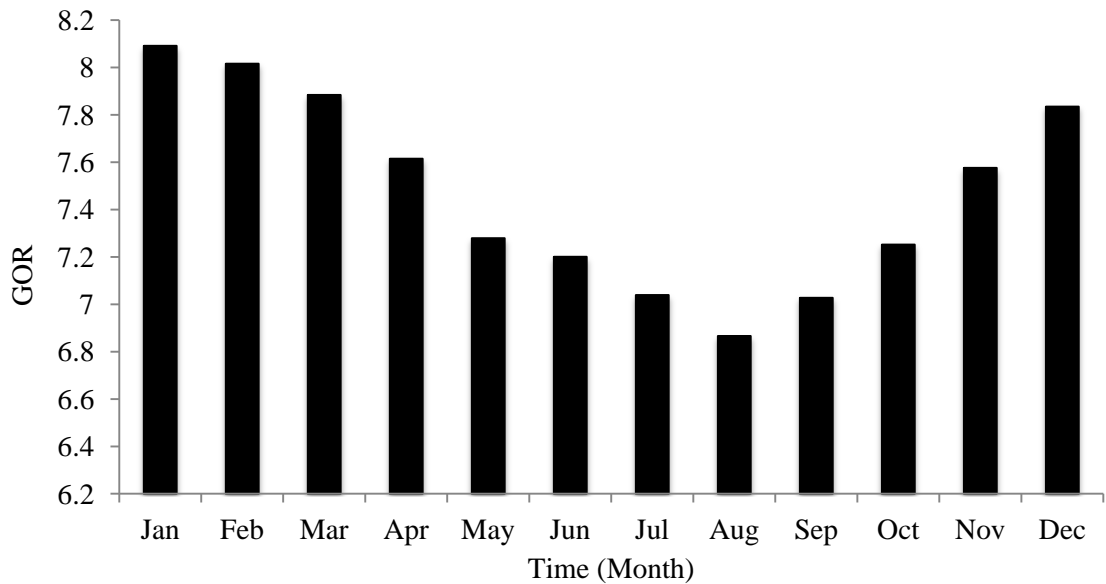


Figure 5.19 Variation of performance (GOR) throughout the year

## 5.6 Conclusion

A simple linear dynamic brine heater fouling factor profile is developed based on actual MSF plant operation data. Sensitivity analysis of brine heater fouling and seawater temperature on the production of fresh water and other operating parameters such as top brine temperature, steam consumption, brine recycling and performance ratio are presented.

It can be seen from the results that increase of brine heater fouling by (90%) will cause a reduction in overall heat transfer coefficient and consequentially lowers TBT and higher R with fixed seawater temperature. This leads to a decrease in the fresh water production by (5.5%). The simulation also shows that for demand fixed water and constant TBT, the higher the brine heater fouling factor the higher steam consumption and higher the steam temperature.

The simulation results also clearly show that it is possible to supply fixed freshwater demand throughout the year with changes in seawater temperature and brine heater fouling. Interesting observation shows that for a given brine heater fouling the top brine temperature decreases as seawater temperature increases. However, interestingly it can

be noted that the plant can be operated successfully at lower top brine temperature (TBT) with higher steam consumption and higher brine recycling.

Steam temperature is strongly affected with brine heater fouling factor rather than seawater temperature. Even though the seawater temperature decreases at the end of year, the highest steam temperature required is noticed in December at maximum brine heater fouling factor. Both steam flow rate and brine recycle flow rate increase with increased seawater temperature and decrease as the seawater temperature decreases, even the fouling factor is increased. However, the maximum flow rates for both are in August at maximum seawater temperature.

Even in summer time, the MSF process could fulfil the demand of fresh water by operating with lower top brine temperature, higher steam, higher brine recycle flow rate and lower performance, but this will reduce scale formation rate and therefore the frequency for shutdown for cleaning will be lower and therefore the cost of maintenance will be lower. In this work, the performance ratio (GOR) does not reflect the maintenance cost.

In this chapter, for a given design and fixed freshwater demand the sensitivity of operating parameters such as top brine temperature, steam temperature and brine recycling (R) with variable brine heater fouling and seawater temperature on plant performance of MSF desalination process were studied. The simulation shows significant variation in the amount of the total brine recycle ( $W_R$ ) ( $W_R = R+F$ ) and steam temperature when the operating condition such as seawater temperature and brine heater fouling factor are changed (for all cases). The next reasonable step would be to formulate a suitable optimization problem where design and the above operating parameters (R and F) are simultaneously optimized while minimize the total operation costs of the MSF desalination process.

# Chapter 6

## Effect of Brine Heater Fouling on Optimal Design and Operation of MSF Process

### 6.1 Introduction

The accurate calculation of the overall heat transfer coefficient (which is also a function fouling factor) is of substantial importance in MSF processes. Scaling leads to dynamic adjustment of operating conditions if certain freshwater demand is to be met. Rather than playing with an operating plant to determine the new set points it is always economical to determine the optimal set points based on accurate process model and optimization techniques before the operating set-points are applied in the actual plant (Tanvir and Mujtaba, 2008a; Mussati et al., 2004). However, in the past several modelling, simulation and optimisation studies of MSF process have been carried out using fixed fouling factor for the brine heater (Tanvir and Mujtaba, 2008a; Mussati et al., 2004; EL–Dessouky and Ettouney, 2002).

In this chapter, the role of changing brine heater fouling factor with varying seawater temperatures (during a year from January to December) and its effect on the plant performance and the operating costs for fixed water demand and fixed top brine temperature are studied. The total monthly operation cost of the MSF desalinations required, are minimised while the operating parameters such as make up, brine recycle flow rate and steam temperature are optimised.. Two cases with different TBT and anti-scaling dosages are considered in this work: (a) TBT (90°C) and anti-scaling dosages (0.8 ppm) (b) TBT (108°C) and anti-scaling dosages (3ppm).



The optimal design and operation of MSF desalination process for different monthly freshwater demand throughout the year and with seasonal variation in seawater temperature and brine heater fouling is also studied.

Note, the anti-scaling agent addition is not considered in the optimisation decision variables due to shortage experimental data which could show the behaviour of fouling factor with different dosage of anti-scaling (ppm) and different TBT during the whole year.

## 6.2 Fixed Design and Fixed Freshwater Demand Throughout the Year

### 6.2.1 Optimization Problem Formulation

The optimization problem is described below.

Given: Fixed number of stages, heat exchangers areas, design specification of each stages, seawater flow and fixed freshwater demand.

Optimize: Steam temperature ( $T_s$ ), Recycled brine flow rate ( $R$ ), Make-up seawater ( $F$ ).

Minimize: The total monthly operating cost (TOC) or maximize GOR

Subject to: Any constraints.

The Optimization Problem (OP1) can be described mathematically by:

$$\begin{array}{ll}
 \text{OP1} & \begin{array}{l} \text{Min} \\ T_s, R, F \end{array} \qquad \text{TOC} \\
 \text{s.t.} & f(x,u,v) = 0 \text{ (model equations)} \\
 & D_N = D_N^* \\
 & \text{TBT} = \text{TBT}^* \\
 & (92^\circ\text{C}) T_s^L \leq T_s \leq T_s^U (115^\circ\text{C}) \\
 & (2 \times 10^6 \text{ kg/h}) R_L \leq R \leq R_U (7.55 \times 10^6 \text{ kg/h})
 \end{array}$$

$$(2 \times 10^6 \text{ kg/h}) F_L \leq F \leq F_U (7.55 \times 10^6 \text{ kg/h})$$

Where,  $D_N$  is the total amount of fresh water produced and  $D_N^*$  is the fixed water demand ( $9.45 \times 10^5$  kg/h). TBT\* is the fixed TBT (90 or 108°C). Subscripts  $L$  superscripts  $U$  refer to lower and upper bounds of the parameters. The model equations presented in Chapter 4 can be described in a compact form by  $f(x,u,v) = 0$  where  $x$  represents non linear sets of all algebraic variables,  $u$  is the optimization variable, such as steam temperature, recycle flow rate, etc.,  $v$  is a set of constant parameters such as number of stages, heat exchangers areas, etc.

Total Annual Operating Cost can be described (Helal et al., 2003):

$$\text{Where, } C1 \text{ (Steam cost, \$/year)} = 8000 W_s [(T_s - 40) / 85] \text{ (0.00415)} \quad (6.1)$$

$$C2 \text{ (Chemical cost, \$/year)} = 8000 [\sum (\text{Unit cost (\$/g) Dosing rate (ppm)}) (F/D_b)] \quad (6.2)$$

Where  $D_b$  = density of brine ( $\text{kg/m}^3$ ).

Chemical cost ( $\$/\text{kg}$ ) and dosing rate (ppm) (Nafey et al., 2006) is given in Table 6.1

$$C3 \text{ (Power cost, \$/year)} = 8000 [D_N / 1000] 0.109 \quad (6.3)$$

$$C4 \text{ (Maintenance and spares cost, \$/year)} = 8000 [D_N / 1000] 0.082 \quad (6.4)$$

$$C5 \text{ (Labour cost, \$/year)} = 8000 [D_N / 1000] 0.1 \quad (6.4)$$

$$\text{TOC (Total Monthly Operating Cost, \$/Month)} = (C1 + C2 + C3 + C4 + C5) / 12 \quad (6.6)$$

Table 6.1 Pre-treatments for make-up

Chemical	Unit cost ( $\$/\text{kg}$ )	Dosing rate (ppm)
Sulphuric acid, $\text{H}_2\text{SO}_4$	0.504	24.2
Caustic Soda, NaOH	0.701	14
Anti- scaling	1.9	(0.8 or 3)
Chlorine	0.482	4

### 6.2.2 Case Study

Here the effect of dynamic brine heater fouling on the performance of MSF process (in terms of  $GOR = D_N / W_S$  and operating costs) is studied for a fixed freshwater demand  $D_N = 9.45 \times 10^5$  kg/h. Two cases are considered. In Case 1, TBT = 90°C with anti-scaling (polyphosphates) rate of 0.8 ppm is considered. In Case 2, TBT = 108°C with anti-scaling rate of 3 ppm is considered. Note, the concentration (ppm) of H<sub>2</sub>SO<sub>4</sub>, Caustic Soda and Chlorine are constant for both case studies.

The configuration investigated in this work refers to the case study reported by Rosso et al. (1996) (Chapter 4). The total number of stages is 16, with 13 stages in the recovery section and 3 in the rejection section. The specifications and constant parameters (except for  $f_{bh}$ ), which are used in this work, are shown in Table 4.1. Seasonal variation of seawater temperature is shown in Tables 6.2 and 6.3 (based on Abdel-Jawad and AL-Tabtabael, 1999). For different seawater temperatures (at different seasons) corresponding brine heater fouling factors are calculated using equation (5.5). The optimization problem OP1 is then solved for each  $T_{sw}$  and  $f_{bh}$ . Tables 6.2 and 6.3 also show the optimal monthly operating cost, chemical required, steam consumption and the operating parameters such as make up, brine recycle flow rate, steam temperature and GOR throughout the year. Note, in this section December is assumed to be overhauling period.

Table 6.2 Summary of optimization results (Case 1)

Month	$T_{sw}$ °C	$f_{bh}$ m <sup>2</sup> K/kw	F×10 <sup>6</sup> kg/h	R×10 <sup>6</sup> kg/h	$T_s$ °C	Anti-scalant kg/Month	TOC×10 <sup>5</sup> \$/Month	Steam kg/h	GOR
Jan	15	0.065	3.91	4.74	93.61	2252.21	4.48	116955	8.08
Feb	17	0.078	4.09	4.78	94.02	2360.73	4.54	118095	8.00
Mar	20	0.093	4.40	4.85	94.43	2539.92	4.65	120122	7.86
Apr	25	0.108	5.02	4.98	95.24	2892.04	4.85	124260	7.60
May	28	0.121	5.48	5.05	95.65	3159.01	5.01	127307	7.42
Jun	30	0.135	5.80	5.13	96.16	3341.00	5.12	12947	7.28
Jul	32	0.150	6.15	5.21	96.78	3542.02	5.25	132241	7.14
Aug	35	0.164	6.75	5.35	97.45	3891.41	5.47	136718	6.91
Sep	33	0.178	6.34	5.26	97.54	3652.02	5.34	133739	7.06
Oct	30	0.192	5.79	5.13	97.48	3340.03	5.18	129986	7.27
Nov	25	0.206	5.02	4.98	97.22	2892.01	4.94	124555	7.58
Total						33862.25	54.83		

Table 6.3 Summary of optimization results (Case 2)

Month	$T_{sw}$ °C	$f_{bh}$ m <sup>2</sup> K/kw	F×10 <sup>6</sup> kg/h	R×10 <sup>6</sup> kg/h	$T_s$ °C	Anti-scalant kg/Month	TOC×10 <sup>5</sup> \$/Month	Steam kg/h	GOR
Jan	15	0.065	2.45	4.40	110.3	5309.12	4.52	98823	9.56
Feb	17	0.078	2.47	4.42	110.7	5557.53	4.57	99535	9.49
Mar	20	0.093	2.75	4.45	111.0	5952.94	4.64	100677	9.38
Apr	25	0.108	3.09	4.52	111.4	6685.95	4.78	102839	9.18
May	28	0.121	3.32	4.57	111.8	7177.26	4.87	104345	9.05
Jun	30	0.135	3.48	4.60	112.1	7529.04	4.94	105457	8.96
Jul	32	0.150	3.65	4.64	112.5	7902.82	5.01	106657	8.86
Aug	35	0.164	3.94	4.71	112.9	8520.52	5.13	108625	8.69
Sep	33	0.178	3.75	4.67	113.1	8098.64	5.06	107344	8.80
Oct	30	0.192	3.48	4.60	113.2	7529.66	4.97	105584	8.95
Nov	25	0.206	3.04	4.52	113.1	6687.45	4.84	103050	9.17
Total						76950.56	53.33		

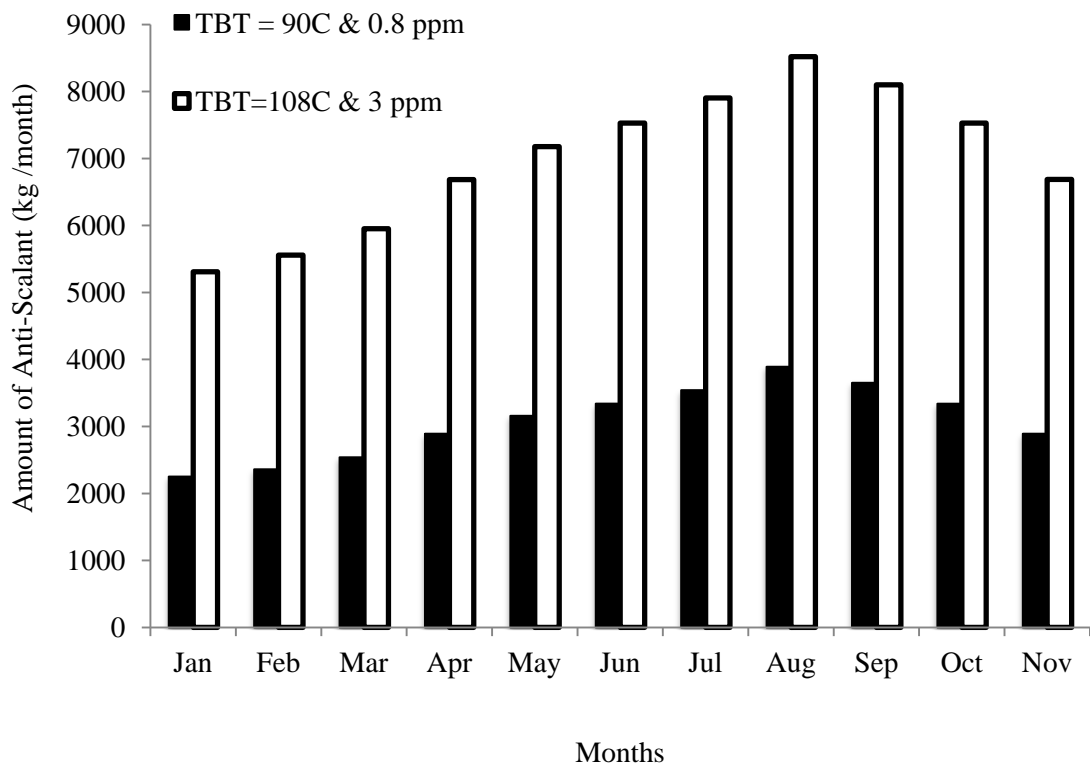


Figure 6.1 Variation of optimal monthly anti-scalant consumption throughout the year

From January onward  $f_{bh}$  increases and so does the  $T_{sw}$ . This consequently demands higher  $F$  and  $R$  and steam consumption ( $W_s$ ) leading to higher TOC (monthly) for both cases. However, with decrease in  $T_{sw}$  from August onward,  $F$ ,  $R$  and TOC decrease (even though  $f_{bh}$  kept on increasing). Clearly, the effect of  $T_{sw}$  on  $F$ ,  $R$  and TOC is more pronounced compared to the effect of  $f_{bh}$ . Note, the highest total TOC is noted in August at the maximum yearly  $T_{sw}$  ( $35^\circ\text{C}$ ). For all cases,  $F$  and  $R$  vary significantly. Low TBT required higher  $R$  and  $F$  (compare the results in Table 6.2 with 6.3). Although there is a decrease (only slightly) in steam cost for Case 1, the total chemical cost is higher due to higher requirement of  $F$ . The overall optimization results also show higher performance ratio GOR is achieved with higher TBT and chemical additives (see amount of anti-scale in Figure 6.1). Although the operating cost is slightly lower in

Case 2 (about 2.6%), the residual anti-scaling concentration present is higher in the brine blow down. It is expected that the impact on marine environment will be higher if this blow down is discharged to the sea without treatment.

Finally, note that at the same  $T_{sw}$  of 25 °C in April and November, although  $F$  and  $R$  remain the same,  $W_s$ ,  $T_s$  and TOC increase due to increase in  $f_{bh}$ .

### **6.3 Variable Design and Freshwater Demand throughout the Year**

Most recently, a number of authors studied optimization using gPROMS software technique, but their works were limited to investigating optimal design and operation for fixed fouling factor and fixed freshwater demand throughout the year (Mussati et al., 2004; Tanvir and Mujtaba, 2008a). However, in reality the freshwater demand (Alvisi et al., 2007) and also the seawater temperature (Adel-Jawad and AL-Tabtabael, 1999) vary throughout the year. This section focuses on the role of changing fouling factor with monthly variation in seawater temperatures and freshwater demand/consumption during a year from January to December and their effect on the total monthly cost of MSF desalination process. Top brine temperature is considered to be fixed. The total monthly cost of the MSF desalination process required is selected to minimise while optimising the design and operating parameter such as total number of stages, seawater make up and brine recycle flow rate.

#### **6.3.1 Optimization Problem Formulation**

The optimization problem is described below.

Given: the MSF plant configurations, fixed design specification of each stage, seawater flow, top brine temperature (TBT), variable average monthly seawater temperature, and monthly freshwater demand.

Determine: the optimum total number of stages, optimum recycled brine flow rate  $R$ ; make-up seawater,  $F$  throughout the year.

Minimize: the total monthly cost (TMC).

Subject to: process constraints.

The Optimization Problem (OP2) is described mathematically as:

$$\begin{array}{ll}
 \text{OP2} & \text{Min} \\
 & \text{R, F, N} \\
 & \text{TMC} \\
 \text{s.t.} & f(x, u, v) = 0 \text{ (model equations)} \\
 & \text{TBT} = \text{TBT}^* \\
 & (2 \times 10^6 \text{ kg/h}) R_L \leq R \leq R_U (7.55 \times 10^6 \text{ kg/h}) \\
 & (2 \times 10^6 \text{ kg/h}) F_L \leq F \leq F_U (7.55 \times 10^6 \text{ kg/h})
 \end{array}$$

Where, is TBT\* is the fixed top brine temperature (90°C).

The objective function TMC is given by  $TMC = \frac{TAC}{12}$  where, TAC (Total Annual Cost) is defined as:

$$TAC (\$/\text{year}) = CPC + TOC \quad (6.7)$$

Where,

$$CPC (\text{MSF Annualised Capital Cost, } \$/\text{year}) = 182 \times 8000 N^{0.65} \quad (6.8)$$

The details of TOC are presented in section 6.2. The optimization problem OP2 is solved for each  $T_{sw}$ , (representing a month of the year)  $f_{bh}$  and freshwater demand/consumption. The optimisation problem presented OP2 minimises the total monthly cost while optimising R and F meeting the demand. Note, the steam temperature is not optimised here but is calculated.

### 6.3.2 Results and Discussions

For different total number of stages, here, the total monthly cost of the process is minimised by optimising operation parameters. The feed seawater flow rate is



$1.13 \times 10^7$  kg/h with salinity 5.7 wt% and TBT = 90 °C. The rejection section consists of three stages. The specifications and constant parameters, which are used in this work, are shown in Table 4.1. The brine heater fouling factor is calculated using equation (5.5). Monthly variation of average seawater temperature (based on Abdel-Jawad and AL-Tabtabael, 1999) and monthly freshwater demand/consumption profiles based on Alvisi et al. (2007) for all months are shown in Figure 6.2. It is noticed that the freshwater demand is low in January and high in August.

Table 6.4 summarises the total operating cost and total capital cost of MSF process a monthly basis and the optimum total number of stages for all months. The results also show the optimal steam consumption and the operating parameters such as make up, and brine recycle flow rate throughout the year. Figure 6.3 illustrates the variations of monthly total cost with different number of stages in different months.

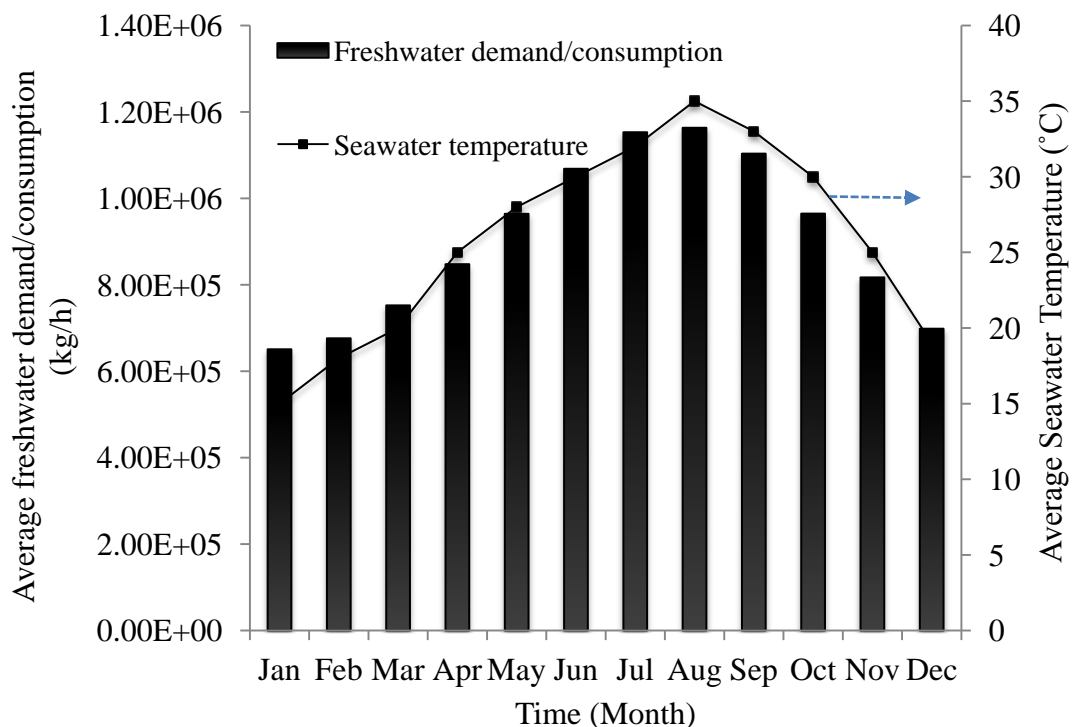


Figure 6.2 Average monthly seawater temperature and freshwater demand/consumption profiles during a year

It is noticed from the optimisation results that, the total monthly cost and total number of stages required in August (Table 6.4 and Figure 6.3) are the highest due to higher seawater temperature and freshwater demand/consumption (Figure 6.2). In addition, steam temperature and consumption, seawater make up and brine recycle (Table 6.4) and therefore total operating cost is higher in July and August. Figure 6.3 proves this fact in terms of minimum monthly total cost as a function of total number of stages policy.

The results also show that to meet the demand of variable freshwater demand/consumption in August, there has to be an increase in total number of stages from 10 to 19 (compare August and January in Table 6.4). Furthermore, the total monthly cost and total monthly operating cost have been increased by about 55% and 59% respectively in August compared with that for January to meet the freshwater demand. Although the optimum total number of stages in December to March are the same 10 stages, the total monthly operating cost is increased by about 19% (compare March and January in Table 6.4) to meet the demand. However, based on the results it is proposed to design MSF desalination process based on August condition with highest number of stages. This would allow operators to connect as many (August) or as few (January) of these individual units as are needed. In this way it is possible to meet variable monthly freshwater demand/consumption with varying seawater temperature and adding flexible scheduling and maintenance opportunity of the plant without interrupting or fully shutting down the plant at any month throughout the year.

Table 6.4 Summary of optimization results

Month	$f_{bh}$ m <sup>2</sup> K/kw	N	F×10 <sup>6</sup> kg/h	R×10 <sup>6</sup> kg/h	T <sub>s</sub> °C	Ws kg/h	TOC \$/M	TMC \$/M
Jan	0.065	10	2.40	3.48	93.63	119386	346837	856056
Feb	0.078	10	3.25	3.06	94.67	140774	395139	870652
Mar	0.093	10	3.75	3.61	93.57	144784	413188	922358
Apr	0.108	11	4.39	4.64	96.63	157034	470029	1011793
May	0.121	12	5.55	5.48	98.14	175697	538310	1111598
Jun	0.135	14	6.40	6.41	98.93	178609	570792	1204499
Jul	0.150	15	7.30	7.35	100.29	192269	624094	1286866
Aug	0.164	19	7.55	7.55	98.93	158491	551316	1324165
Sep	0.178	15	7.04	7.04	100.54	181176	593126	1255898
Oct	0.192	13	5.78	5.59	99.68	165034	526707	1130611
Nov	0.206	11	4.46	4.29	98.84	151604	466344	1008108
Dec	0.222	10	3.49	3.33	97.69	133263	400363	909583

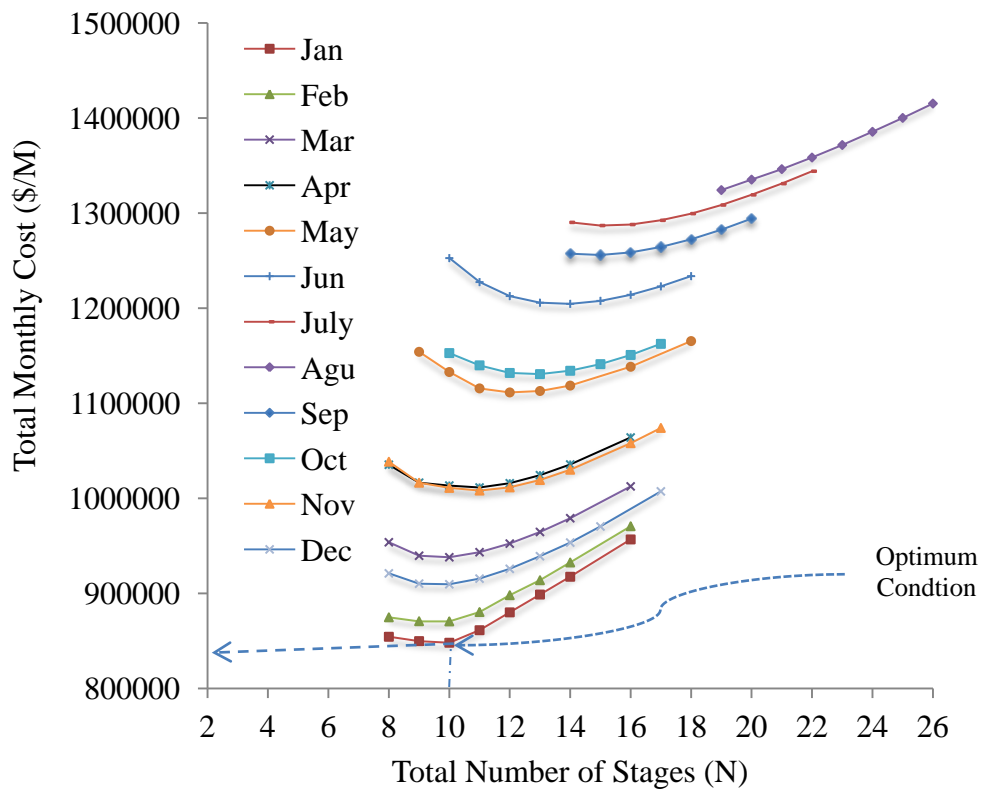


Figure 6.3 The variation of total monthly cost with total number of stages during a year

## 6.4 Conclusions

Optimal design and operation of MSF desalination processes are studied here using optimisation techniques in gPROMS models builder 2.3.4. Firstly, for a fixed design and fixed fresh water demand, two different operations in terms of TBT and anti scalant dosing were considered. The change in brine heater fouling factor with time (at different seawater temperature) was calculated by using the linear relationship for anti-scaling (Chapter 5) for a fixed design (number of stages in recovery and rejection section). The operating parameters such as make up flow rate, brine recycle flow rate and steam temperature were optimized while minimizing total monthly operation costs of MSF desalination.

The results of cost optimization clearly show that as seawater temperature increases from winter to summer seasons, the steam consumption and brine flow rates in the recovery section increase. However, the highest total monthly operating cost is noticed in August.

Effect of seawater temperature on total monthly operating cost (TOC) is more pronounced compared to the effect of fouling factor. Even though the brine heater fouling factor attains the maximum value at the end of year, the highest total monthly operating cost is noted at the maximum yearly seawater temperature.

The cost of fresh water production was reduced when the unit is operated for a higher TBT with a maximum of chemical additives. Even though the operating cost is slightly lower in the second case, the higher residual of anti-scalant concentration was presented in the brine blow down. Therefore, the impact on the marine environment will be higher in the second case if the blow down is discharged into the sea directly. Furthermore, higher TBT operation will lead to high costing materials for construction.

Finally, for fixed top brine temperature, the role of changing fouling factor with monthly varying of seawater temperatures and freshwater demand/consumption during a year and they're effect on the total monthly cost of MSF desalination process. Optimization problem was formulated to optimize the total number of flash stages and operating parameters such as recycle brine and seawater make up while minimizing the total monthly cost (including capital cost and operating cost) of the process for all months.

The optimization results provides that August operation requires the desalination process to use more flash stages than in other months to meet the variable demand of freshwater with high seawater temperature. The results also indicate that higher F and R at higher seawater temperature and freshwater demand during a month leading to higher total cost (monthly) by about 55% in August compared with that for January.

# Chapter 7

## Meeting Variable Freshwater Demand by Flexible Design and Operation of MSF Desalination Process

### 7.1 Introduction

Seawater temperature is subject to variation during 24 hs a day and throughout the year. This variation will affect the rate of production of freshwater using MSF process throughout the year. Most recently, a number of authors including Tanvir and Mujtaba (2008b) and Hawaidi and Mujtaba (2010) focused on optimal design and operation of MSF processes based on fixed freshwater demand 24 hs a day, 7 days a week and 365 days a year. However, in reality the demand (Alvisi et al., 2007) and also the seawater temperatures (Yasunaga et al., 2008) vary throughout the day and throughout the year. With the design and operating conditions being fixed, the freshwater production varies considerably with the variation of the seawater temperature, producing more freshwater at night (low seawater temperature) than during the day (high temperature) (Tanvir and Mujtaba, 2008a). Interestingly, this production pattern goes exactly counter to demand profile, which is greater during peak hours (morning, noon and evening) than after mid night. In addition, there is more freshwater demand in summer than in winter season (Alvisi et al., 2007).

This Chapter investigates how the design and operation of multistage flash (MSF) desalination processes are to be optimised and controlled in order to meet variable demands of freshwater with changing seawater temperature throughout the day and throughout the year. In order to avoid dynamic changes in operating conditions of the process (which would be required to cope with the variable demand) and in order to restrict these changes only at discrete time in a day, storage tank is added to the MSF

process (Figure 7.1). The operation parameters, such as make-up and brine recycle flow rates are optimized at discrete time intervals (based on the storage tank level which is monitored dynamically and maintained within a feasible limit) while the total daily cost is minimised.

A steady state process model (presented in Chapter 4) for the MSF process coupled with a dynamic model for the storage tank is developed which is incorporated into the optimisation framework within gPROMS modelling software. Based on actual data, correlations for seawater temperature profiles are developed. In addition, Neural Network (NN) technique has been used to develop a correlation which can be used for calculating dynamic freshwater demand/consumption profiles at different time of the day and season. These correlations are also embedded within the process model in gPROMS. Mid night is considered to be the starting time.

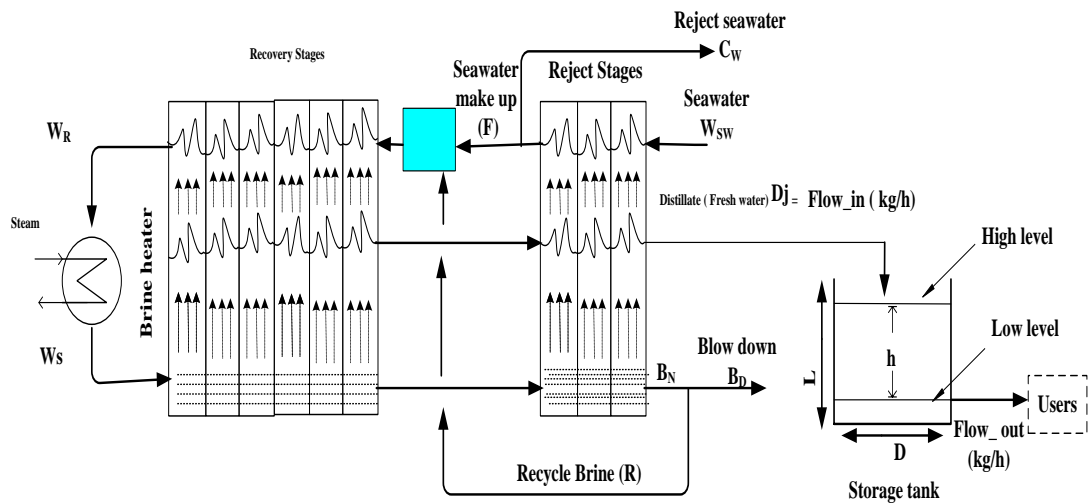


Figure 7.1 A typical MSF desalination process with storage tank

## 7.2 Estimation of Dynamic Freshwater Demand/Consumption Profile Using NN

Use of neural network (NN) based physical property correlation is not new in MSF desalination process modelling, simulation and optimisation (Tanvir and Mujtaba,

2006b). Table 7.1 presents typical hourly water demand/consumption for the Mondays of the week in Winter, Spring, Summer and Autumn taken from Alvisi et al., (2007). These data were selected from the published data presented in graphical form with time range (0 – 24 h) for different seasons.

In this work, a NN based correlation is developed to estimate dynamic freshwater demand/consumption profile (Flow\_out) as a function of time (h), and season S (S =1,... 4, winter, spring, summer, autumn respectively). A 4 layers NN architecture shown in Figure 7.2 is used for this purpose.

A neuron ( $a$ ) is a mathematical processing component of the NN. The neurons in the input layer are called the input, which receive information from the input layer and process them in a hidden way. The neurons in the output layer (e.g.  $a_1^4$ ) receive processed information from previous layers and sends output signals out of the system. In the NN architecture used in this work (4 layered) there is one input, two hidden layers and one output layer, the correlation is given by:

$$a_1^4 = f_1^4 \left( \sum_{k=1}^2 (w_{1k}^4 a_k^3) + b_j^4 \right) \quad (7.1)$$

Where  $a_k^3$  is given by:

$$a_k^3 = f_j^3 \left( \sum_{k=1}^4 (w_{jk}^3 a_k^2) + b_j^3 \right) \quad (7.2)$$

For  $j=1$  in layer 3, Equation (7.2) can be expressed as:

$$a_1^3 = f_1^3 (w_{11}^3 a_1^2 + w_{12}^3 a_2^2 + w_{13}^3 a_3^2 + w_{14}^3 a_4^2 + b_1^3) \quad (7.3)$$

Where  $a_k^2$  is given by:

$$a_k^2 = f_j^2 \left( \sum_{k=1}^2 (w_{jk}^2 a_k^1) + b_j^2 \right) \quad (7.4)$$



For  $j=1$  in layer 2, Equation (7.4) can be expressed as:

$$a_1^2 = f_j^2(w_{11}^2 a_1^1 + w_{12}^2 a_2^1 + b_1^2) \quad (7.5)$$

Table 7.1 Demand Profile from Alvisi et al. (2007)

Season	Time (h)	Flow_out (l/s)
S= 1 (Winter)	<b>0</b>	<b>27.50</b>
	<b>2</b>	<b>22.31</b>
	4	24.62
	6	50.00
	<b>8</b>	<b>63.85</b>
	<b>10</b>	<b>62.69</b>
	12	62.69
	14	57.50
	<b>18</b>	<b>61.54</b>
	<b>20</b>	<b>57.50</b>
	22	41.92
	24	26.35
S= 2 (Spring)	<b>0</b>	<b>28.16</b>
	<b>2</b>	<b>22.96</b>
	4	22.43
	6	49.86
	<b>8</b>	<b>67.96</b>
	<b>10</b>	<b>66.84</b>
	12	68.06
	14	64.03
	<b>18</b>	<b>68.21</b>
	<b>20</b>	<b>63.59</b>
	22	44.42
	24	31.07
S= 3 (Summer)	<b>0</b>	<b>35.58</b>
	<b>2</b>	<b>29.23</b>
	4	27.50
	6	55.77
	<b>8</b>	<b>75.96</b>
	<b>10</b>	<b>74.23</b>
	12	70.19
	14	65.00
	<b>18</b>	<b>81.15</b>
	<b>20</b>	<b>83.46</b>
	22	58.08
	24	35.00
S= 4 (Autumn)	<b>0</b>	<b>28.65</b>
	<b>2</b>	<b>23.46</b>
	4	19.42
	6	56.35
	<b>8</b>	<b>74.23</b>
	<b>10</b>	<b>71.35</b>
	12	70.19
	14	65.58
	<b>18</b>	<b>69.62</b>
	<b>20</b>	<b>67.88</b>
	22	45.96
	24	30.38

The transfer function between the input and the first hidden and between the hidden layers are a hyperbolic tangent function ( $f_j^2, f_j^3 = \tanh$ ) and between the last hidden layer and output is linear function ( $f_j^4 = 1$ ).

For efficient development of NN based correlation data with wide range are usually scaled between (-1, 1) and de-scaled at the end (Tanvir and Mujtaba, 2006b). The data (time and season) shown in Table 7.1 are used as input data for the NN and are scaled with mean and its standard deviation as:

$$time_{scaled} = \frac{(time - time_{mean})}{time_{std}} \quad (7.6)$$

$$S_{scaled} = \frac{(S - S_{mean})}{S_{std}} \quad (7.7)$$

$$flow\_out_{scaled} = \frac{(flow\_out - flow\_out_{mean})}{flow\_out_{std}} \quad (7.8)$$

Where  $time_{mean}$  is the average  $time$ ,  $S_{mean}$  is the average value of all  $S$  values,  $time_{std}$  is standard deviation of time,  $S_{std}$  is standard deviation of  $S$  values used to develop the correlation.  $flow\_out_{mean}$  and  $flow\_out_{std}$  are the average and standard deviation respectively of the freshwater demand/consumption.

The equation (7.6) scales the time between (-1.706, 1.548), equation (7.7) scales the value of  $S$  between (-1.398, 1.298) and equation (7.8) scales the value of freshwater demand/consumption between (-1.7616, 1.897). The mean values of time,  $S$  and  $flow\_out$  together with the standard deviation are presented in Table 7.2.

There are two input neurons in the NN based correlations. The values are:

$$a_1^1 = time_{scaled} \quad \text{and} \quad a_2^1 = S_{scaled} \quad (7.9)$$

There is one output neuron in the NN based correlations:

$$a_1^4 = flow\_out_{scaled} \quad (7.10)$$

The output value is rescaled to find the value in original units.

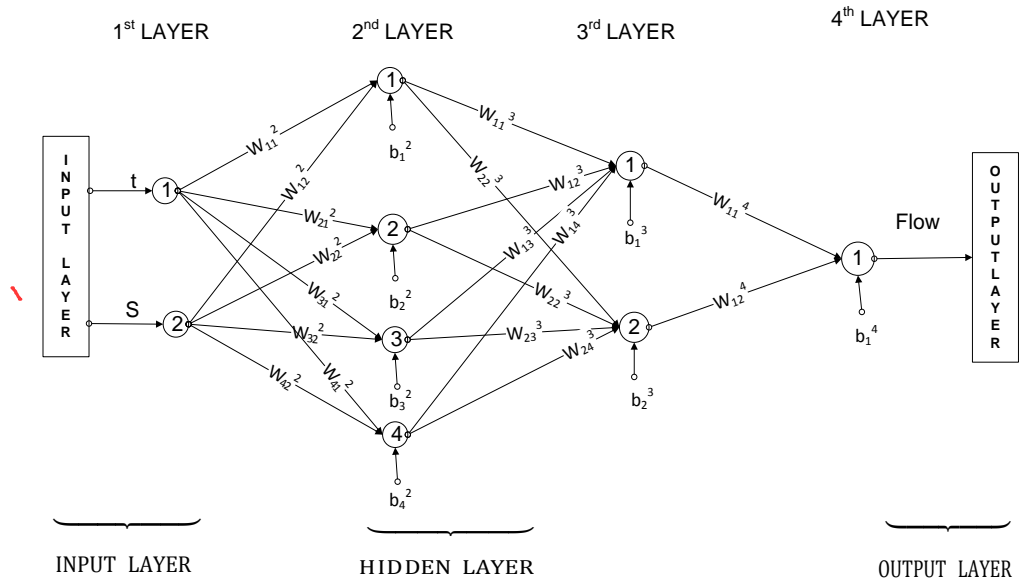


Figure 7.2 A Four layer neural network

The values of the first layer, second and third layer neurons can be written as:

$$a_1^2 = \tanh(w_{11}^2 \text{time}_{scaled} + w_{12}^2 S_{scaled} + b_1^2) \quad (7.11)$$

$$a_2^2 = \tanh(w_{21}^2 \text{time}_{scaled} + w_{22}^2 S_{scaled} + b_2^2) \quad (7.12)$$

$$a_3^2 = \tanh(w_{31}^2 \text{time}_{scaled} + w_{32}^2 S_{scaled} + b_3^2) \quad (7.13)$$

$$a_4^2 = \tanh(w_{41}^2 \text{time}_{scaled} + w_{42}^2 S_{scaled} + b_4^2) \quad (7.14)$$

$$a_1^3 = \tanh(w_{11}^3 a_1^2 + w_{12}^3 a_2^2 + w_{13}^3 a_3^2 + w_{14}^3 a_4^2 + b_1^3) \quad (7.15)$$

$$a_2^3 = \tanh(w_{21}^3 a_1^2 + w_{22}^3 a_2^2 + w_{23}^3 a_3^2 + w_{24}^3 a_4^2 + b_2^3) \quad (7.16)$$

The final NN based correlation for the estimation of demand/consumption profile can be written as:

$$\text{flow\_out}_{scaled} = a_1^4 = w_{11}^4 a_1^3 + w_{12}^4 a_2^3 + b_1^4 \quad (7.17)$$

The total input data (Table 7.1) are divided into three sets: first 2 input data points are selected for training (50%, bold), the next input data points for validation (25%, italic) and fourth one is selected for testing (25%, normal) (Table 7.1). Levenberg-Marquardt

back propagation algorithm (Tanvir and Mujtaba, 2006b) is used for training to determine the weights and biases of multi-layered network (Figure 7.3). The weights and transfer functions are shown in Table 7.2.

The neural network architecture (the number of hidden layers, neurons and transfer functions in each layer) is selected based on simulation by training the network using various configurations and selecting the one, which gives the network output close to the actual data

Table 7.2 Weights, biases, transfer functions (TF) and Scaled up parameters for 4-layered network

2 <sup>nd</sup> layer	weights	Bias	TF		
$w_{11}^2 = 4.03169$	$w_{12}^2 = -0.00619$	$b_1^2 = -3.753461$	tanh		
$w_{21}^2 = -0.54501$	$w_{22}^2 = -0.53621$	$b_2^2 = 0.54613$	tanh		
$w_{31}^2 = -7.8365$	$w_{32}^2 = -.045366$	$b_3^2 = -7.01898$	tanh		
$w_{41}^2 = 0.56025$	$w_{42}^2 = 0.51196$	$b_4^2 = -0.57975$	tanh		
3 <sup>rd</sup> layer	weights	Bias	TF		
$W_{11}^3 = 0.2399$	$W_{12}^3 = 28.6726$	$W_{13}^3 = -0.037$	$W_{14}^3 = 29.5340$	$b_1^3 = 0.33252$	tanh
$W_{21}^3 = 0.6816$	$W_{22}^3 = 1.20067$	$W_{23}^3 = -0.143$	$W_{24}^3 = 1.1377$	$b_2^3 = 2.74325$	Tanh
4 <sup>th</sup> layer	Weights	Bias	TF		
	$W_{11}^4 = 4.29131$ $W_{12}^4 = 169.606$	$b_1^4 = -167.88$	1		
$time_{mean}$	$S_{mean}$	$flow\_out_{mean}$	$time_{std}$	$S_{std}$	$flow\_out_{std}$
12.5818	2.55	52.611	7.3727	1.1126	17.304

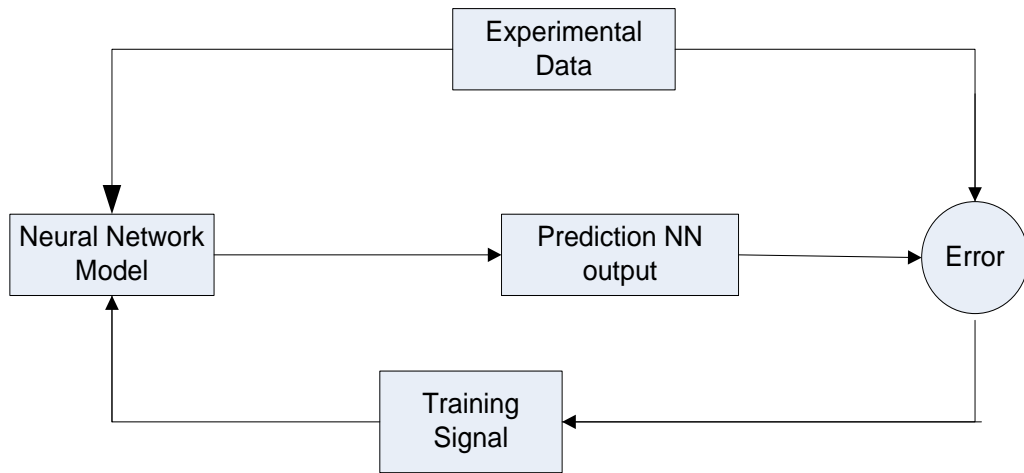


Figure 7.3 Neural Network back propagation training scheme

The statistical regression between calculated values of the average freshwater demand/consumption (flow\_out) by NN correlations and experimental data is plotted to find the overall trends of the predicted data (Figure 7.4). The above correlation has coefficient of determination equal to 0.99 (Figure 7.5) which clearly shows that NN based correlation can predict the freshwater demand/consumption profile very accurately and dynamically. The correlation is also used to predict the freshwater demand/consumption based on (time, season), which were never used for training, validation or testing the correlation. For example, the NN correlation is used to predict the demand/consumption profile between winter and spring at  $S = 1.5$  (Figure 7.6). The results clearly show that the prediction by correlation follows the expected trend.

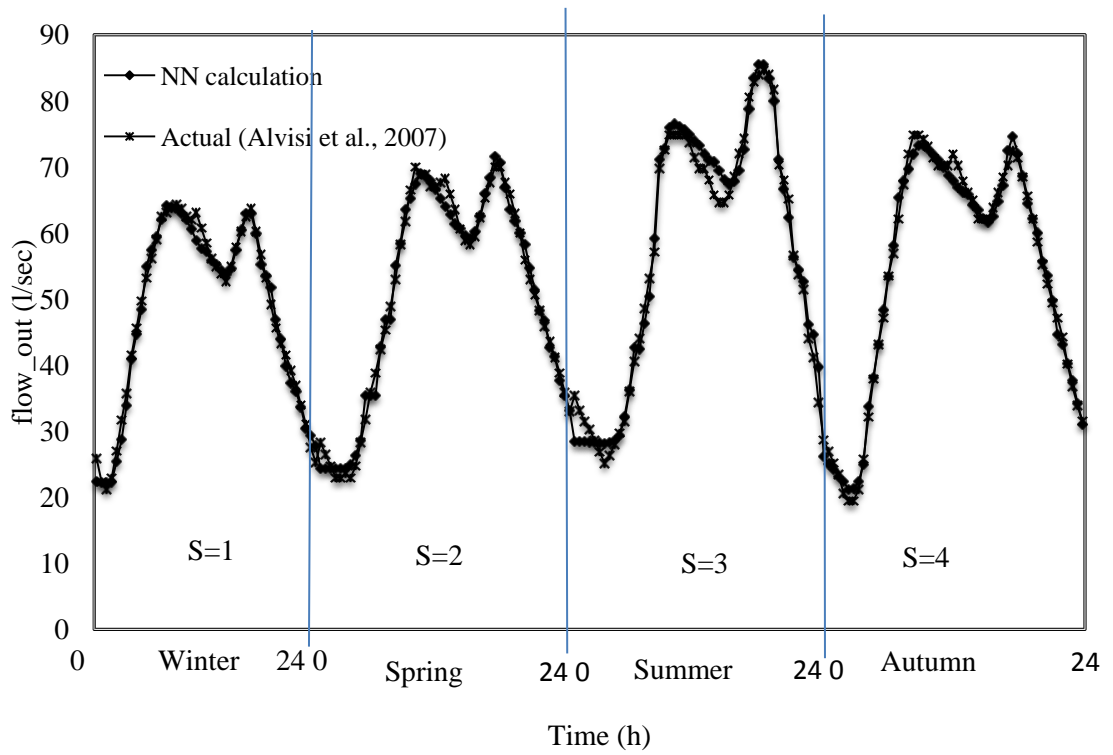


Figure 7.4 Freshwater demand/consumption(*flow\_out*) profiles at different season

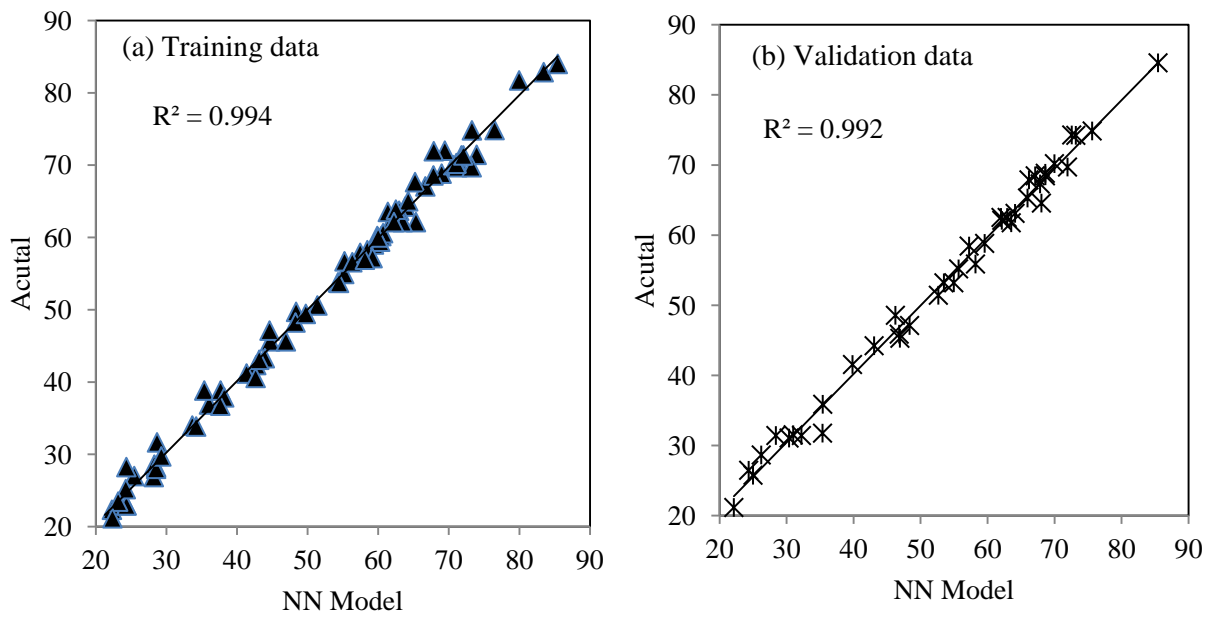


Figure 7.5 Calculated and measured freshwater demand/consumption (*flow\_out*)

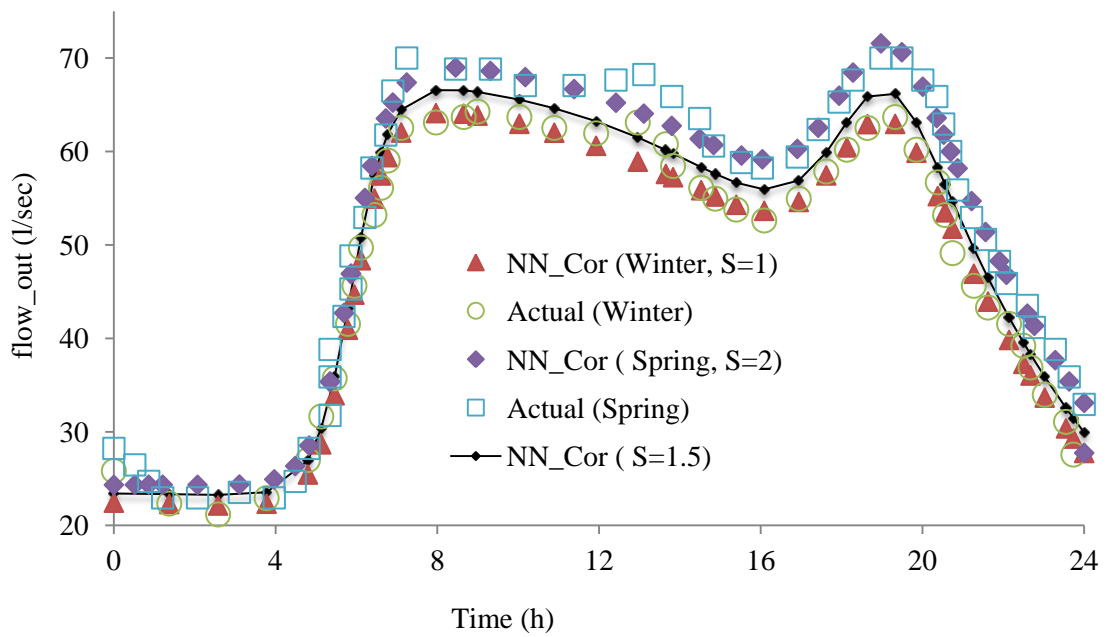


Figure 7.6 Actual freshwater demand/consumption by Alvisi et al. (2007) and predicted profile

### 7.3 Estimation of Dynamic Seawater Temperature Profile

Figure 7.7 shows the actual seawater temperature ( $^{\circ}\text{C}$ ) over 24 h in October (autumn season) (Yasunaga et al., 2008). Using regression analysis, the following polynomial relationship is obtained (also shown in Figure 7.7) with a correlation coefficient greater than 90%.

$$T_{\text{sw}} = 6 \times 10^{-6} t^5 - 0.0003 t^4 + 0.0032 t^3 + 0.007 t^2 - 0.1037 t + 28.918 \quad (7.18)$$

Equation (7.18) represents the relationship between the seawater temperature and time (h). The temperature at  $t = 0$  represents the seawater temperature at midnight. In this chapter, the seawater temperature profile in October is assumed to represent the temperature profile of the autumn season.

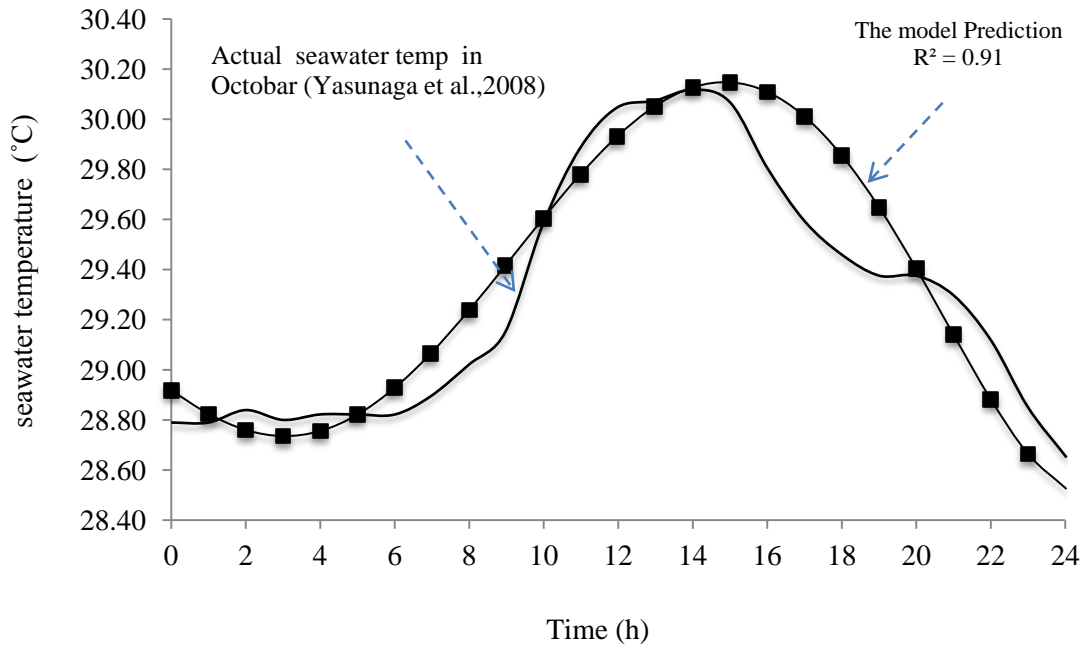


Figure 7.7 Seawater temperature profiles

#### 7.4 MSF Process Model

In this chapter, no disturbances in process input parameters (such as seawater feed rate, steam flow rate) are considered (which can make the MSF process dynamic) except the change in feed seawater temperature. However, in a particular day the variation of seawater temperature is very small (0.1- 0.2°C variation per hour) (Figure 7.7) and the dynamics imparted due to this I believe will be very negligible (Aly and Marwan, 1995; Tanvir, 2007). Hence a steady state process model for the MSF is considered. However, the variation in the storage tank throughout the day is significant and therefore dynamic model for the storage tank is considered. However, note, change in demand required changes in some of the operating parameters (e.g. R and F) which are optimised at discrete time intervals. No doubt, discrete changes of these parameters will impart transient states into the process, however, for the sake of simplicity it is assumed that these transient states will be of short period and therefore neglected. A steady state process model for the MSF is given in Chapter 4 and dynamic model for the storage



tank is given in the following. Note, the overall process model consists of steady state MSF process model plus the dynamic storage tank model leading to a coupled system of differential and algebraic equations.

### 7.4.1 Tank Model

The dynamic mathematical model of the tank takes the following form:

Mass balance:

$$\frac{dM}{dt} = \text{Flow\_in} - \text{Flow\_out} \quad (7.19)$$

Relation between liquid level and holdup:

$$M = \rho A_s h \quad (7.20)$$

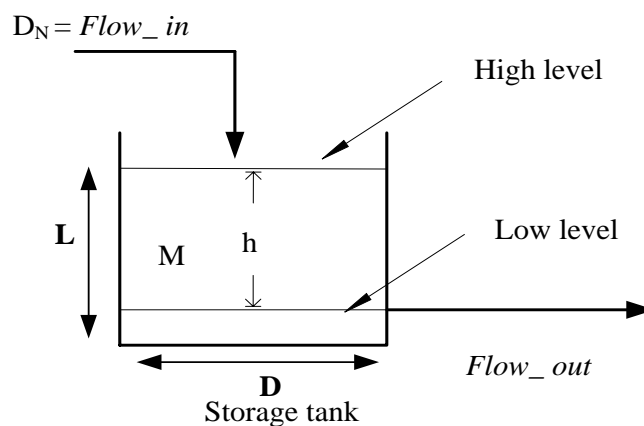


Figure 7.8 Storage Tank

### 7.5 Storage Tank Level Constraints

In Figure 7.8, the storage tank is assumed to operate without any control on the level, and therefore  $h$  goes above the limit  $h_{max}$  or below the limit  $h_{min}$  during the operation of MSF process as shown in Figure 7.9 a. At any time, this violation ( $v_1, v_2$ ) of safe operation can be defined as:

$$v_1 = \begin{cases} (h(t) - h_{max})^2 & \text{if } h > h_{max} \\ 0 & \text{if } h < h_{max} \end{cases} \quad (7.21)$$

and

$$v_2 = \begin{cases} (h(t) - h_{min})^2 & \text{if } h < h_{min} \\ 0 & \text{if } h > h_{min} \end{cases} \quad (7.22)$$

A typical plot of  $v_1$  and  $v_2$  versus time  $t$  is shown in Figure 7.9 b. The total accumulated violation for the entire period can be calculated using:

$$V_T = \int_{t=0}^{t_f} (v_1(t) + v_2(t)) dt \quad (7.23)$$

Therefore,

$$\frac{dV_T}{dt} = v_1(t) + v_2(t) = (h(t) - h_{max})^2 + (h(t) - h_{min})^2 \quad (7.24)$$

This equation is added to the overall process model equations presented in Chapter 4. Also an additional terminal constraint ( $0 \leq V_T(t_f) \leq \varepsilon$ ) is added to the optimisation formulations presented in the next section, where  $\varepsilon$  is a very small finite positive number ( $10^{-6}$ ). The above constraint will ensure that  $h(t)$  will always be equal or less than  $h_{max}$  and equal or above  $h_{min}$  throughout the 24 h.

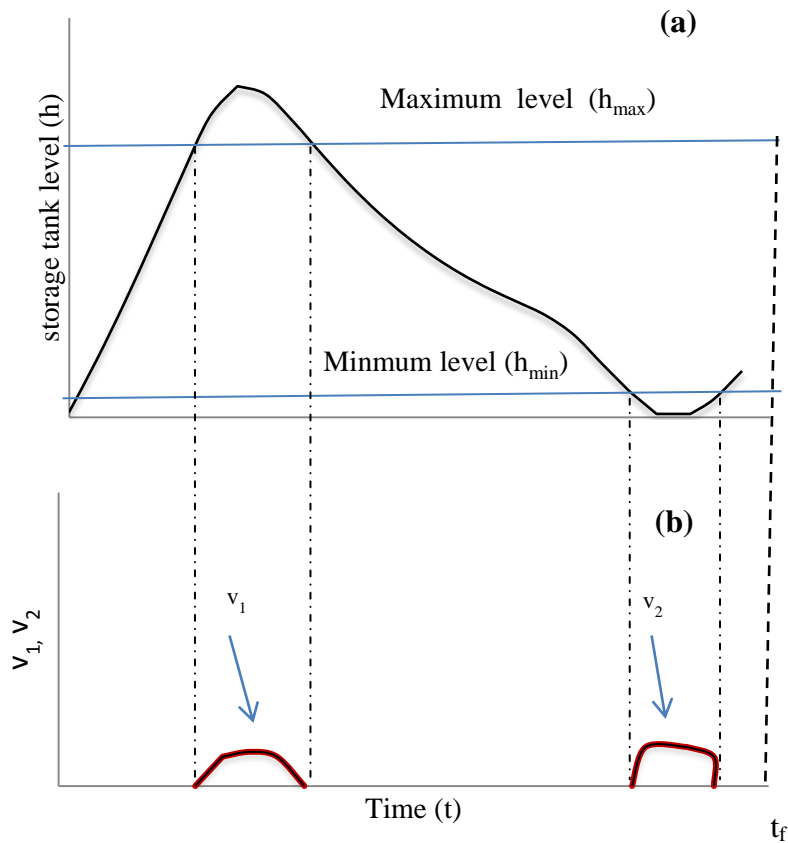


Figure 7.9 (a) A typical storage tank level profile (b) Tank level Violations during the operation

## 7.6 Description of Case Studies

In this Chapter a number of case studies are carried out which is summarised in Table 7.3. Note, the top brine temperature is fixed for (TBT=90°C) all case studies in this Chapter.

Table 7.3 Summary of all case studies in this chapter

<b>Case Study</b>	<b>Objective function</b>	<b>Optimisation Variables</b>	<b>Conditions and given</b>
1. Section 7.7	Minimise Total daily operating cost	Recycled brine flow rate ( $R$ ), Make-up seawater ( $F$ )	Variable freshwater demand/consumption and seawater temperature over 24 h for one season, Fixed number of stage
2. Section 7.8	Minimise Total daily operating cost	Recycled brine flow rate ( $R$ ), Make-up seawater ( $F$ )	Variable freshwater demand/consumption and seawater temperature over 24 h for one season, Variable number of stage
3. Section 7.9	Minimise Total daily operating cost	Recycled brine flow rate ( $R$ ), Make-up seawater ( $F$ )	Variable freshwater demand /consumption and seawater temperature(with increasing 0.5, 1, 1.5C°) over 24 h for one season, Fixed number of stage
4. Section 7.10	Minimise Total daily Cost (including operating and capital costs)	Recycled brine flow rate ( $R$ ), Make-up seawater ( $F$ ), Total number of stages ( $N$ )	Variable freshwater demand/consumption and seawater temperature over 24 h for four season

## 7.7 Case Study 1: Minimise Total Daily Operating Cost under Fixed Design

### 7.7.1 Optimisation Problem Formulation

The performance of MSF desalination process is evaluated in terms of minimising the total daily operating cost.

The optimization problem is described below.

Given: the MSF plant configurations, fixed design specification of each stage, volume of the storage tank, seawater flow, seawater temperature and fresh water demand profile

Determine: the optimum recycled brine flow rate ( $R$ ), make-up seawater ( $F$ ) at different intervals within 24 h.

Minimize: the total daily operating cost (TOC).

Subject to: process constraints.

The Optimization Problem (OP3) is described mathematically for any interval as:

$$\begin{aligned}
 \text{OP3} \quad & \text{Min} \\
 & R, F \quad \text{TOC} \\
 \text{s.t.} \quad & f(t, \dot{x}, x, u, v) = 0 \text{ (model equations)} \\
 & T_{BT} = T_{BT}^* \\
 & 0 \leq V_T \leq \varepsilon \\
 & (2 \times 10^6 \text{ kg/h}) R_L \leq R \leq R_U (7.55 \times 10^6 \text{ kg/h}) \\
 & (2 \times 10^6 \text{ kg/h}) F_L \leq F \leq F_U (7.55 \times 10^6 \text{ kg/h})
 \end{aligned}$$

Where,  $T_{BT}^*$  is the fixed top brine temperature ( $90^\circ\text{C}$ ). Subscripts (L) and (U) refer to lower and upper bounds of the parameters. The model equations presented in the previous section can be described in a compact form by  $f(t, \dot{x}, x, u, v)$  where  $\dot{x}$  represents all the state variables,  $x$  represent non linear sets of all algebraic and differential variables,  $u$  is the control variable, such as seawater make up, recycle flow rate, etc.,  $v$  is a set of constant parameters.

Total Annual Operating Cost can be described

$$\text{Where, } C_1 \text{ (Steam cost, \$/year)} = 8000 W_s [(T_s - 40) / 85] (0.00415) \quad (7.25)$$

$$C_2 \text{ (Chemical cost, \$/year)} = 8000 [D_N / 1000] (0.025) \quad (7.26)$$

$$C_3 \text{ (Power cost, \$/year)} = 8000 [D_N / 1000] (0.109) \quad (7.27)$$

$$C_4 \text{ (Maintenance and spares cost, \$/year)} = 8000 [D_N / 1000] 0.082 \quad (7.28)$$

$$C5 \text{ ( Labour cost, \$/year)} = 8000 [D_N / 1000] \cdot 0.1 \quad (7.29)$$

$$\text{TOC (Total Annual Operating Cost, \$/year)} = (C1 + C2 + C3 + C4 + C5) \quad (7.30)$$

MSF process model is given in Chapter 4 and the dynamic tank model is mentioned above. This optimisation problem minimises the total daily operating cost while considering variable seawater temperature change and customer demand throughout 24 hs and optimises R and F. The time intervals 24 h is also discretised into multiple intervals and in each intervals R and F are optimised. Results obtained using single and multiple intervals are then compared.

### 7.7.2 Results and Discussions

The case study is carried out in a 16 stages (including 13 stages in recovery section and 3 stages in rejection section) with fixed top brine temperature (TBT= 90°C). The feed seawater flow rate is  $1.13 \times 10^7$  kg/h with salinity 5.7 wt%. The storage tank has diameter (D =18 m), and aspect ratio: L/D = 0.55 (Virella et al., 2006). The initial value of 'h' is 0.5 meter. The specifications and constant parameters which are used in this work are shown in Table 7.4.

One, two and three time intervals within 24 h are considered within which F and R are optimised with intervals length while minimising the total daily operating cost. In this chapter, the daily variations of average seawater temperature and freshwater demand/consumption profiles for autumn season are calculated using equation (7.18) and equation NN respectively as shown in Figure 7.10. Note, the actual freshwater consumption at any time is assumed to be 5 times more than that shown in Figure 7.4.

Table 7.4 Constant parameters and input data

	$A_j/A_H$	$ID_j/ID_H$	$OD_j/OD_H$	$f_j/f_{bh}$	$w_j/L_H$	$H_j$
Brine heater	3530	0.022	0.0244	$1.864 \times 10^{-4}$	12.2	-----
Recovery stage	3995	0.022	0.0244	$1.4 \times 10^{-4}$	12.2	0.457
Rejection stage	3530	0.0239	0.0254	$2.33 \times 10^{-5}$	10.7	0.457

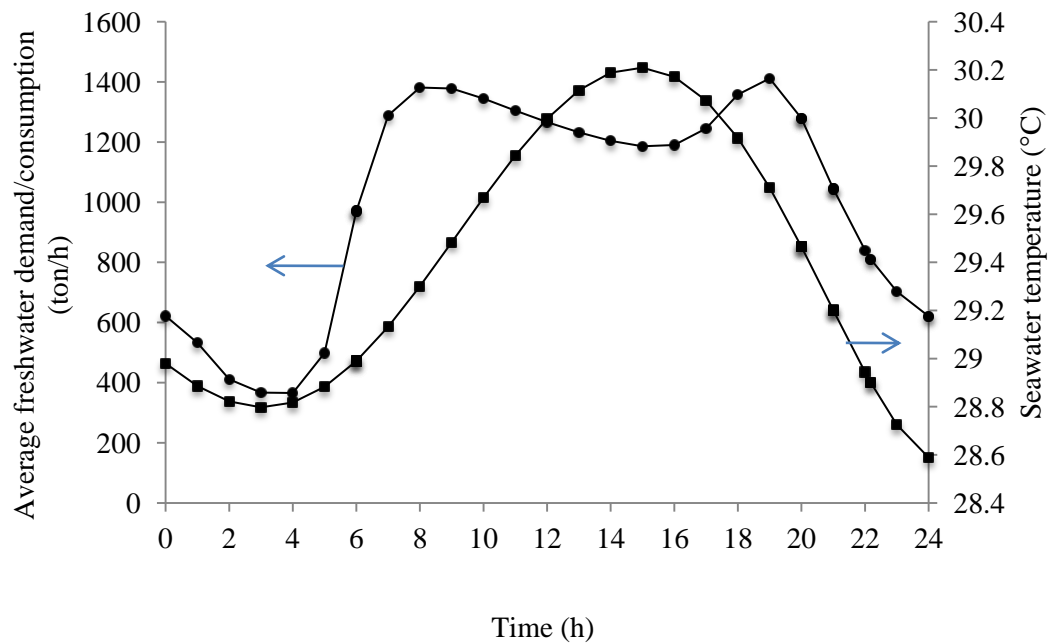


Figure 7.10 variations of seawater temperature and freshwater demand/consumption profiles

The optimisation results for each interval in terms of optimal recycle flow rate (R) and make-up flow rate (F) and total minimum daily operating cost are shown in Table 7.5 and Figure 7.11. The variations of steam temperature and consumption profiles for two and three intervals time is also shown in Figure 7.12. Figure 7.13 presents the storage tank levels profile for different intervals throughout the day. Figure 7.14 also shows that the variations of freshwater production and consumption profile for fixed total number of stages (N=16) during a day.

It is noticed from the optimisation results that, the MSF desalination operated with single interval for seawater make up F and brine recycle R were not sufficient to produce the variable freshwater demand.

The multi (F and R) interval strategies (2 and 3) were found to produce variable freshwater demand with varying seawater temperature. The optimisation results also show that the total daily operating cost using three time intervals is reduced by 130 \$/day compared to that obtained by using two intervals (Table 7.5). This is due to the fact that the MSF desalination process has to be operated at higher steam flow rate, higher steam temperature and with higher rate of F and R using two time intervals (Figures 7.11 and 7.12). Moreover, Figure (7.12) shows an increase in the steam temperature profile using two intervals by 1°C for 12 h compared with three intervals and consequently leads to increased fouling in brine heater. In addition, the consequence of this will be increased bottom brine temperature (Figure 7.15). On top of all these, the impact on the marine environment will be higher when the MSF plant operated using two time intervals. This clearly shows the benefit of using 3 time intervals.

Table 7.5 Summary of optimisation results using different intervals

	C1(\$/d)	C2(\$/d)	C3(\$/d)	C4(\$/d)	C5(\$/d)	TOC(\$/d)
One interval	*	*	*	*	*	*
Two intervals	10282	611	2703	2033	2480	18112
Three intervals	10175	609.8	2697	2029	2475	17980

\* No results obtained



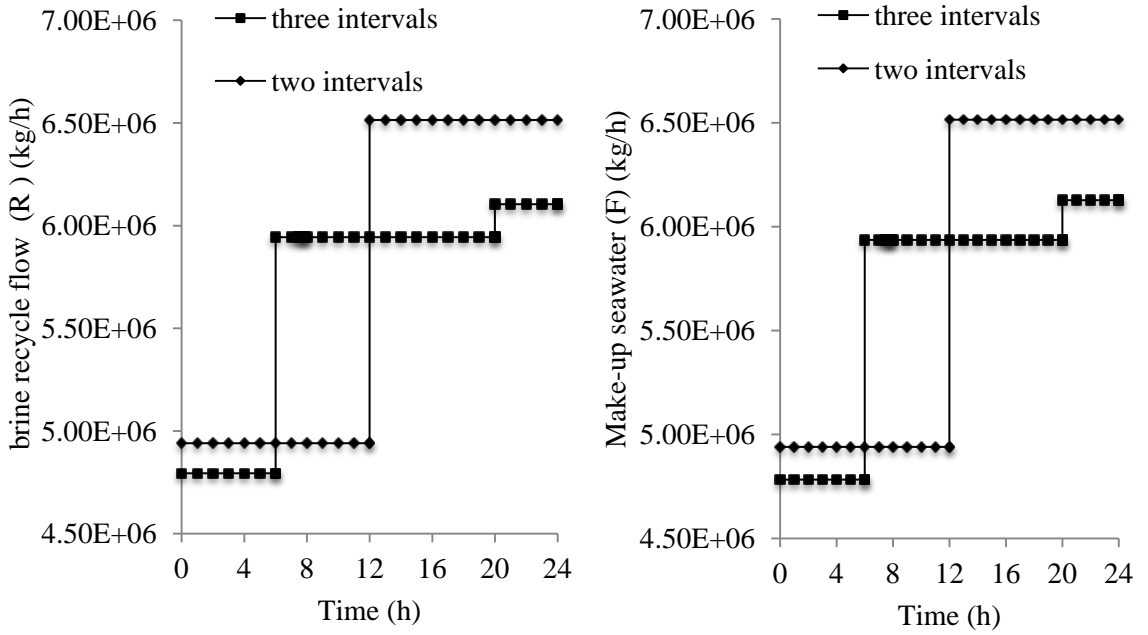


Figure 7.11 Optimum seawater makeup (F) and brine recycle flow rate (R) profiles at two and three intervals

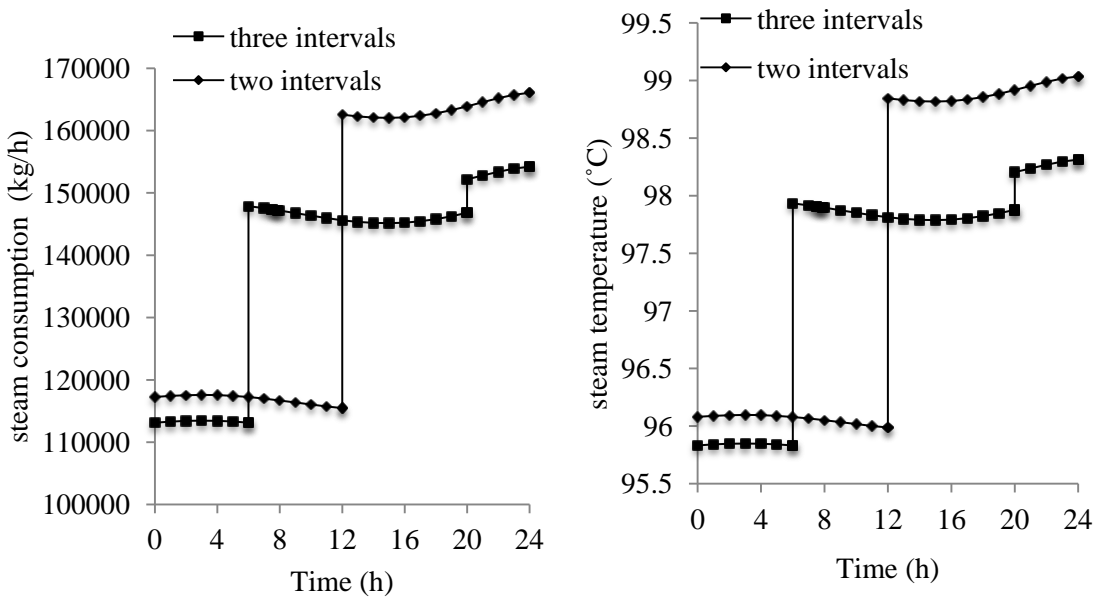


Figure 7.12 Variations of steam temperature and consumption profiles at two and three intervals time

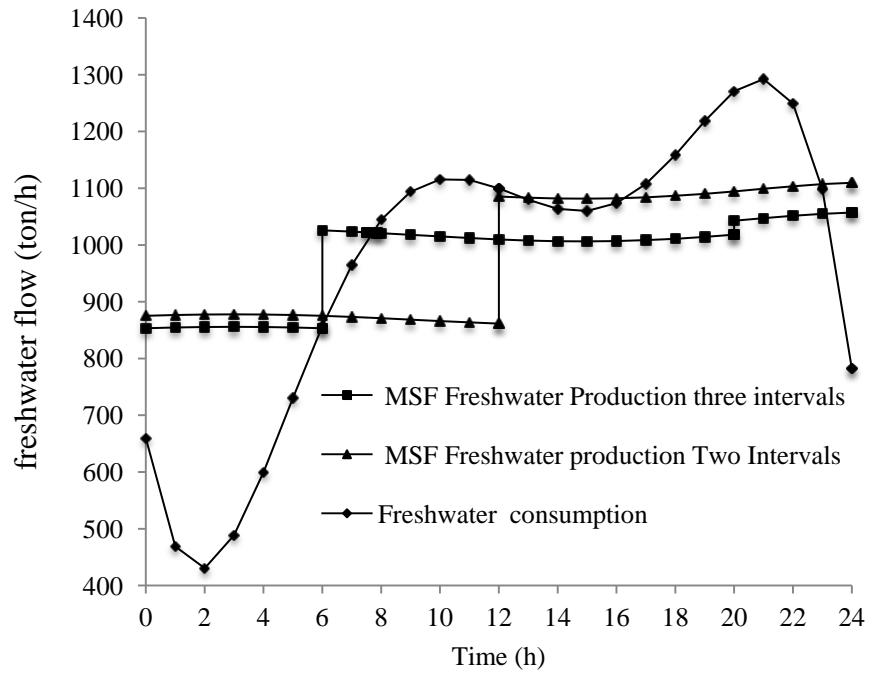


Figure 7.13 Freshwater production and consumption profile at different intervals

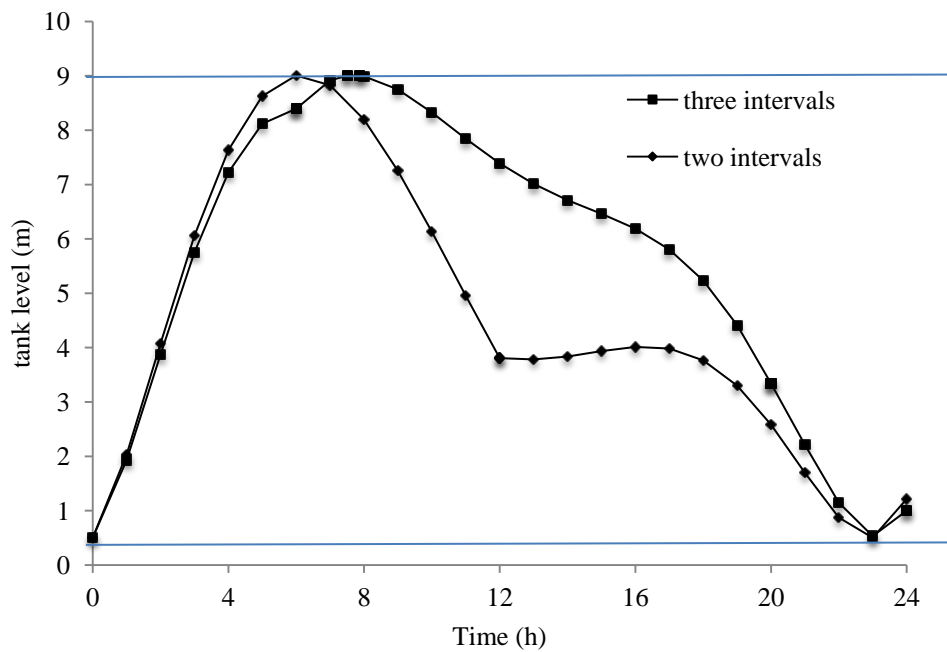


Figure 7.14 Storage tank level profiles at different intervals

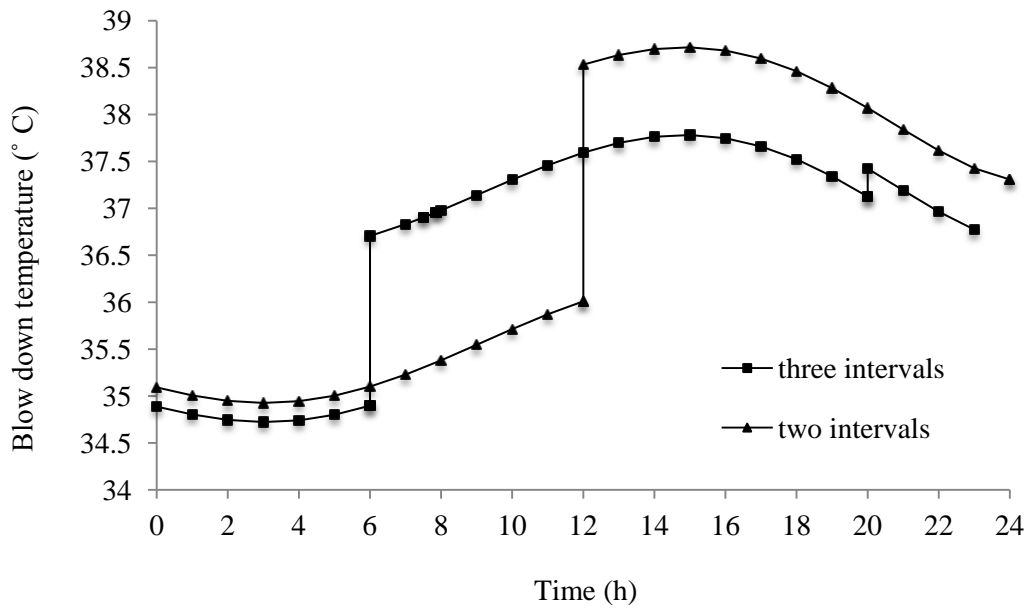


Figure 7.15 Variations of blow down temperature profiles at different intervals

## 7.8 Case Study 2: Minimise Total Daily Operating Cost with Variable Design

For a given total number of stages, this work investigates how the operation MSF desalination process are to be optimised and controlled in order to maintain a variable demand of freshwater with changing seawater temperatures throughout the day. The optimisation problem is same as OP3 (section 7.7).

The specifications and constant parameters of MSF process and storage tank which are used in this work are the same as that used in pervious case. In this work, three intervals within 24hs is considered within which F and R are optimised with interval length. The rejection section consists of three stages and the number of stages in the recovery section varies in different cases.

Table 7.6 summarises the cost components and total operating cost on a daily basis.

Figure 7.16 represents the optimum recycle flow rate (R) and make-up flow rate (F) at

discrete time intervals. Figure 7.17 illustrates the variations of steam temperature and consumption profile. The storage tank levels for different number of stages profile are shown in Figure 7.18. Figure 7.19 demonstrates the variations of freshwater production and consumption profile with N=16.

Table 7.6 Summary of optimisation results

N	TBT	C1 (\$/d)	C2 (\$/d)	C3 (\$/d)	C4 (\$/d)	C5 (\$/d)	TOC (\$/d)
16	90	10175.18	609.80	2697.86	2029.58	2475.10	17987.52
15	90	10929.27	609.67	2697.28	2029.15	2474.57	18739.95
14	90	11816.78	609.52	2696.62	2028.65	2473.97	19625.55

As the total number of stages decreases, the total operating cost is increased for fixed TBT (Table 7.6) due to higher F and R and steam consumption (Figures. 7.16 and 7.17). Although there is a decrease (only slightly) in chemical costs, maintenances & spear parts and labour costs, the contribution of the steam cost is higher. However, the intermediate storage tank adds the operational flexibility, and maintenance could be carried out without interrupting the production of water or full plant shut-downs at any time throughout the day. Figure 7.17 illustrates that the steam temperature and consumption are low at night time and approximately constant between 0 h and 6 h (first interval). There is a peak in the morning to evening which reaches maximum around 7-19 h (second interval) then a slight high 20 -24 h (third interval).

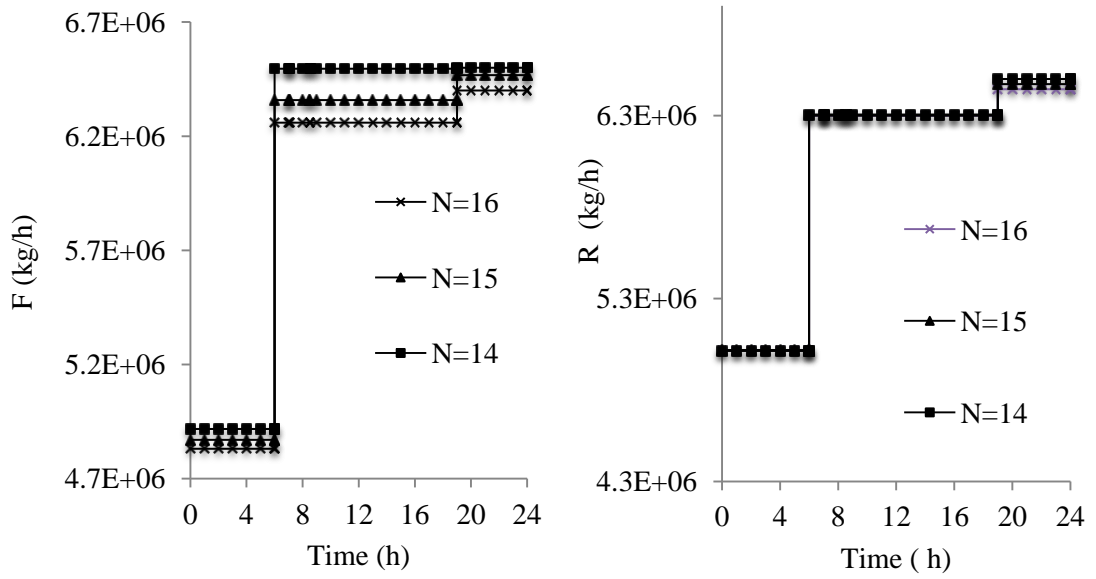


Figure 7.16 Optimum seawater makeup and brine recycle flow rates throughout profiles

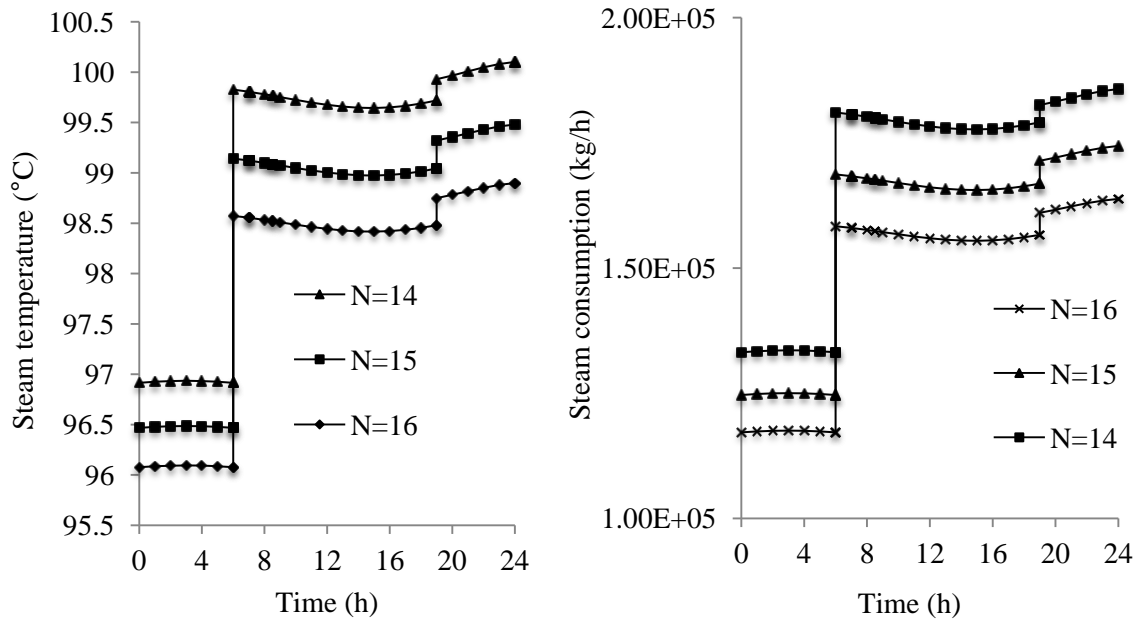


Figure 7.17 Steam temperature and consumption profile

The results also show that when the freshwater consumption rate is more than the freshwater production rate (Figure 7.19), the storage tank level falls down (Figure 7.18) and in order to maintain the demand the makeup and brine recycle flow rates need to be increased (Figure 7.17). The opposite happens when freshwater consumption rate is less than the freshwater production rate and consequently the tank level increases. The highest tank level 'h' is noted at 8 am and the lowest level at 23 am.

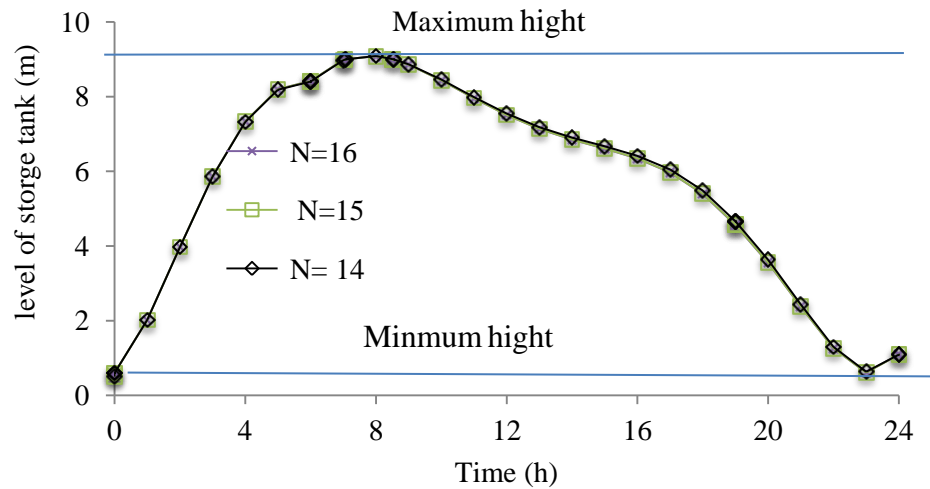


Figure 7.18 Storage tank level profiles at different number of stages

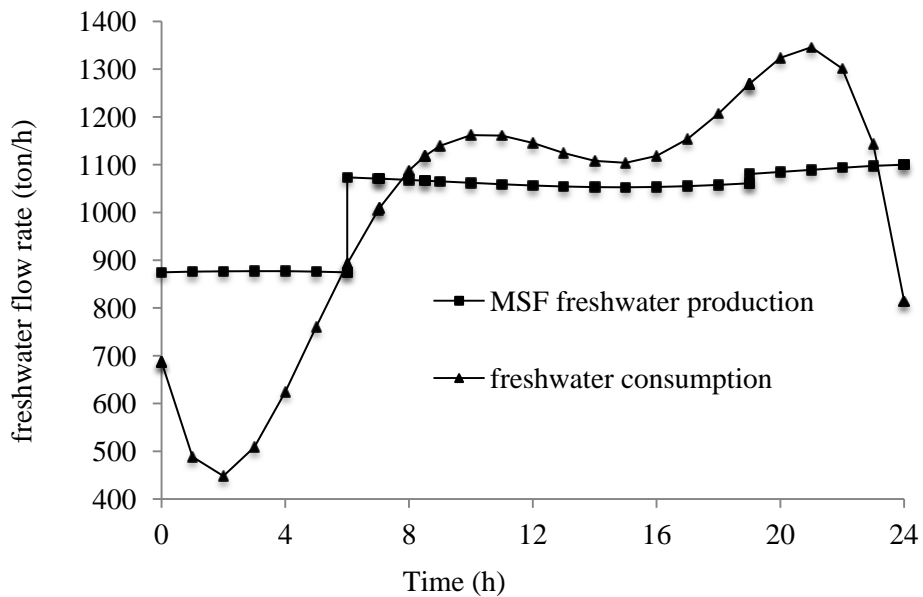


Figure 7.19 Freshwater production and consumption profile (N=16)

### **7.9 Case Study 3: Sensitivity of Seawater Temperature Profile**

The sensitivity of seawater temperature profile on the operating cost and operation parameters of MSF desalination process are carried out. The seawater temperature profile has been increased by 0.5°C, 1°C and 1.5°C respectively as shown in Figure 7.20 (the base case values are shown in the pervious case (section 7.8) with total number of stages 16) to see its effect on the operation (operating cost, recycled brine flow rate, seawater make up flow rate, steam consumption, steam temperature, bottom brine temperature, etc.). The daily freshwater demand/consumption profile is kept the same as in the previous case (Figure 7.10).

A 16 stages MSF desalination process with fixed top brine temperature (TBT= 90°C) is considered here. The all other parameters of MSF process and storage tank were fixed as shown in the previous case. The optimisation problem is same as that used in the previous case (OP3). Three intervals within 24 h are considered within which F and R are optimised with intervals length while minimising the total daily operating cost.

Effect of increasing the seawater temperature on the total daily operating cost of process including pro-rata steam cost, chemical cost, power cost, maintenance and spares cost and labour cost are summarized in Table 7.7. Figure 7.21 represents the optimum recycle flow rate (R) and make-up flow rate (F) at discrete time intervals. Figure 7.22 illustrates the steam temperature and consumption profiles.

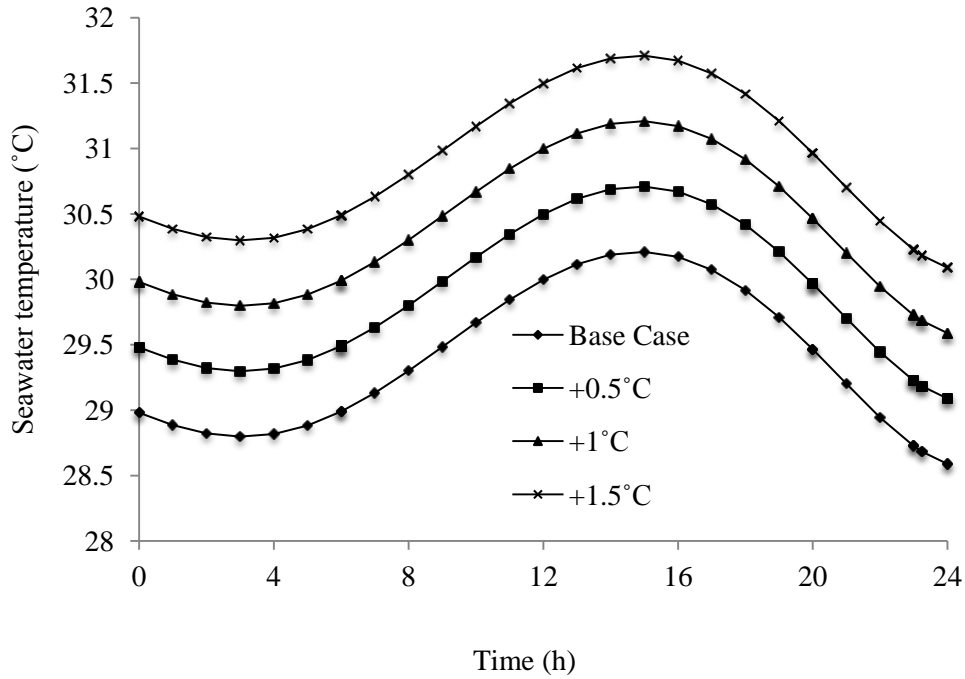


Figure 7.20 Seawater temperature profile during 24 h

It is observed that the increase in the seawater temperature profile increases the total daily operating cost (Table 7.7). The reason behind this behaviour is that, with increasing seawater make up and brine recycle flow rates (Figure 7.21), brine flow entering brine heater ( $W_R$ ) will increase and therefore, it will need to operate at higher steam temperature with higher consumption to maintain the demand level (Figure 7.22). Increasing the steam temperature will decrease its latent heat and consequently leads to increased steam consumption to meet the fixed top brine temperature. This consequently will increase the total daily operating cost by 0.6 % per 1°C increasing in the seawater temperature profile.

Figure 7.23 illustrates the effect of increasing the seawater temperature profile on the blow down brine temperature during 24 h. As is shown, increasing the seawater temperature increases the blow down brine temperature. The minimum and maximum blow down temperature has been achieved at 3 am and 2 pm respectively. On the other



hand, the results also show that the average blow down temperature increases by 1-1.25°C per 1°C increase in the seawater temperature profile.

Table 7.7 Summary of optimisation results

	C1(\$/d)	C2(\$/d)	C3(\$/d)	C4(\$/d)	C5(\$/d)	TOC(\$/d)
Base case (section 7.8)	10175	609	2697	2029	2475	17980
+0.5°C	10225	610	2698	2030	2475	18038
+1°C	10274	610	2698	2030	2475	18086
+1.5°C	10323	610	2698	2030	2475	18132

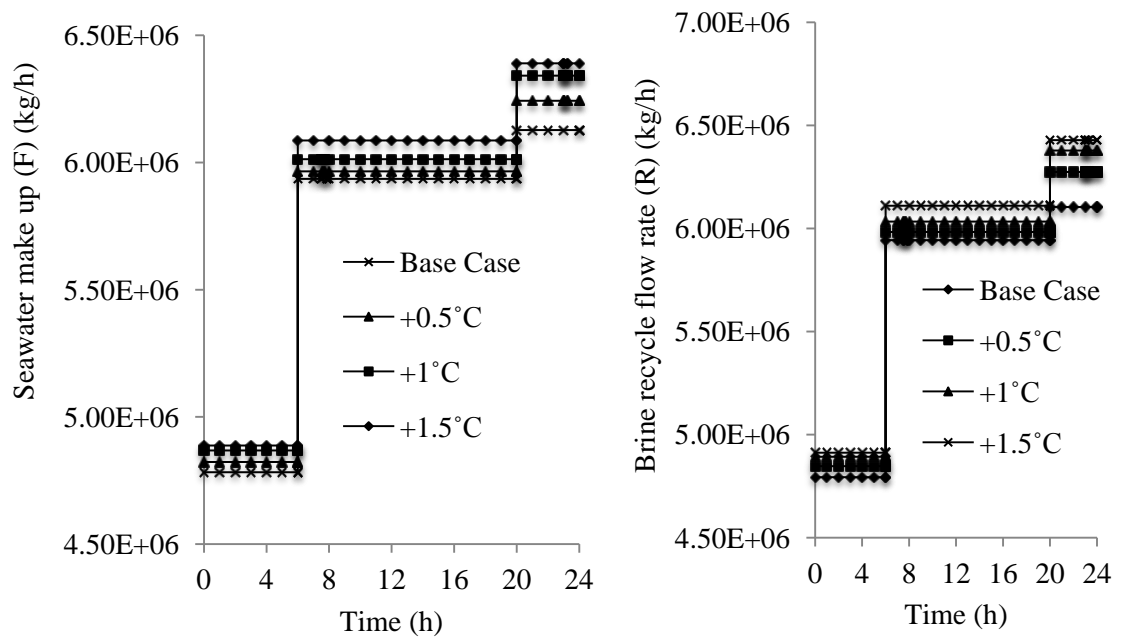


Figure 7.21 Optimum seawater makeup and brine recycle flow rates at different seawater temperature profiles

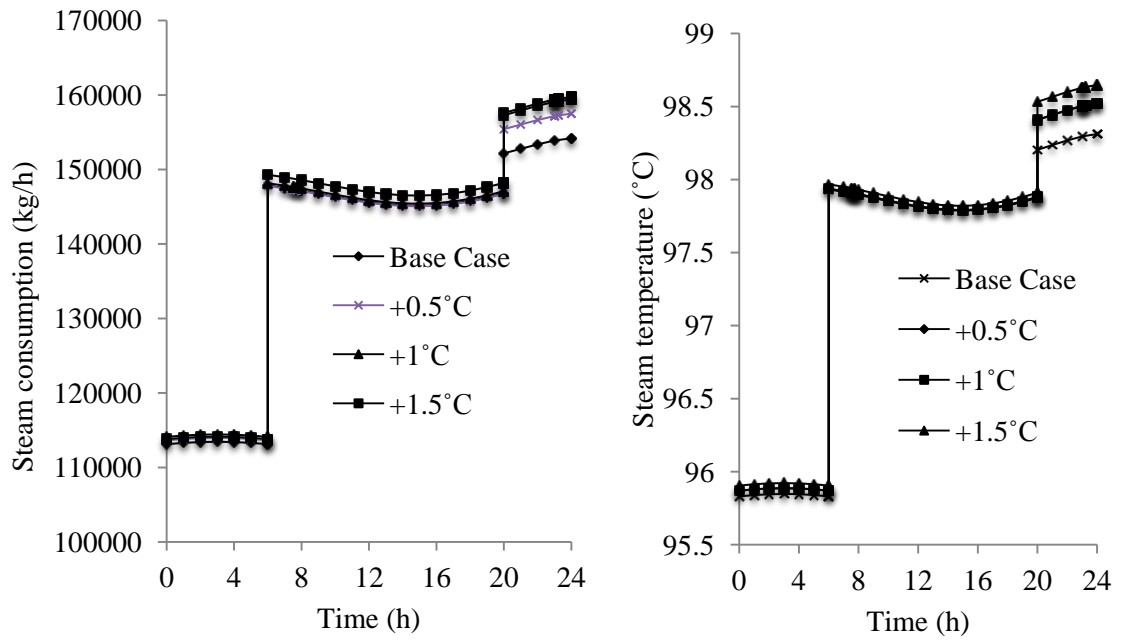


Figure 7.22 Steam temperature and consumption profile at different seawater temperature profiles

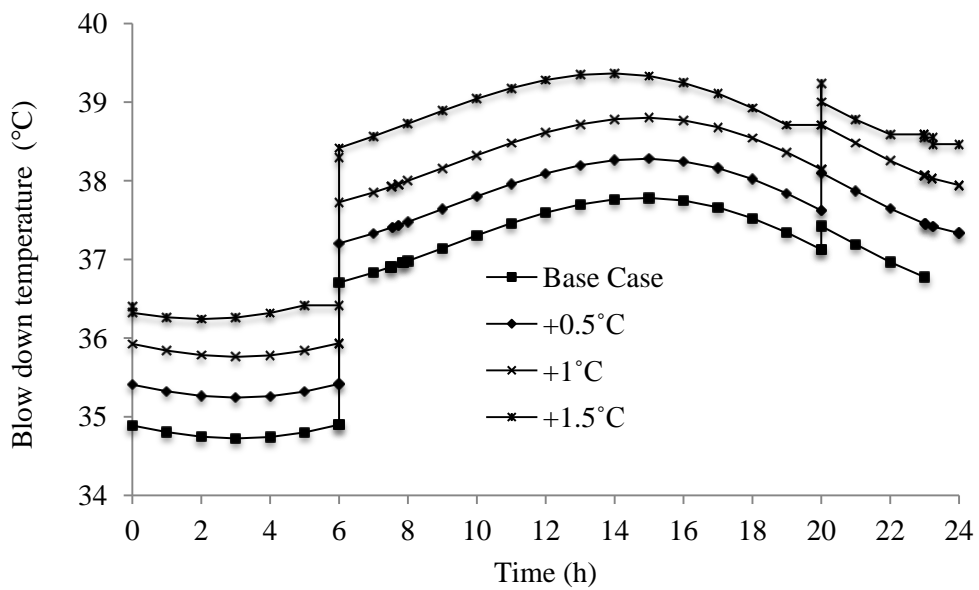


Figure 7.23 Variations of blow down temperature profiles at different seawater temperature profiles

## 7.10 Case Study 4: Flexible Design and Operation of MSF Process with Variable Seasonal Demand during a Year

For fixed top brine temperature (TBT), the design and operation of MSF desalination process are to be optimised and controlled in order to maintain a variable demand of seasonal freshwater demand/consumption with changing seasonal seawater temperature throughout the day and throughout the year is considered here using gPROMS model builder 2.3.4.

The optimization problem is described below.

Given: the MSF plant configurations, fixed design specification of each stage, volume of the storage tank, seawater flow, variable seawater temperature, top brine temperature (TBT) and freshwater demand profile.

Determine: the optimum total number of stages, optimum recycled brine flow rate  $R$ ; make-up seawater,  $F$  at different intervals within 24 h.

Minimize: the total daily cost (TDC).

Subject to: process constraints.

The Optimization Problem (OP4) is described mathematically over 24 h period as:

$$\begin{aligned}
 OP4 \quad & \text{Min} && \text{TDC} \\
 & R, F, N \\
 \text{s.t.} \quad & f(t, \dot{x}, x, u, v) = 0 \text{ (model equations)} \\
 & TBT = TBT * \\
 & (0.1\text{m}) \quad h_{\min} \leq h \leq h_{\max} (10.5\text{m}) \\
 & 0 \leq V_T(t_f) \leq \varepsilon_T \\
 & (2 \times 10^6 \text{ kg/h}) R_L \leq R \leq R_U (7.55 \times 10^6 \text{ kg/h}) \\
 & (2 \times 10^6 \text{ kg/h}) F_L \leq F \leq F_U (7.55 \times 10^6 \text{ kg/h})
 \end{aligned}$$

Where,  $T_{BT}^*$  is the fixed top brine temperature (90°C). Subscripts (L) and (U) refer to lower and upper bounds of the parameters. The model equations presented in the previous section can be described in a compact form by  $f(t, \dot{x}, x, u, v)$  where  $\dot{x}$  represents all the state variables,  $x$  represent non linear sets of all algebraic and differential variables,  $u$  is the control variable, such as seawater make up, recycle flow rate, etc.,  $v$  is a set of constant parameters.

The values of seawater makeup (F) and brine recycle (R) are chosen based on controlling the velocity in the condenser tubes between of 1 m/s as a minimum to a maximum of 3 m/s (El-Nashar,1998). The lower limit is dictated by heat transfer and flashing efficiency considerations and the higher limit by the tube erosion damage and higher pumping costs. The minimum and maximum levels of storage tank are arbitrarily assumed as 0.1 and 10.5 m, respectively.

The objective function TDC is given by  $TDC = \frac{TAC}{365}$  where, TAC (Total Annual Cost) is defined as:

$$TAC (\$/year) = CPC + STC + TOC \quad (7.31)$$

Where,

$$CPC (\text{MSF Annualised Capital Cost, } \$/\text{year}) = 182 \times 8000 N^{0.65} \quad (7.32)$$

$$STC (\text{Storage tank, } \$/\text{year}) = [2300 (\text{Storage tank volume (m}^3\text{)})^{0.55}] \times 3.1 \times 0.0963 \quad (7.33)$$

The depreciation period of the storage tank is 15 years with 5% interest rate giving the capital recovery factor equal to 0.0963. The detailed references on the calculation of CPC of the MSF plant can be found in Tanvir and Mujtaba (2008a) (the depreciation period/interest rate and the capital recovery factor are assumed to be included).

### 7.10.1 Results and Discussions

For different total number of stages, here, the total daily cost of the process including pro-rata capital cost of the storage tank is minimised by optimising operation parameters at discrete time intervals with the storage tank level, being monitored dynamically between a maximum and minimum limit. The storage tank has diameter ( $D = 20$  m), and aspect ratio:  $L/D = 0.55$ . The feed seawater flow rate is  $1.13 \times 10^7$  kg/h with salinity 5.7 wt%. The rejection section consists of three stages.

The initial level of the storage tank is 0.1 meter. The total operating time is 24 h and midnight is considered to be the starting time. In this work three discrete time intervals is used. The lengths of these intervals and in each interval seawater make up 'F' and brine recycle 'R' are optimised.  $h_{min} = 0.1$  m and  $h_{max} = 10.5$  m are used as lower and upper tank levels. Table 7.4 lists all the constant parameters of the model equations including various dimensions of the flash stages and brine heater.

During a particular day of the autumn season, the daily variation of average seawater temperature is calculated using equation (7.18). The average seawater temperatures profiles is assumed to increase by 4 °C (in the summer season) and falls by 10 °C (in the winter season) and 1 °C (in the spring season) as shown in Figure 7.24. The daily freshwater demand/consumption profiles for four seasons are calculated using NN as shown in Figure 7.25. Note, the actual freshwater consumption at any time is assumed to be 5 times more than that shown in Figure 7.4.

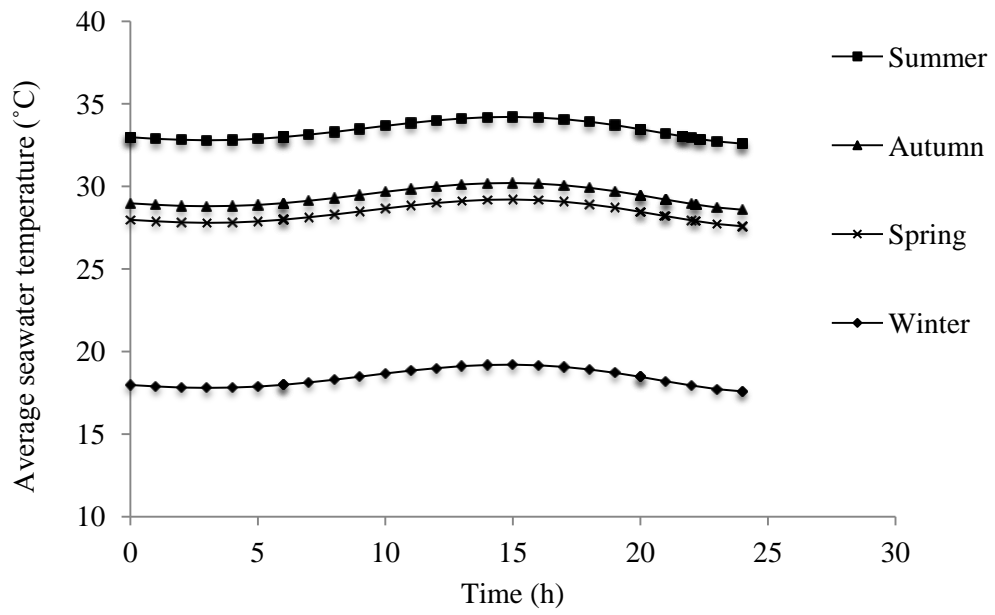


Figure 7.24 Seawater temperature Profiles for different season

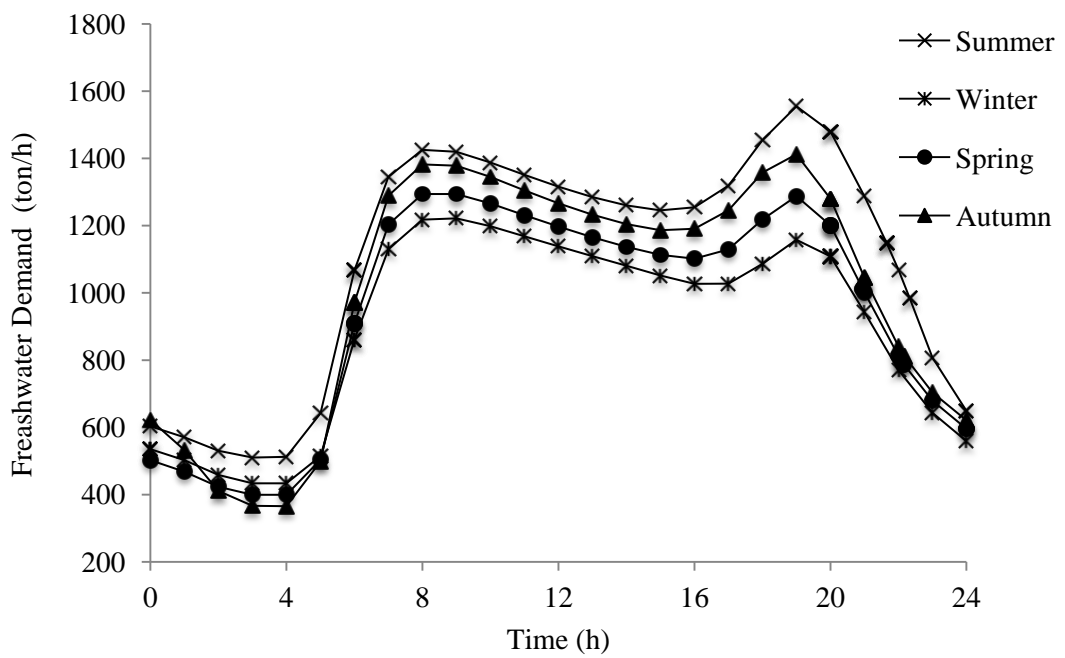


Figure 7.25 Freshwater consumption/demand profiles for different season

Table 7.8 summarises the cost of storage tank, capital cost of MSF process based on total number of stage, total operating cost, total cost on a daily basis and the optimum total number of stages for four seasons. Figure 7.26 illustrates the variations of total cost with different number of stages in different seasons. Figures 7.27 and 7.28 represent the optimum operating cost components in different seasons. Figure 7.29 represents the optimum recycle flow rate ( $R$ ) and make-up flow rate ( $F$ ) at discrete time intervals in different seasons. Figure 7.30 illustrates the steam temperature and demand/consumption profiles in different seasons.

It is noticed from the optimisation results that, the total daily cost and total number of stages required in summer season (Table 7.7 and Figure 7.26) are the highest due to higher seawater temperature and freshwater consumption (Figures 7.24, 7.25). In addition,  $F$  and  $R$  (Figure 7.29) and therefore total operating cost are higher in summer season. Although the steam consumption decreases slightly compared to the other seasons except winter season (Figure 7.28), the contribution of the other operating and capital costs are relatively higher (Figure 7.27). Figure 7.26 proves this fact in terms of minimum total cost as a function of total number of stages policy. Observation also shows that to meet the demand of variable freshwater in summer, there has to be an increase in total number of stages from 11 to 16 (compare summer and winter in Table 7.8). Observation also shows that the total cost has been increased by about 18% in summer season compared with that for winter season to meet the variable freshwater demand.

The optimised interval lengths within which  $R$  and  $F$  are optimised are found to be 6, 14 and 4h (Figure 7.29) within 24h operation. Figure 7.30 illustrates that the steam temperature and consumption for different seasons are low at night time (first interval) and approximately constant for all seasons except the winter season. The freshwater

demand is higher between morning to evening therefore steam temperature and consumption rate reach to maximum (second interval) except the winter season. At night time (8pm to midnight) when the freshwater demand drops, the steam temperature and consumption rate becomes considerably lower (third interval) for all seasons. Note, steam can not be supplied at the same temperature throughout the day for any season to meet fixed TBT and variable demand. Note, the highest steam cost is noted in autumn season and the lowest steam cost in winter season (Figure 7.28).

Table 7.8 Summary of optimisation results for all seasons

Season	N	STC (\$/d)	CPC (\$/d)	TOC (\$/d)	TDC (\$/d)
Summer	16	176.06	26750.10	21307.62	48233.67
Autumn	13	176.06	23372.75	21028.86	44577.61
Spring	12	176.06	22187.85	20316.55	42673.27
Winter	11	176.06	20967.75	19669.16	40810.63

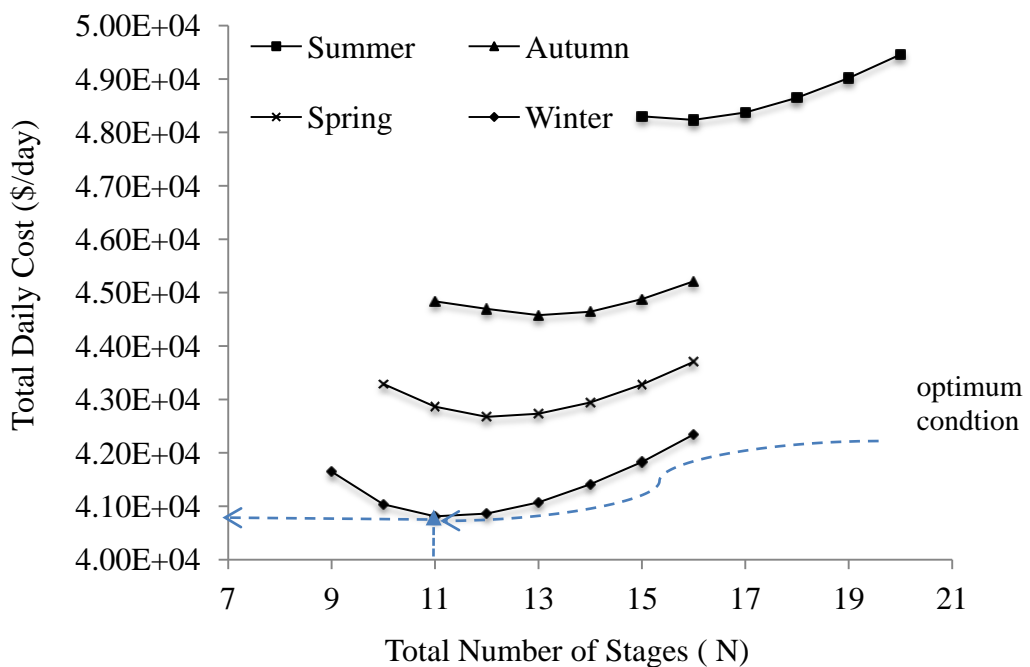


Figure 7.26 The variation of total annual cost with total number of stages at different season



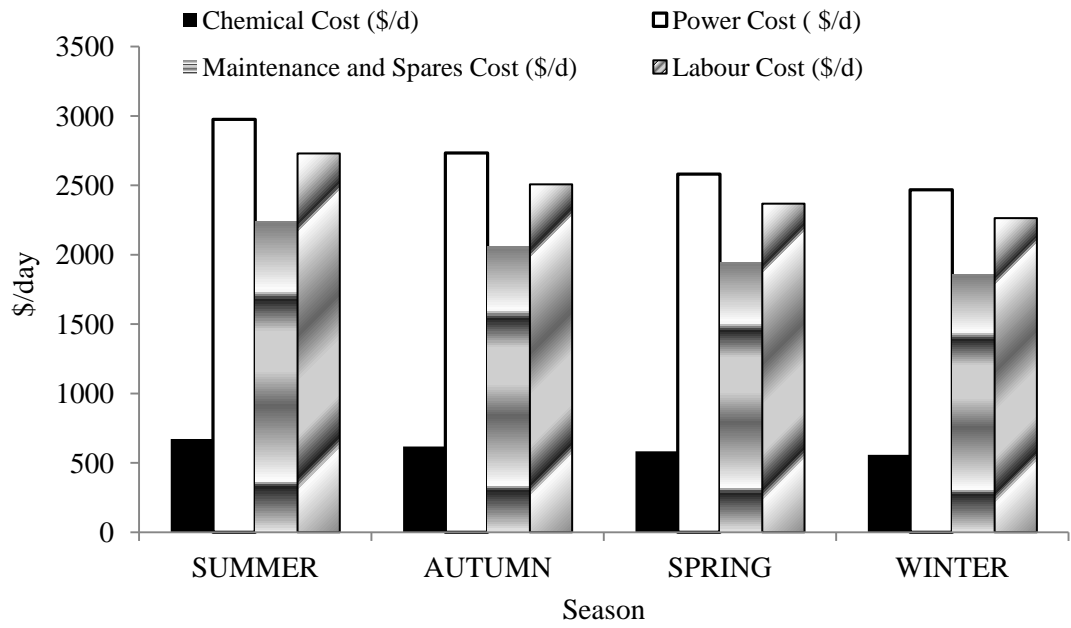


Figure 7.27 Variation of optimal operation cost at different season

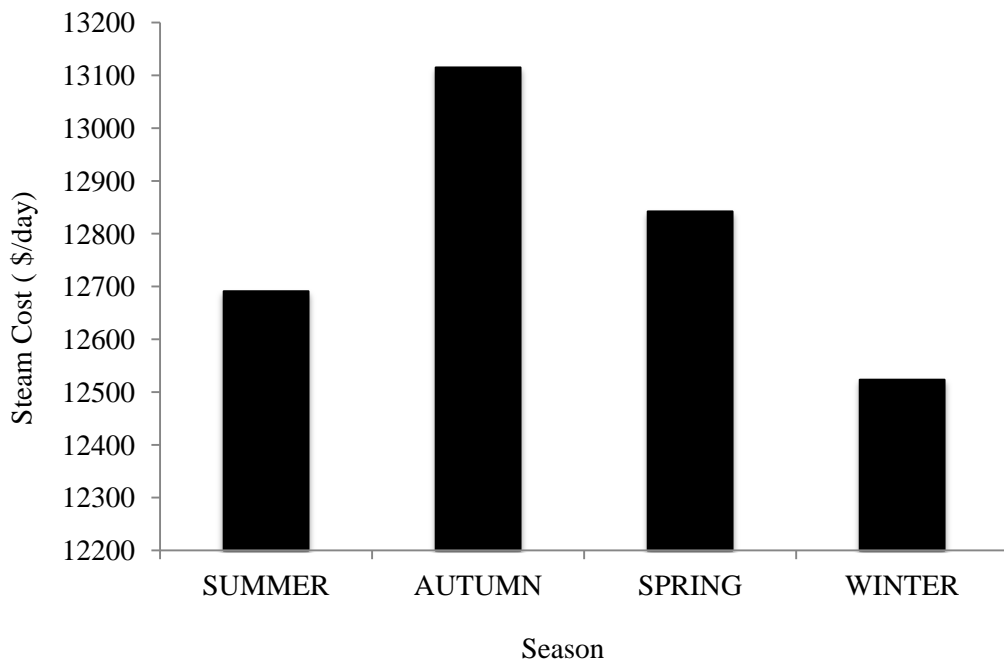


Figure 7.28 Variation of optimal steam cost at different season

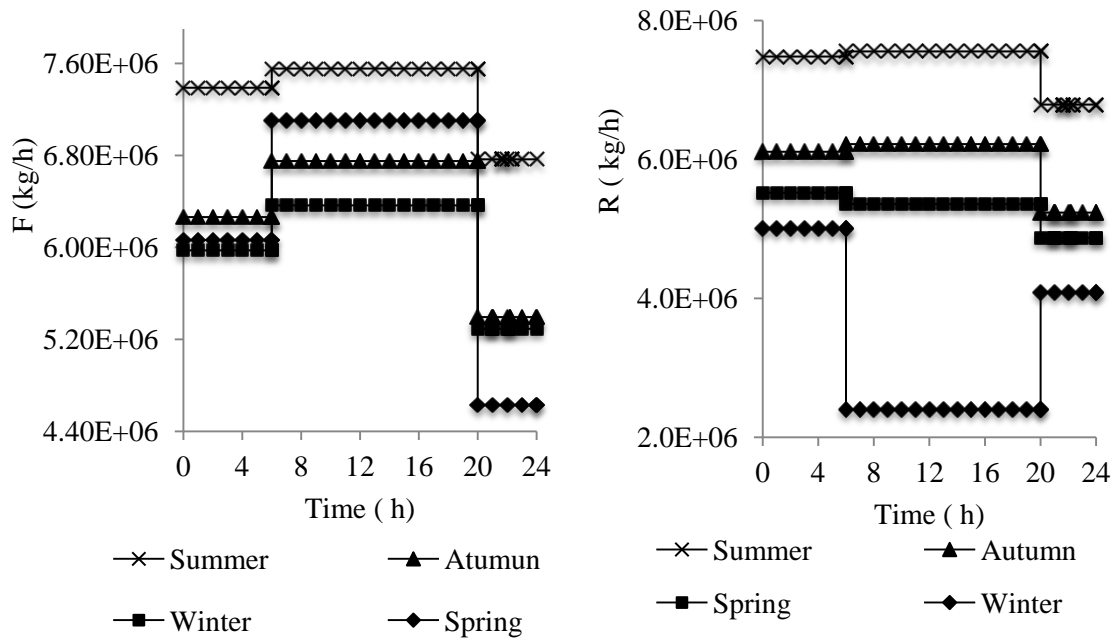


Figure 7.29 Optimum seawater makeup (F) and brine recycle flow rate (R)

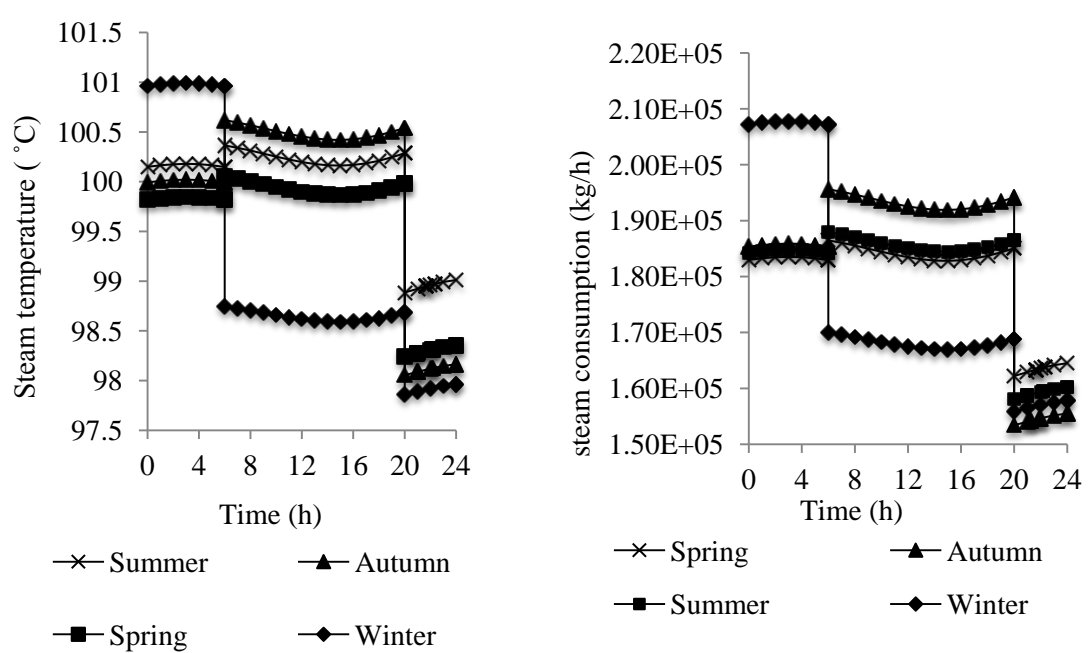


Figure 7.30 Variations of steam temperature and consumption profiles at different season

The dynamic storage tank levels for all seasons are shown in Figure 7.31. Freshwater production from MSF process, consumption (as per demand, Figure 7.25) and accumulated freshwater hold-up (in storage tank) profiles for all seasons are shown in Figure 7.32.

It can be seen from the results that when the freshwater demand is more than the freshwater production rate, the freshwater hold-up decreases (Figure 7.32), the storage tank level falls down (Figure 7.31) for all seasons. The opposite happens when the freshwater consumption rate is less than the freshwater production rate. The highest tank level  $h$  is noted at 8 am and the lowest level at 10 pm.

Based on the results, it can be proposed to design a plant with storage tank based on summer condition, make the design of individual flash units as stand-alone module and connect as many of them as needed due to variation in weather condition (Figure 7.24) to supply a variable amount of freshwater (Figure 7.25) throughout the day and throughout the year. This clearly shows the benefit of using the intermediate storage tank which adds the operational flexibility e.g. maintenance could be carried out without interrupting the production of water or full plant shut-downs at any time throughout the day and the year just by adjusting the number of stages and controlling the seawater make up and brine recycle. Note, although the optimum total number of stages in summer is 16, the minimum total number of stages that could be used to meet the demand 15 (Figure 7.26).

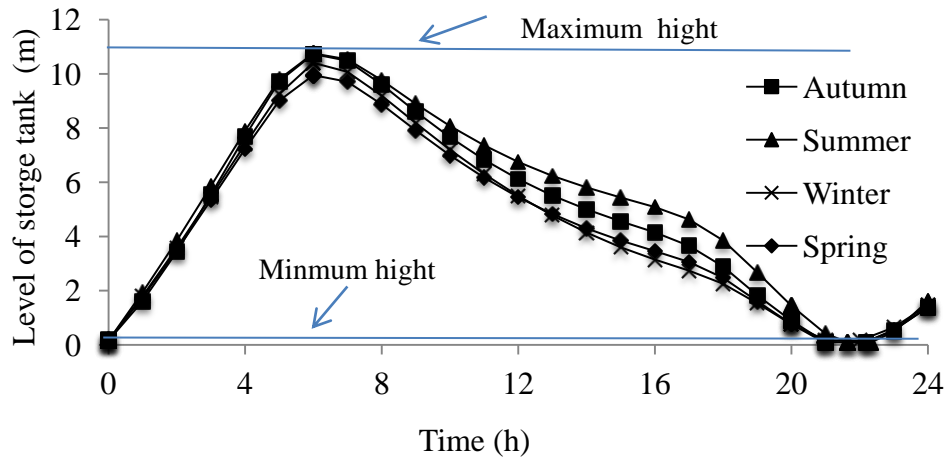


Figure 7.31 Storage tank level profiles for all seasons

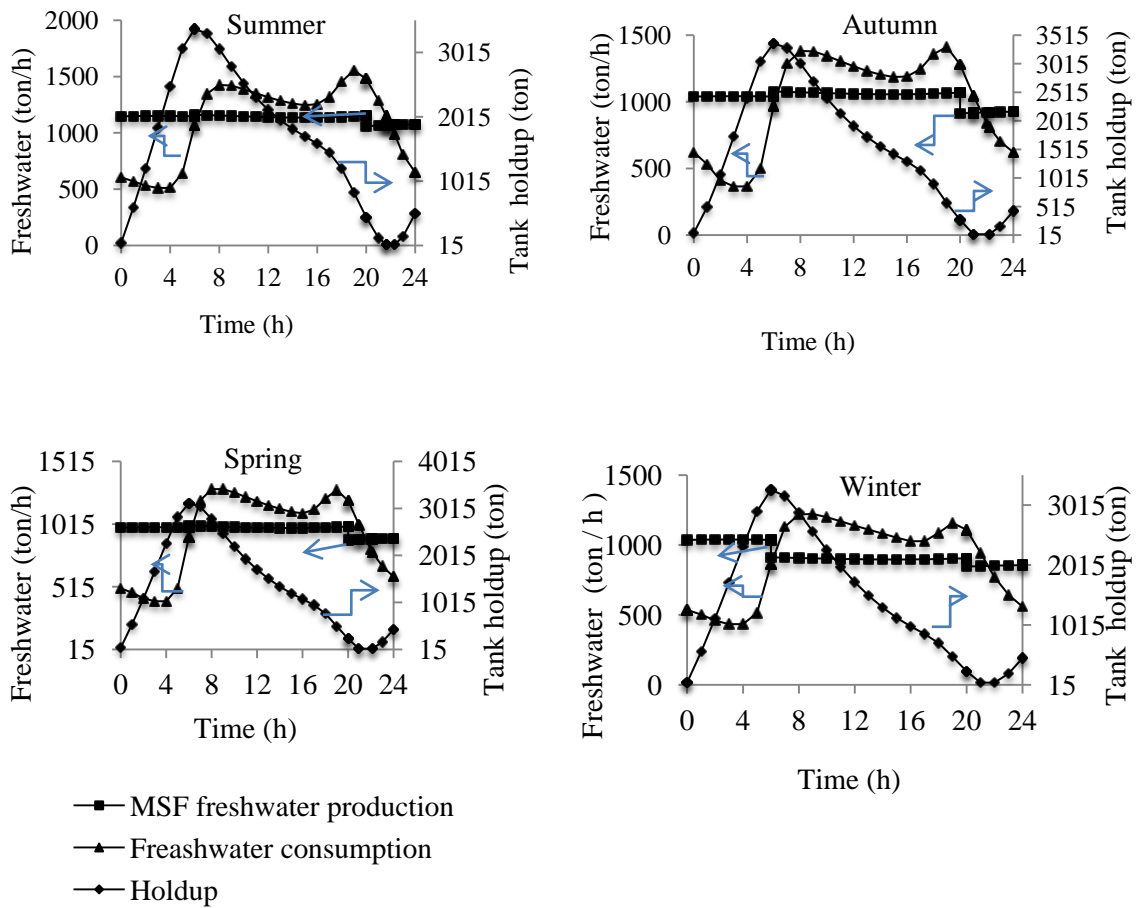


Figure 7.32 Variations of freshwater production of MSF, consumption and freshwater holdup during a day for all seasons

## 7.11 Conclusions

Here, based on actual data, neural network (NN) technique is used to develop a correlation which allows calculation of freshwater demand/consumption profile at different time of the day and seasons of the year. Also, a simple polynomial dynamic seawater temperature profile is developed based on actual data to predict seawater temperature at different time of the day and at different season. An intermediate storage tank is considered between the MSF process and the client to add flexibility in meeting the customer demand throughout the day and throughout the year. A steady state process model for the MSF process coupled with a dynamic model for the storage tank is developed within gPROMS modeling software.

For several process configuration (the design), the operation of the MSF desalination process at discrete time intervals are optimized, while minimizing the total operation costs. Although the optimization results show increase in total operating costs with decreasing total number of stages at fixed TBT, the intermediate storage tank adds flexible scheduling and maintenance of MSF desalination process.

The total number of flash stages and some significant operating parameters such as recycle brine and seawater make up at discrete time interval are optimized, minimizing the total daily cost (including capital cost component of the process and the storage tank and the operating cost) of the process for all seasons.

The optimization results show that summer operation requires the desalination process to use more flash stages than in other seasons to meet the variable demand of freshwater. This consequently demands higher  $F$  and  $R$  at higher seawater temperature and freshwater demand during a day leading to higher total cost (daily) by about 18% in the summer season compared with that for winter season. Note, the steam cannot be

supplied at the same temperature throughout the day for any season to meet the variable demand with varying seawater temperature at fixed TBT.

The results clearly also show that the benefit of using the intermediate storage tank adds flexible scheduling and maintenance opportunity of individual flash stages and makes it possible to meet variable freshwater demand with varying seawater temperatures without interrupting or fully shutting down the plant at any-time during the day and for any season.

# Chapter 8

## Effect of Demister Separation Efficiency on the Freshwater Purity in MSF Desalination Process

### 8.1 Introduction

The purity of freshwater is very important for consumption by living beings and for industrial services such as boiler feed to produce steam and also as process and utility water and demister plays an important role in determining the purity of freshwater coming from MSF desalination plants. In MSF process (Figure 8.1), demisters are used to reduce the mist with salt passing to distillate trays. They are made of a metal mesh made of thin wires (stainless steel) installed inside the evaporator flash chamber. The wire mesh is made by knitting wires to form many layers as shown in Figure 8.2. These wire-meshes are placed horizontally facing the stream of vertically rising vapour (Figure 8.3). The wire which is used in the demister typically has a diameter in between 80-280 $\mu$ m and the typical thickness used for the pads is in the 65-150-mm range (Brunazzi and Paglianti, 1998).

Water with soluble salts allows deposits to form at high temperature which is commonly referred to as 'scale' or 'foul'. However, scale formation also occurs on demister sheets in the flash stage during operation due to instability in some parameters (such as brine level, anti-foam, anti-scale injection rate and concentration factor, etc.) (Fatha and Ismail, 2008). Scale formation is mainly caused by crystallization of calcium and magnesium hydroxides.

The efficiency of the demister depends markedly on two factors: (a) the distance between the top of the brine pool and the bottom of the demisters. (b) the demister area (Ettouney, 2005). In addition, the performance of the demister, also depends on

many design variables such as: void fraction, wire diameter, packing density, pad thickness and material of construction (El-Dessouky et al., 2000).

The final purity of freshwater depends on the brine vapour weight ratio reaching the demister and the separation efficiency of the demister. A small variation of efficiency can have a large influence on the final freshwater purity (Sommariva et al., 1991). As the vapour/droplets flow through the demister, the droplets are captured and accumulated on the surface of the demister wires and results in the formation of a small thin brine film (Ettouney, 2005).

Sommariva et al. (1991) described different theories which regulate the salt entertainment and the distillate purification in both clean and fouled demister conditions and supported them with real plant (19 stages) experimental data at seawater temperature 32 °C. Ettouney (2005) focused on droplet and mist re-entrainment from the demister, which occurs at high vapor velocities. He used a clean demister in a 24 stage MSF process.

For fixed top brine temperature, this chapter studies the effect of separation efficiency of demister on the final purity of freshwater for both clean and fouled demister with seasonal variation of seawater temperatures. The objectives were to (i) find the variation of the purity of produced freshwater when the plant operates with clean and fouled demister (ii) estimate the required total number of stages to maintain the purity of freshwater at the desired level using clean demister.



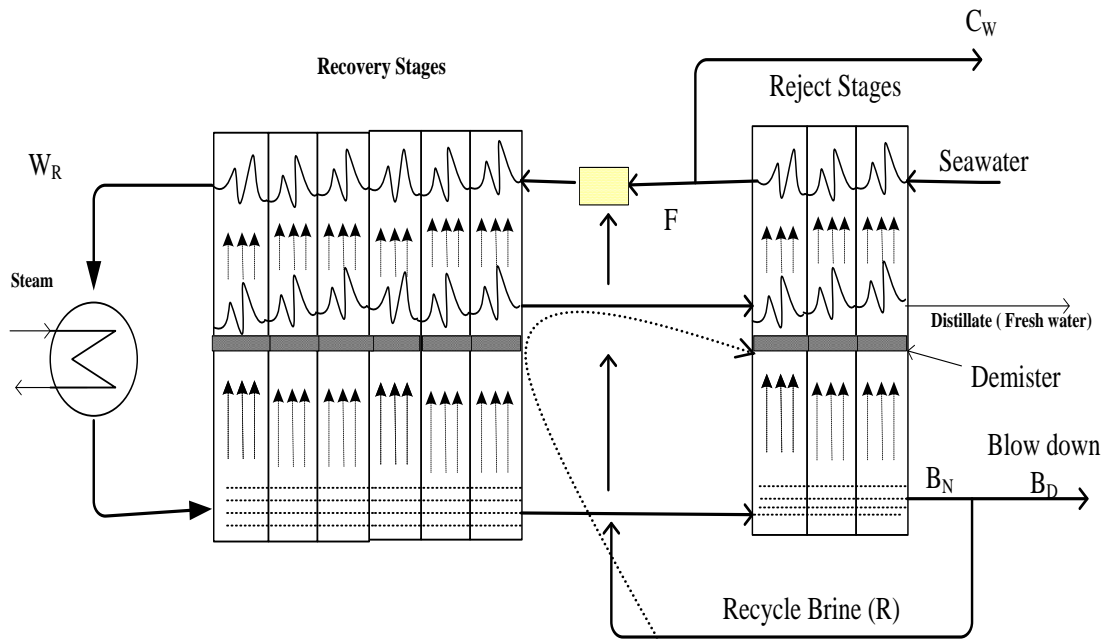


Figure 8.1 A typical MSF Process



Figure 8.2 Wire-mesh mist eliminator (Fatha and Ismail, 2008)

## 8.2 Demister Model

Models for flash chamber, brine heater, demister, splitter, etc. are developed and connected via a high level modelling language using gPROMS. With reference to Figure 8.1, a typical MSF desalination process mathematical model description is therefore based on mass balance, energy balance, heat transfer equations and supported by physical correlations are given in chapter 4. The theoretical demisters

efficiency correlations and the distillate purity calculations for both clean and fouled conditions (Figure 8.3) are given in the following.

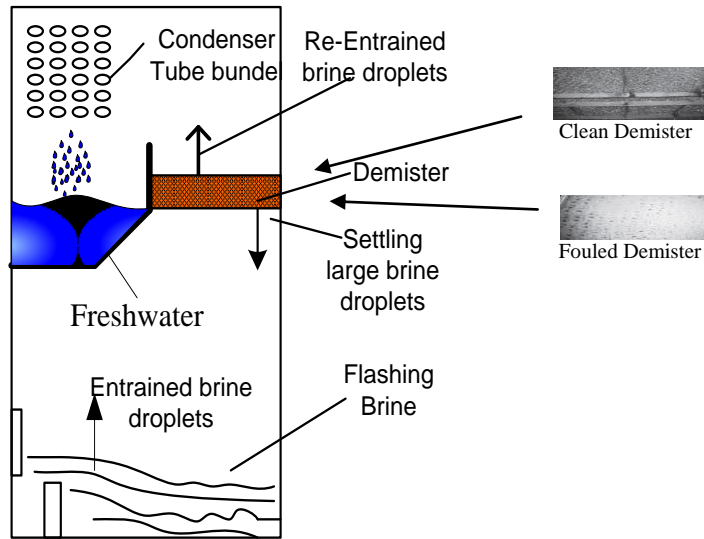


Figure 8.3 typical flash stage

Maximum Liquid Entrainment Mechanism (Sommariva et al., 1991)

$$E = \begin{cases} 34100 \times [G^3 V^2 2.205 \cdot 10^{-8}]^{-0.157} & \text{if, } G^3 V^2 2.205 \cdot 10^{-8} < 347 \\ 84 \times [G^3 V^2 2.205 \cdot 10^{-8}]^{0.87} & \text{if, } G^3 V^2 2.205 \cdot 10^{-8} > 347 \end{cases} \quad (8.1)$$

E: Liquid entrained vapour ratio (ppm), G: specific evaporation (kg/h m<sup>2</sup>), V: vapours specific volume (m<sup>3</sup>/ kg)

Mass Balance (El-Dessouky et al., 2000)

$$M_{out} = M_{in} - \eta M_{in} \quad (8.2)$$

M<sub>in</sub> and M<sub>out</sub> are the mass of entrained brine droplet by the vapour in and out of the mist eliminator.

Separation Efficiency( η)

$$\eta = 1 - e \left( \frac{-v_s A_{ss} k_f \rho_v D_z}{v} \right) \quad (8.3)$$

$D_z$  is demister thickness for industrial ranges from 0.1m to 0.15 m and  $k_f$  is a shape coefficient.

$k_f$  for clean condition (Sommariva et al., 1991)

$$k_f = \left(1 - \frac{1}{\tau}\right) 0.6233 \left[1 - 2.168 e^{(-0.0127 v_s^{3.05} + 0.005)}\right] \quad (8.4)$$

$\tau$  is the ratio between the length of the vapour path and the thickness of the packed bed.

A typical value ( $\tau$ ) for such in wire packed bed is 1.3 .

$k_f$  for fouled condition (Sommariva et al., 1991)

$$k_f = \left(1 - \frac{1}{\tau}\right) 0.6233 \left[1 - 2.168 e^{(-0.064 v_s^{1.675} + 0.005)}\right] \quad (8.5)$$

Superficial Vapour Velocity  $v_s$  (m/sec) (Sommariva et al., 1991)

$$\text{Ln} \left[ \frac{v_s^2 A_{ss} \mu_l^{0.2} \rho_v}{g \epsilon^3 \rho_l} \right] = -4.995 - 0.7252 \text{Ln} \left[ \left(\frac{\rho_v}{\rho_l}\right)^{0.5} \frac{L}{G} \right] - 0.03016 \left[ \text{Ln} \left( \left(\frac{\rho_v}{\rho_l}\right)^{0.5} \right) \frac{L}{G} \right]^{0.2} \quad (8.6)$$

$A_{ss}$  is demister specific surface ( $\text{m}^2/\text{m}^3$ ) for industrial demister  $A_{ss}$  ranges from 140 to 300  $\text{m}^2/\text{m}^3$  and  $\epsilon$  is demister void fraction for industrial ranges from 0.975 to 0.99 (El-Dessouky et al., 2000)

### 8.3 Case Study

Using the process model (presented in Chapter 4), a series of simulations has been carried out to study the effect of the separation efficiency of demister with seasonal variation of seawater temperatures on the final purity of freshwater. In this work, the freshwater demand ( $D_f = 9.35 \times 10^5$  kg/h), and top brine temperature (TBT = 90 °C) are fixed. The feed seawater flow rate is  $1.13 \times 10^7$  kg/h with salinity 5.7 wt% and seawater makeup is  $5.62 \times 10^6$  kg/h. The specifications and constant parameters of MSF process and the demister features are shown in Tables 8.1 and 8.2.

Table 8.1 Constant parameters and input data

	$A_j/A_H$	$ID_j/ID_H$	$OD_j/OD_H$	$f_j/f_{bh}$	$w_j/L_H$	$H_j$
Brine heater	3530	0.022	0.0244	0.159	12.2	--
Recovery stage	3995	0.022	0.0244	0.120	12.2	0.457
Rejection stage	3530	0.0239	0.0254	0.020	10.7	0.457

Table 8.2 Demister features

Free volume (void fraction, $\varepsilon$ ) = 97.5 %
Demister thickness ( $D_z$ ) = 0.15m
Demister specific surface ( $A_{ss}$ ) = 300 m <sup>2</sup> /m <sup>3</sup>

## 8.4 Results and Discussions

### 8.4.1 Variation in the Product Salinity for an MSF Process for Different Seawater Temperature

The total number of stages is 16. Figure 8.4 shows the variations in the product salinity for clean and fouled demister situation. For clean demister the simulation results show that the freshwater purity was within the allowable limits (salt concentration below 25 ppm) for seawater temperature above 20 °C. Rapid increase of the product salinity occurs as the intake seawater temperature drops to 20 and 15°C. Most of the salinity increase in the product water occurs in the last stages for both cases. This is due to lower stage temperatures, reduction in the stage pressure, decreases in the vapour density and increases in the vapour velocity (Figures 8.5, 8.6). Note, for a given seawater temperature fouled demister situation will lead to significant decrease in purity of fresh water (e.g. at seawater temperature 35°C the product salinity is 3.0 ppm with clean condition while it is 30 ppm for fouled demister).

The variation of the demister efficiency for both clean and fouled demister throughout the stages is shown in Figure 8.7 for seawater temperature 30°C. The demister

efficiency is at maximum value in the first stage and then decrease with stages. Note, the lowest demister efficiency is noted in the last stage (75%) for fouled demister.

The variation of product salinity with seawater temperature is shown in Figure 8.8. It can be seen that for both conditions the purity is increased with increased seawater temperature and decrease as the seawater temperature decreases. However, the maximum purity for both conditions is in summer season at maximum average seawater temperature about 35 °C.

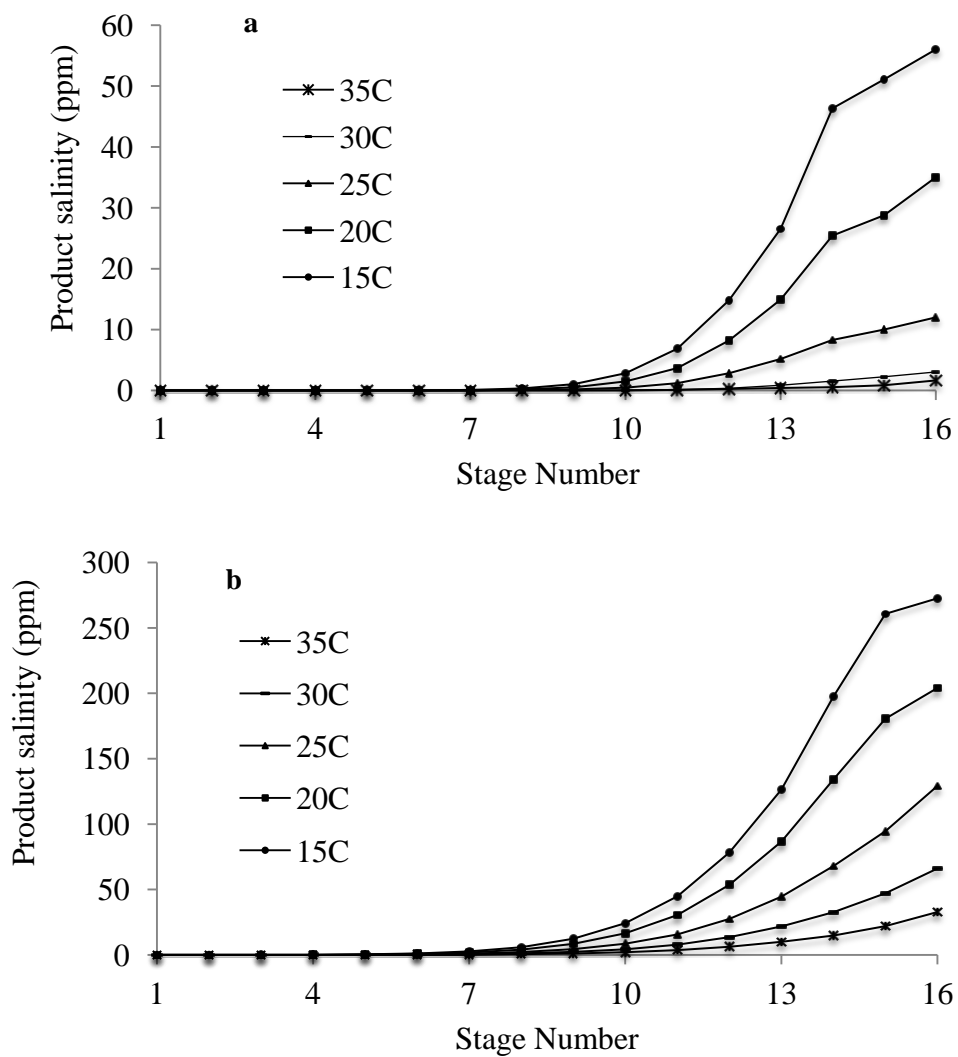


Figure 8.4 The variation in the product salinity as function of the intake seawater temperature and number of stage for (a) clean demister, (b) fouled demister

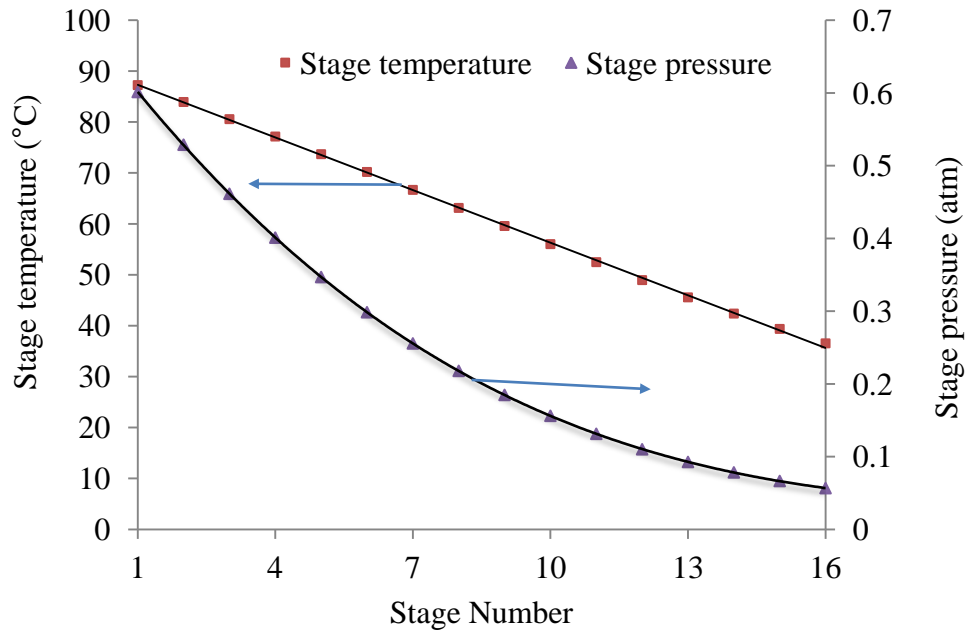


Figure 8.5 Temperature and pressure variation through stages

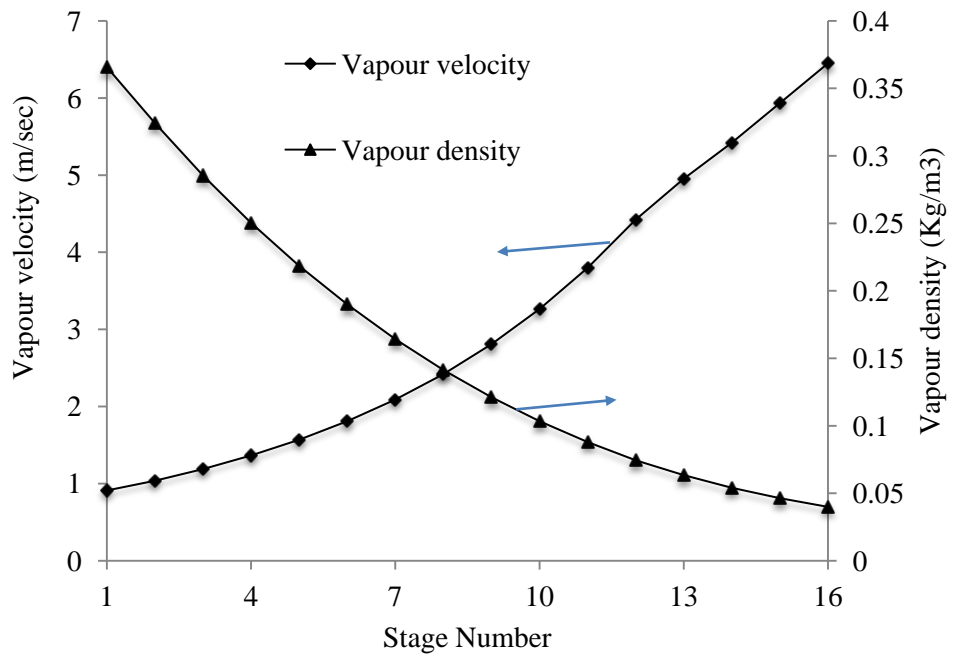


Figure 8.6 Variation of vapour velocity and density through stages

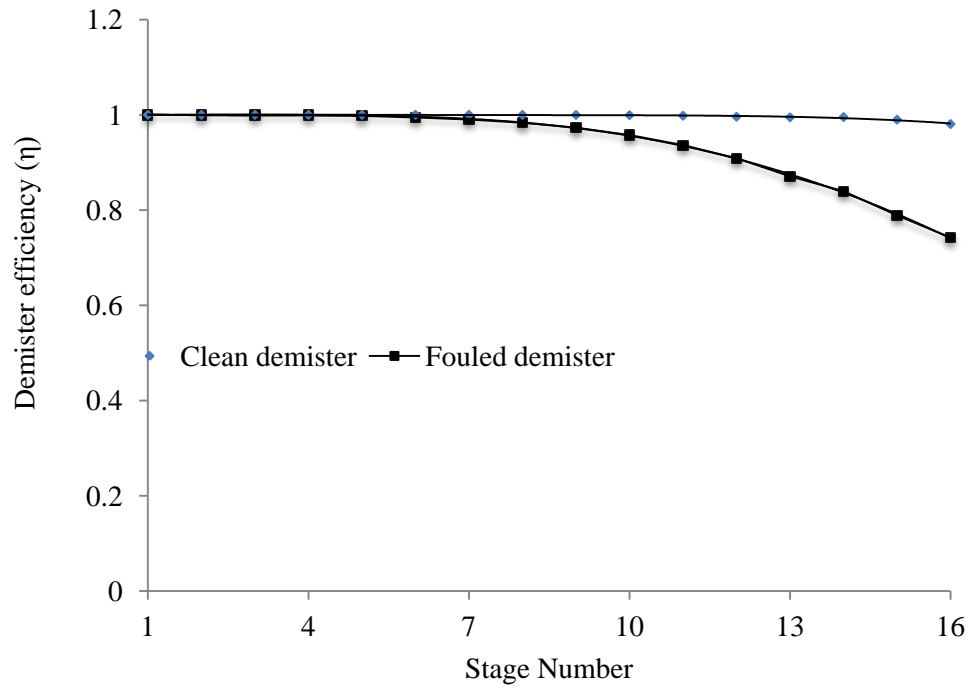


Figure 8.7 The variation in the demister efficiency through stages at seawater temperature (30°C)

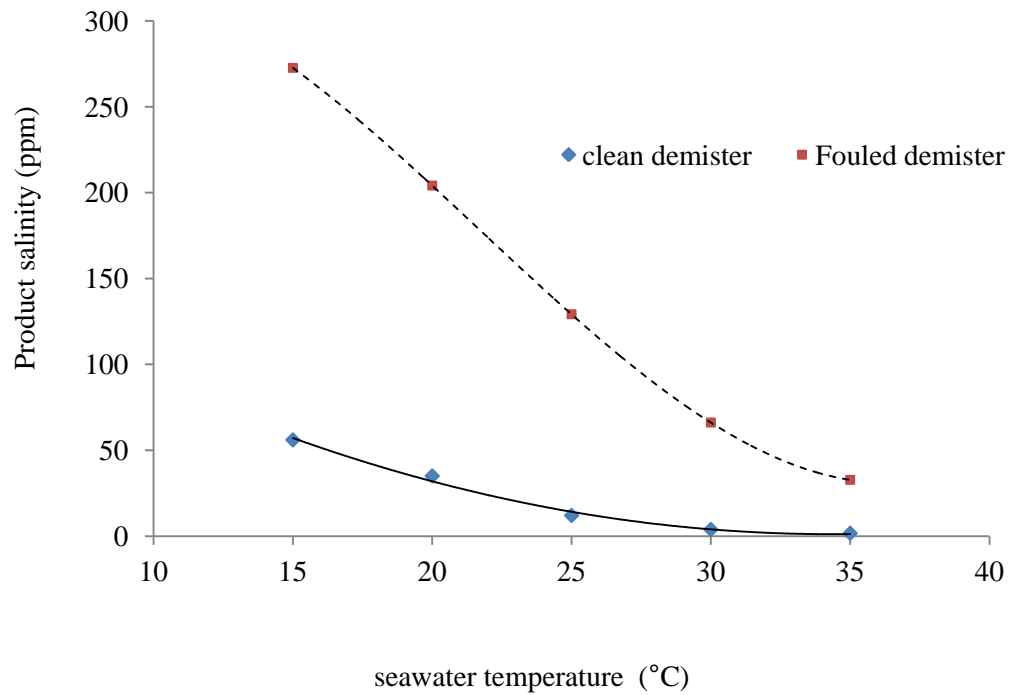


Figure 8.8 The variation in the product salinity with seawater temperature

#### **8.4.2 Effect of Total Number of Stages on the Purity of Freshwater for Clean Demister**

The sensitivity of total number of stages on the purity of freshwater for different seawater temperature (20 and 35 °C), fixed demand ( $D_j = 9.35 \times 10^5$  kg/ h) and fixed TBT = 90°C are shown in Figure 8.9. The total number of stages is varied from (14, 15, 16, 17, 19 and 21). In all cases the rejection section is consisted of 3 stages and the number of stages in the recovery section is only varied. The higher the number of stages the lower the product salinity. This means that the salinity can be lowered at the expense of capital cost. The amount of salinity of freshwater in 20°C is about 7 times higher than in 35°C at any total number of stages. It is interesting to reflect that for fixed freshwater demand and TBT at low seawater temperature the higher number of stages to maintain high purity of fresh water at the desired level.

Finally for 3 different sets of plant configuration (10, 14 and 19 stages) a series of simulation is carried out to study the effect of variation of freshwater demand on the purity at fixed average seawater temperature (20 °C winter season) and fixed TBT = 90°C (Figure 8.10). It can be seen that, as the demand of freshwater increases, for a given design of the plant, the purity of freshwater decreases. Note, the results of the optimization problem (OP2) in Chapter 6 presented in Table 6.4 and Figure 6.3 showed the minimum number of stages (NR=10) in December (seawater temperature = 20 °C winter season) to produce  $7.0 \times 10^5$  kg/h of freshwater with product salinity zero ppm. However, according to Figure 8.10, the salinity with  $7.0 \times 10^5$  kg/h of freshwater production is 30 ppm and is within tolerance (< 250 ppm for drinking purpose (Al-Khudhiri, 2006))



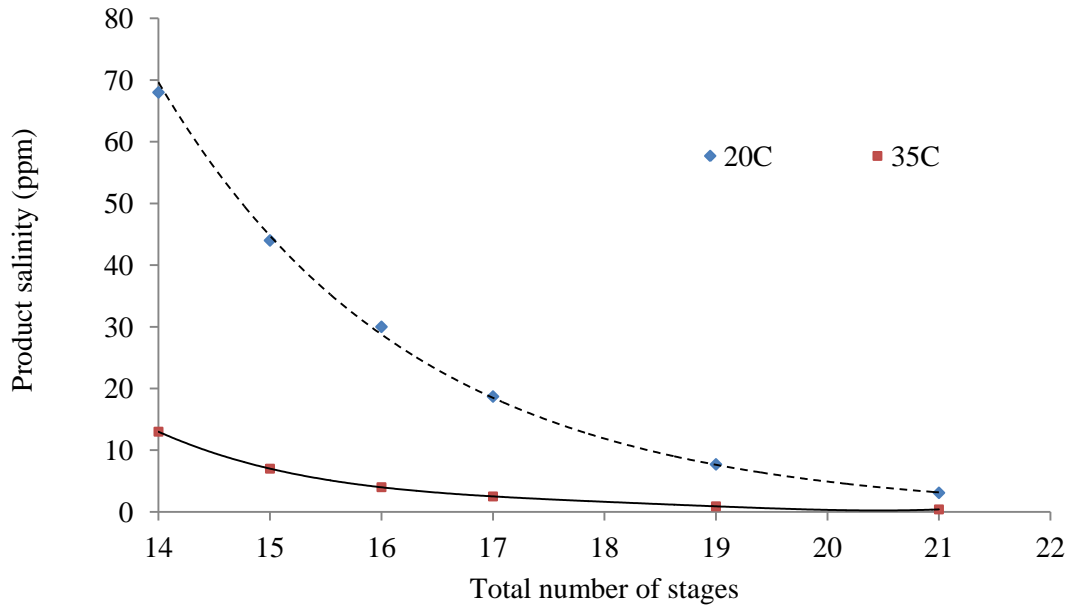


Figure 8.9 The variation in product salinity with total stages at 35°C and 20°C for clean demister

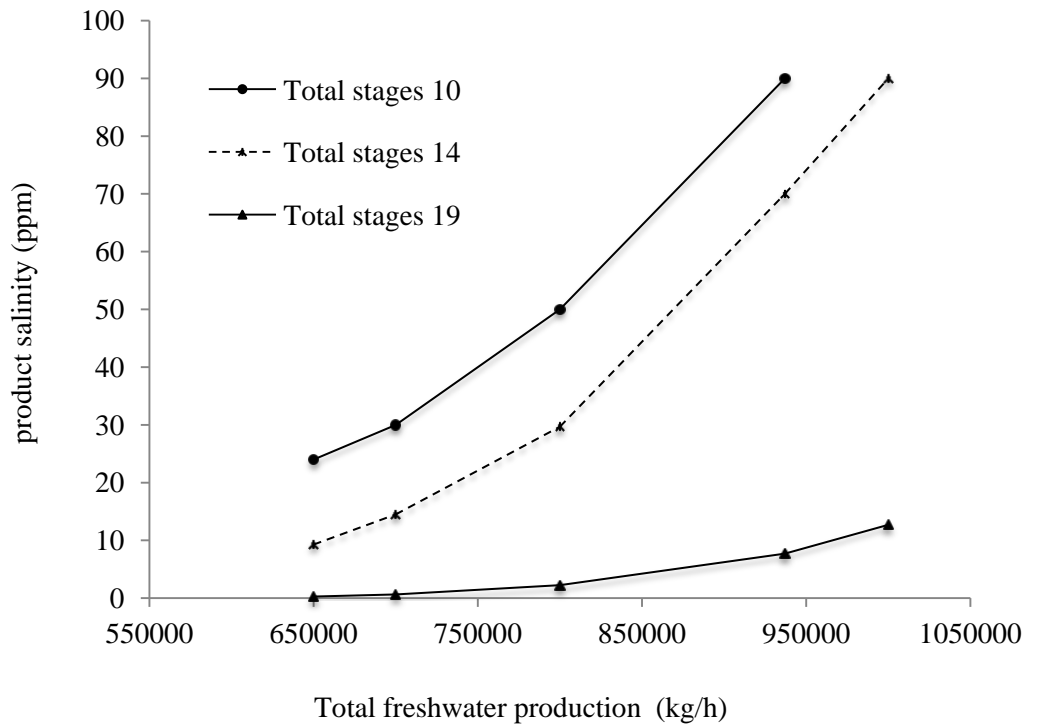


Figure 8.10 The variation in the product salinity with total fresh water production at 20°C for clean demister

## 8.5 Conclusions

With seasonal variation of seawater temperature, the effect of demister separation efficiency on the final purity of freshwater for both clean and fouled demister conditions at fixed TBT and freshwater demand has been studied here.

The results show that the product salinity remains within the desired limit (below 25ppm) as long as the seawater temperature remains above 20 °C. Rapid decreases in product purity occur as the seawater temperature drops below 20 °C. Most of the salinity increase in the product water occurs in the last stages of the process. This is due to lower stage temperatures, reduction in the stage pressure, decreases in the vapour density and increases in the vapour velocity.

The simulation results also show that the purity of freshwater is affected by the total number of stages. It is observed that with top brine temperature and fresh water demand being fixed, the total number of stages needs to increase when the seawater temperature decreases. This is required to maintain the purity of freshwater production at the desired level for industrial services and human consumption.

# Chapter 9

## Conclusions and Future Work

### 9.1 Conclusions

Desalination processes produce high quality freshwater from sea, estuary or brackish water. As highlighted in Chapter 1 and 2, several desalination technologies exist in the world and among various desalination processes, the multistage flash (MSF) desalination process is a thermal process and is a major source of fresh water around the world (EL-Dessouky and Ettouney, 2002).

Fouling/scaling and corrosion lead to more costly designs and operating problems in seawater desalination. The fouling tendency requires about 20 to 25% excess design allowance and the design of the heat transfer area constitutes about 30% of the total cost (Gill, 1999). Simulation and optimisation help in getting better operation of MSF processes leading to high performance and low operating costs. This research was focused on the optimal design and operation of MSF desalination process with brine heater and demister fouling; flexible design operation and scheduling under variable demand and seawater temperature using gPROMS.

The following conclusions are drawn from this work.

#### *Chapter Five*

A simple linear dynamic brine heater fouling factor profile is developed based on actual MSF plant operation data. gPROMS modelling tool has been used to model and simulate MSF desalination process. The simulation results using the gPROMS modelling were in good agreement with the simulation results reported by published results. The model was then used to study the sensitivity of two parameters: brine

heater fouling factor, which is affected by heat transfer efficiency process by plugging the exchanger and the seawater temperatures, which is subject to seasonal variation on the plant performance such as top brine temperature, steam consumption, and brine flow rate recycling with fixed water demand and fixed steam temperature.

For a given brine heater fouling factor, the simulation results clearly show that it is possible to supply fixed demand fresh water throughout the year with varying seawater temperature and brine heater fouling factor. However, higher top brine temperature requires a lower amount of steam at any given seawater temperature due to lower brine heater fouling factor.

An interesting observation shows that even though the plant has high brine heater fouling factor with fixed steam temperature, it can be operated successfully at lower top brine temperature (TBT) with higher steam consumption and higher brine recycling. Even in summer time the MSF process could fulfil the demand of fresh water by operating at lower top brine temperature, higher steam consumption and higher brine recycle flow rate. This will reduce the scale formation rate and therefore frequent shut downs of the plant for cleaning will be lower. Therefore, specific energy consumption, operating costs and maintenance will be lower.

### *Chapter six*

The sensitivity of the fouling factor on the optimal performance of MSF process is studied at discrete time zone corresponding to different seawater temperature. Two different operations in terms of TBT and anti-scale dosing were considered. With freshwater demand fixed throughout the year, for each discrete time interval (season), the operating parameters such as make up flow rate, brine recycle flow rate and steam temperature are optimized while an objective function (total monthly operation costs of MSF desalination).

The optimization results provided that steam temperature strongly depends on brine heater fouling factor and cannot supply the steam at the same temperature during a year. However, steam consumption and brine flow rates increase as seawater temperature increases.

The optimisation results clearly show that as the scale builds up with time, there will be increase in the steam temperature, steam consumption, brine flow rates, total operating costs and decrease in GOR even though the seawater temperature remains the same throughout the year. The variation in seawater temperature throughout the year together with changes in the brine heater fouling factor adds further changes in the operating parameters, costs and GOR. High TBT and anti-scaling dosing although preferable in terms of steam consumption and GOR, this will lead to further environmental impact. Furthermore, higher TBT operation will lead to high costing materials for construction.

### *Chapter seven*

Accurate estimation of freshwater demand/consumption profile at different time of the day and at different season is developed using neural network (NN) technique. The NN based correlation predicted the freshwater demand/consumption (day/night) and the data from the literature was very closely. In addition, the correlation predicted the freshwater demand/consumption based on (time, season) very well even outside the range of training, validation or testing. Also, based on actual data from the literature a simple polynomial dynamic seawater temperature profile is developed to predict seawater temperature at different time of the day and for main seasons.

An intermediate storage tank was added between the MSF process and the users to add flexibility in meeting the client demand throughout the day and for main seasons. In this work, the high level modelling language (gPROMS modelling software) has been

used to model an MSF process embedding NN based correlation coupled with a dynamic model for the storage tank.

An optimisation problem was formulated to optimise the number of stages, and few significant operating parameters such as recycle brine flow and make up seawater at discrete time intervals (assumed piecewise constant) while minimizing an objective function (minimizing the total daily cost) with fixed TBT, variable freshwater demand/consumption and seasonal variation of seawater temperature. However, the results in terms of minimizing the total daily cost indicated that summer operation requires the desalination process to use more flash stages than in other seasons to meet the variable demand of freshwater. In addition, it can be noted that the plant with intermediate storage tank can operate successfully to achieve clear benefits for more flexible scheduling of individual flash stages and maintenance opportunity, even though the operation provide freshwater at a variable demand during a day with changeable seawater temperature. This will reduce the interrupting or fully shutting down the plant at any-time during the day and for any season. It is interesting to note that the storage tank adds significant flexibility to the operation and maintenance of the process while coping with the variable freshwater demand/consumption. The optimisation framework presented in this work can be applied to any freshwater demand profile with any seawater temperature profile.

### *Chapter eight*

This work was devoted to study the sensitivity of the demister separation efficiency on the final purity of freshwater for both clean and fouled demister conditions. The results are shown as a function of the intake seawater temperature. The product salinity remains within limits at values below 25ppm as long as the intake seawater temperature is above 25°C. Another feature of these results is that the purity of

freshwater production is decreased when the plant is operated for a fouled demister with a minimum of intake seawater temperature.

The interaction of design (total number of stages) and the purity of freshwater in the context of fixed freshwater demand and fixed TBT with different seawater temperature were studied. The results showed that the purity of freshwater is affected by the total number of stages i.e. as the number of stages increase the purity increases. However, it is interesting to reflect that the total number of stages increase as the seawater temperature decreases to maintain the purity of freshwater production at the desired level.

## **9.2 Future Work**

Some suggestions for future are outlined below

- The result presented in this thesis is dependent on the models used which may not be completely in agreement with the real plant. Therefore, the results achieved in this thesis should be validated experimentally in the future work.
- The correlations of seawater properties such as fouling and corrosion by using neural network based correlations can be developed
- The model can be updated to include the effect of recovery and rejection sections fouling factor with time on operation of MSF desalination process.
- Also the MSF process model can be further developed incorporating the effect of demister on purity of freshwater, condensable and non-condensable gas behaviour and corrosion behaviour.
- The correlation of dynamic brine heater fouling factor can be updated to include the effect of many variables such as temperature, pH, concentration of

bicarbonate ions, and rate of CO<sub>2</sub> release, concentration of Ca<sup>2+</sup> and Mg<sup>2+</sup> ions, and total dissolved solids.

- Steady state and dynamic optimization of design and operation with rigorous model of MSF desalination process for material selection such as carbon steel, copper-nickel, steel alloys etc., maintenance and scheduling/operation for variable water demand (day/night) can be studied.
- A steady state process model for the MSF process coupled with a dynamic model for the storage tank can be validated with real plant data gPROMS validation tool (Experimental Design tools).
- A dynamic model for the MSF process coupled with a dynamic model for the storage tank can be developed for control design and studies.
- Variable demands of freshwater with changing seawater temperature (during the day and during the year) could be built up in optimisation framework considering hybrid desalination (Mixed MSF, RO) process with intermediate storage.
- Fixed and variable demand (during the day and during the year) could be built up in optimisation framework considering the anti-scaling agent as an additional optimisation decision variables.



## Reference

Abdel-Jabbar, N. M., Qiblawey, H. M., Mjalli, F. S. and Ettouney, H. (2007). Simulation of large capacity MSF brine circulation plants, *Desalination*, **204**, 501-514.

Abdel-Jawad, M. and AL-Tabtabael, M. (1999). Impact of current power generation and water desalination activities on Kuwaiti marine environment. Proceedings of IDA World Congress on desalination and water reuse, San Diego, USA.

Al-Abri, M. and Hilal, N. (2008). Artificial neural network simulation of combined humic substance coagulation and membrane filtration, *Chemical Engineering Journal*, **14**, 127-34.

AL-Ahmad, M. and Aleem, F. A. (1994). Scale formation and fouling problems and their predicted reflection on the performance of desalination plants in Saudi Arabia, *Desalination*, **96**, 409-419.

AL-Anezi, K. and Hilal, N. (2007). Scale formation in desalination plants: effect of carbon dioxide solubility. *Desalination*, **204**, 385-402.

Al-Bakeri, F. and El Hares, H. (1993). Experimental optimization of sponge ball cleaning system operation in Umm AI Nar MSF desalination plants, *Desalination*, **94**, 133-150.

AL-Deffeeri, N. S. (2007). Heat transfer measurement as a criterion for performance evaluation of scale inhibition in MSF plants in Kuwait, *Desalination*, **204**, 423-436.

Al-Khudhiri, A. I. (2006). Optimal Design of Hybrid MSF/RO Desalination Plant. Master thesis. University of Kingdom of Saudi Arabia King Saud.

AL-Odwani, A., Carew, J., Al-Tabtabaei, M. and Al-Hijji, A. (2001). Materials performance in SWRO desalination plant at KISR research and development program, *Desalination*, **135**, 99-110.

AL-Rawajfeh, A. E. (2008). Simultaneous desorption–crystallization of CO<sub>2</sub>–CaCO<sub>3</sub> in multi-stage flash (MSF) distillers, *Chemical Engineering and Processing*, **47**, 2262–2269.

AL-Rawajfeh, A. E., Glade, H. and Ulrich, J. (2005). Scaling in multiple-effect distillers: the role of CO<sub>2</sub> release, *Desalination*, **182**, 209- 219.

AL-Sahali, M. and Ettouney, H. (2007). Developments in thermal desalination processes: Design, energy, and costing aspects, *Desalination*, **214**, 227-240.

Al-Sofi, M. A. (1999). Fouling phenomena in multi stage flash (MSF) distillers, *Desalination*, **126**, 61-76.

AL-Sofi, M. A., Al-Hussain, M. A. and Al-Zahrani, S. G. (1987). Additive scale control optimization and operation modes, *Desalination*, **66**, 11-32.

Alvisi, S., Franchini, M. and Marinelli, A. (2007). A short-term pattern-based model for water-demand forecasting, *Journal of Hydroinformatics*, **91**, 39-50.

Aly, N. H. and El-Fiqi, A. (2003). Thermal performance of seawater desalination systems. *Desalination*, **158**, 127-142.

Aly, N. H. and Marwan, M. A. (1995). Dynamic behaviour of MSF desalination plants, *Desalination*, **101**, 287-293.

Aminian, A. (2010). Prediction of temperature elevation for seawater in multi-stage flash desalination plants using radial basis function neural network, *Chemical Engineering Journal*, **162**, 552–556

Aziz, N., Mujtaba, I. M. and Hussain, M. A. (2001). ‘Set point tracking in batch reactor: Use of PID and Generic Model Control with Neural Network Techniques’. *Application of Neural Network and other Learning Technologies in process Engineering* (Eds I. M. Mujtaba and M. A. Hussain Imperial College Press, London, pp 217-2424.

Beamer, J. H. and Wilde, D. J. (1971). The simulation and optimization of a single effect multi-stage flash desalination plant. *Desalination*, **9**, 259-275.

Bomberger, J. D., Seborg, D. E. and Ogunnaike, B. A. (2001). ‘ RBFN identification of an industrial polymerisation reactor model.’ *Application of Neural Network and other Learning Technologies in process Engineering* (Eds I. M. Mujtaba and M. A. Hussain Imperial College Press, London, pp 23-48.

Borsani, R. and Rebagliati, S. (2005). Fundamentals and costing of MSF desalination plants and comparison with other technologies, *Desalination*, **182**, 29-37.

Brunazzi, E. and A. Paglianti, (1998). Design of Wire Mesh Mist Eliminators,’ *AIChE J.*, **44**, 505.

Buros, O. K. (2000). The ABC’S Second Edition, for the International Desalination Association, Riyadh, Saudi Arabia.

Chan, S. H. and Ghassemi, K. F. (1991). Analytical modelling of calcium carbonate deposition for laminar falling film and turbulent flow in annuli Part II Multispecies model. *ASME J Heat Transfer*, **113**, 741– 746.

Choi, Y. J., Han, S. K., Chung, S. T. and Row, K. H. (2007). Separation of Racemic Bupivacaine Using Simulated Moving Bed with Mathematical Model, *Biotechnology and Bioprocess Engineering*, **12**, 625- 633.

Cipollina, A., Mivale, G. and Rizzuti, L. (2007). Investigation of flashing phenomena in MSF chambers, *Desalination*, **216**, 183-195.

Clelland, W. and Stewart, J. M. (1966). The optimisation and design of large scale multi-stage flash distillation plants, *Desalination*, **1**, 61-76.

Coleman, A. K. (1971). Optimization of a single effect, multi-stage flash distillation desalination system, *Desalination*, **9**, 315-331

Cooper, K. G., Hanlon, L. G., Smart, G. M., Talbot, R. E. A. (1983). Model for the fouling of M.S.F. plants based on data from operating units *Desalination*, **47**, 37-42.

Darwish, M. A., El-Refae, M. M. and Abdel-Jawad, M. (1995). Developments in the multi-stage flash desalting system, *Desalination*, **100**, 35-64.

Delene, G. and Ball, S. J. (1971). A digital computer code for simulating large multi-stage flash evaporator distilling plant dynamics, Oak Ridge National Laboratory Report, ORNL-TM-933.

E1-Dessouky, H. and Bingulac, S. (1996). Solving equations simulating the steady-state behaviour of the multi-stage flash desalination process. *Desalination*, **107**, 171.

Edgar, T. F., Hinnemlauer, D. M. and Lasdon, L. S. (Eds) (2001). Optimization of chemical processes. Second Edition. New York. Mc Graw-Hill.

Eikens, B. Karim, M. N. and Simon, L., (2001a). 'Process identification with self-organising networks' *Application of Neural Network and other Learning Technologies in process Engineering* (Eds I. M. Mujtaba and M. A. Hussain Imperial College Press, London, pp 49-76.

Ekpo, E. E. and Mujtaba I. M. (2008). Evaluation of neural networks-based controllers in batch polymerisation of methyl methacrylate. *Neurocomputing* **71**, 1401–1412.

EL-Bairouty, M., Fath, H., Saddiqi, M., and EL-Rabghy, O. (2005). Design, Construction and Testing of Experimental Education MSF Desalination Unit. Proceeding of IDA Congress in Desalination & Water Reuse Singapore.

El-Dahshan, M. E. (2001). Corrosion and scaling problems present in some desalination plants in Abu Dhabi, *Desalination*, **138**, 371–377.

EL-Dessouky, H. (2000). Multi-stage flash desalination technologies. Euro summer school short course on sustainability assessment of water desalination technologies, Vilamoura, Portugal.

EL-Dessouky, H. T. and Ettouney, H. M. (1999). Multiple-effect evaporation desalination systems thermal analysis, *Desalination*, **125**, 259-276.

EL-Dessouky, H. T. and Ettouney, H. M. (2002). Fundamentals of salt water desalination Amsterdam: Elsevier Science Ltd.

EL-Dessouky, H. T. and Khalifa, T. A. (1985). Scale formation and its effect on the performance of once through MSF plant, *Desalination*, **55**, 199-217.

EL-Dessouky, H., Alatiqi, I. and Ettouney H. (1998). Process synthesis: the multi-stage flash desalination system, *Desalination*, **115**, 155-179.

- El-Dessouky, H., Ettouney, H., Al-Juwayhel, F. and Al-Fulaij, H. (2004) *Chem. Eng. Res. Design* **82**, 1–12.
- EL-Dessouky, H., Shaban, H. I. and Al-Ramadan, H. (1995). Steady-state analysis of multi-stage flash desalination process, *Desalination*, **103**, 271-287.
- El-Dessouky, H.T Alatiqi, I. M. Ettouney, H. M. and Al-Deffeeri, N. S. (2000). Performance of wire mesh mist eliminator, *Chemical Engineering and Processing*, **39** 129 – 139.
- El-Dessouky, H.T. and Ettouney, H. M. (1997). Simulation of combined multiple effect evaporation – vapour compression desalination processes, 1st IDA Int. Desalination Conference, Cairo.
- EL-Moudir, W., ElBousiffi, M. and Al-Hengari, S. (2008). Process modelling in desalination plant operations, *Desalination*, **222**, 431–440.
- EL-Nashar, A. M. (1998). Optimization of operating parameters of MSF Plants through automatic set point control, *Desalination*, **116**, 89-107.
- EL-Sayed, E. E. F., Al-Odwani, A., Ahmed, M. and Al-Tabtabaei, M. (2006). Process design and performance of an MSF distillation test unit for corrosion studies, *Desalination*, **201**, 23-34.
- Ettouney, H. (2005). Brine entrainment in multistage flash desalination, *Desalination*, **182**, 87–97.
- Ettouney, H. M., El-Dessouky, H. T., Faibish, R. and Gowin, P. (2002). Evaluating the economics of desalination, CEP Magazine.

- Falcetta, M. F. and Sciubba, E. (1999). Transient simulation of a real multi-stage flashing desalination process, *Desalination*, **122**, 263-269.
- Fatha, H. E. S. and Ismail, M. A. (2008). An online cleaning system to reduce demister fouling in MSF Sidi Krir Desalination Plant  $2 \times 5000 \text{ m}^3/\text{day}$ , *Desalination*, **220**, 252–257
- Fausett, L. V., (1994). ‘Fundamentals of neural networks: Architectures, algorithms and applications.’ Prentic-Hall, London.
- Finan, M. (1991). Some aspect of scale control in seawater evaporators, First exposition and symposium for new and renewable energy equipment, 4- 6 May, 1991, Tripoli, Libya.
- Fink, F. W., White, E. L. and Boyd, W. K. (1966). US Dept of Interior, R & D Progress Report No. 225.
- Floudas, C. A. (1995) Nonlinear and mixed-integer optimisation: Fundamentals and Applications. USA: Mar combo.
- Furuki, A., Hamanaka, K., Tatsumoto, M. and Inohara, S. (1985). Automatic control system of MSF process (ACSODE), *Desalination*, **55**, 77-89
- Gill, J. S. (1999). A novel inhibitor for scale control in water desalination, *Desalination*, **124**, 43-50.
- Gille, D. (2003), Seawater intakes for desalination plants. *Desalination*, 156, 249
- Glueck, A. R. and Bradshaw, R.W. (1970), A mathematical model for a multistage flash distillation plant. Proc 3rd Int. Symp. on Fresh Water from the Sea, **1**, 95–108.

Gosling, I. (2005) Process simulation and modelling for industrial bioprocessing tools and techniques. *Ind. Biotechnology*, 1 (2), 106-109.

gPROMS (2005) gPROMS User Guide 2005: Process System Enterprise Ltd (PSE).

Grossmann, I. E. (2002). Review on nonlinear mixed-integer and disjunctive programming techniques, *Optim Eng.* 3, 227.

Hagan, M. T., Demuth, H. B. and Beale, M. (1996), *Neural Network Design*. Boston: PWS

Hamed, O. A., AL-Sofi, M. A. K., Imam, M., Ba- Mardouf, K., AL-Mobayed, A. S. and Ehsan, A. (2000). Evaluation of polyphosphonate anti-scalant at low dose rate in the AL-Jubail Phase II MSF plant, Saudi Arabia , *Desalination*, **128**, 275-280.

Hamed, O. A., AL-Sofi, M. A. K., Mustafa, G. M. and Dalvi, A. G. (1999). Performance of different anti-scalants in multi-stage flash distillers. *Desalination*, **123**, 185-194.

Hamed, O. A., Mardouf, K. B. and Al-Omran, A. (2007). Impact of interruption of anti-scalant dosing or cleaning balls circulation during MSF plant operation, *Desalination*, **208**, 192-203.

Handury, W. T. (1995). An analytical simulation of multiple effect distillation plant, *IDA World Congress*, **4**, 375-382.

Harding, K. and Bridle, D.A. (1975). Proc. 6th Int. Symp. on Fresh Water from the Sea, Las Palmas.



Hawaidi, E. A. M. and Mujtaba, I. M. (2010). Simulation and optimization of MSF desalination process for fixed freshwater demand: Impact of brine heater fouling, *Chemical Engineering Journal*, **165**, 545 – 553.

Hawaidi, E. A. M. and Mujtaba, I. M. (2011). Effect of Demister Separation Efficiency on the Freshwater Purity in MSF Desalination Process, In *Computer Aided Chemical Engineering*, vol. 29, 1180-1184, Elsevier B.V., 2011.

Hayakawa, K. Satori, H. and Konishi, K. (1973). Process simulation on multi flash desalination plant, 4th international Symposium on Fresh Water from Sea, 1, 303.

Helal, A. M. (2005). Once-through and brine recirculation MSF designs a comparative study, *Desalination*, **171**, 33-60.

Helal, A. M., El-Nashar, A. M. Al-Katheeri, E. and Al-Malek, S. (2003). Optimal design of hybrid RO/MSF desalination plants Part I: Modelling and algorithms, *Desalination*, **154**, 43-66.

Helal, A. M., Medani, M. S., Soliman, M. and Flower, J. (1986). A TDM model for MSF desalination plants, *Computer Chem. Eng.* **10**, 327–342.

Hilal, N., Kim, G. J. and Somerfield, C. (2011), Boron removal from saline water: A comprehensive review, *Desalination*, **273**, 23–35.

Husain, A. (Ed) (2003). Integrated power and desalination plants. Oxford: Eolss Publishers Co.

Husain, A., Hassan, A., Al-Gobaisi, D. M. K., Al-Radif, A., Woldai, A. and Sommariva, C. (1993). Modelling, simulation, optimization and control of multistage

flashing (MSF) desalination plants Part I: Modelling and simulation, *Desalination*, **92**, 21-41.

Husain, A., Woldai, A., Al-Radif, A., Kesou, A., Borsani, R., Sultan, H. and Deshpandey, P. B. (1994). Modeling and simulation of a multistage flash (MSF) desalination plant, *Desalination*, **97**, 555-586.

IDA, The ABCs of desalting. Topsfield. Second ed. International Desalination Association IDA, Massachusetts, USA, 2000.

IDA. (2006). The 19<sup>th</sup> IDA Worldwide desalting plant inventory. Topsfield, MA, USA, International desalination association.

Khawaji, A., D., Kutubkhanah, I. K. and Wie, J. (2008). Advances in seawater desalination technologies, *Desalination* **221**, 47–69.

Krothapally, M. and Palanki, S. (1997). A neural network strategy for batch process optimisation. *Comput. Chem. Eng.*, 21 (suppl), S463-S468.

Lattemann, S. and Hopner, T. (2008). Environmental impact and impact assessment of seawater desalination, *Desalination*, **220**, 1-15

Lawgali, F. F., (2008), Forecasting water demand for agricultural, industrial and domestic use in Libya, *International Review of Business Research Papers* Vol.4 No. 5 October-November 2008, 231-248.

Lior, N., 17<sup>th</sup> International Congress of Chemical and Process Conference, 27–31 August 2006, Praha Czech Republic.

Malik, A. U. and Kutty, P. C. M. (1992). Corrosion and material selection in desalination plants, SWCC & M Seminar, Al Jubail.653-684.

Mandil, M. A. and Ghafour, E. E. (1970). Optimization of multi-stage flash evaporation plants, *Chemical Engineering Science*, **25**, 611-621

Marian G. M., Mussati, S. F., Aguirre, P. A., Nicola's J. and Scenna, N. J. (2005). Optimization of hybrid desalination processes including multi stage flash and reverse osmosis systems. *Desalination*, **182**, 111-122.

Mazzotti, M., Rosso, M., Beltramini A. and Morbidelli, M. (2000). Dynamic modeling of multistage flash desalination plants, *Desalination*, **127**, 207-218.

Miller, J. P. (1952). A portion of the system  $\text{CaCO}_3 - \text{CO}_2 - \text{H}_2\text{O}$  with geological implications, *American Journal of Science*, 250,161.

Mohsen, M. S. and Al-Jayyousi, O. R. (1999). Brackish water desalination: an alternative for water supply enhancement in Jordan, **124**, 163-174.

Mujtaba, I. M. (2004). Batch distillation: design and operation. London: Imperial College Press.

Mujtaba, I. M. (2007). Meeting the Sustainable Freshwater Demand of Tomorrow's World by Desalination: State of the Art and Future Challenges for the CAPE Community [cape.cperi.certh.gr/files/SitePres/OP40\\_Mujtaba.pdf](http://cape.cperi.certh.gr/files/SitePres/OP40_Mujtaba.pdf).

Mujtaba, I. M. and Hussain, M. A., (Eds), (2001), Application of neural networks and other learning technologies in process engineering. Imperial college pers, London: World Scientific Pub Co INC

Mujtaba, I. M., Aziz, N. and Hussain, M. A. (2006). Neural network based modelling and control in batch reactor. *Trans IchemE*, 48 (A), 635- 644.

Mussati, S. F., Aguirre, P. A. and Scenna, N. J. (2004). A rigorous mixed-integer non linear programming model (MINLP) for synthesis and optimal operation of cogeneration seawater desalination plants, *Desalination*, **166**, 339- 345.

Mussati, S. F., Aguirre, P. A., Scenna, N. J. (2004). Improving the efficiency of the MSF once through (MSF-OT) and MSF-mixer (MSF-M) evaporator, *Desalination*, **166**,141-151.

Mussati, S. F., Aguirre, P. and Scenna, N. (2003). Dual-purpose desalination plants. Part II. Optimal configuration' *Desalination*, **153**, 185-189.

Mussati, S. F., Barttfeld, M., Aguirre, P. A. and Scenna, N. J. (2008). A disjunctive programming model for superstructure optimization of power and desalting plants *Desalination*, **222**, 457-465.

Mussati, S., Aguirre, P., Scenna, N. J. (2001). Optimal MSF plant design, *Desalination*, **138**, 341-347.

Mussati, S.F., Aguirre, P.A. and Scenna, N.J. (2005). Optimization of alternative structures of integrated power and desalination plants, *Desalination*, **182**, 123-129.

Nada, N. (2002). A thermodynamic assessment for the top brine temperature in MSF evaporator. In Bahrain Proceedings, Vol. CD Bahrain: IDA.

Nada, N., Khumayyis, D. and Al Hussain, M. (1985). Economical evaluation of Alkhobar Phase two 50 MIGPD at three different mode of operations, *Desalination*, **55**, 43-54.

Nafey, A. S., Fath, H. E. S. and Mabrouk, A. A. (2006). Thermo-economic investigation of multi effect evaporation (MEE) and hybrid multi effect evaporation—multi stage flash (MEE-MSF) systems, *Desalination*, **201**, 241-254.

Newton, E. H and Birkett, J. D. (1969). Summary report on survey of materials behavior in multistage flash distillation plants, *Desalination*, **6**, 229-237.

Oh, M. and Pantelides, C. C. (1996) A modelling and simulation language for combined lumped and distributed parameter systems. *Computer and Chemical Engineering*, **20**, 611-633

Omar, A. M. (1983). Simulation of MSF desalination plants, *Desalination*, 45, 65-76.

Patel, S. and Finan, M. A. (1999). New anti foulants for deposit control in MSF and MED plants, *Desalination*, **124**, 63-74.

Process Systems Enterprise, Experiment Design for Parameter Precision in gPROMS,2004.

Rao, G. P. (1993). Unity of control and identification in multistage flash desalination processes, *Desalination*, **92**, 103-124.

Rimawi, M. A., Ettouney, H. M. and Aly, G. S. (1989). Transient model of multistage flash desalination, *Desalination*, **74**, 327-338.

Rosso, M., Belmmini, A., Mazzotti, M. and Morbidelli, M. (1996), Modeling Multistage FlashDesalination plants, *Desalination*, **108**, 365-374.

Said, S. A., Emtir, M. and Mujtaba, I. M. (2011). Neural network based correlations for estimating the first and second dissociation constant of carbonic acid in seawater. *Chemical Engineering Transactions* **24**, 523-528.

Sassi, K. M. and Mujtaba, I. M. (2011). Optimal design and operation of reverse osmosis desalination process with membrane fouling. *Chemical Engineering Journal*, **171**, 582-593.

- Schrieber, C-F. and Coley, F.H. (1971). *Materials Performance*, 15 (7), 47.D-6.  
Anderson, NACE Chicago March.
- Shams El Din, A. M. and Makkawi, B. (1998). Operation processes affecting corrosion in MSF distillers, *Desalination*, **115**, 33-37.
- Shams El Din, A. M. and Rizk, M. A. (1994). Brine and scale chemistry in MSF distillers, *Desalination*, **99**, 73-111.
- Sinnott, R. K. (2005). *Chemical Engineering Design*, volume 6, Fourth edition.
- Sommariva, C., Pinciroli, D., Tolle, E. and Adinolfi, R. (1991). Optimization of material selection for evaporative desalination plants in order to achieve the highest cost-benefit ratio, *Desalination*, **124**, 99-103.
- Stoughton, R.W. and Lietzke, M.H. (1967). Thermodynamic properties of sea salt solutions. *Chem. Eng. Data*, **12**, 101–104.
- Tanvir, M. S. (2007). Neural network based hybrid modelling and MINLP based optimization of MSF desalination process within gPROMS. PhD thesis. University of Bradford
- Tanvir, M. S. and Mujtaba, I. M. (2006a). Modelling and simulation of MSF desalination process using gPROMS and neural network based physical property correlation, *Computer Aided Chemical Engineering*, **21**, 315-320.
- Tanvir, M. S. and Mujtaba, I. M. (2008a). Optimization of design and operation of MSF desalination process using MINLP technique in gPROMS, *Desalination*, **222**, 419-430.

Tanvir, M. S. and Mujtaba, I. M., (2006b). Neural network based correlations for estimating temperature elevation for seawater in MSF desalination process, *Desalination* **195**, 251–272.

Tanvir, M. S. and Mujtaba, I. M., (2008b). Less of the foul play: Flexible design and operation can cut fouling and shutdown of desalination plants, *The Chemical Engineer, IChemE*, June, 28-29.

Thomas, P. J., Bhattacharyya, S., Patra, A. and Rao, G. P. (1998) Steady state and dynamicsimulation of multi-stage flash desalination plants: A case study. *Computers & Chemical Engineering*, **22**, 1515-1529.

Tijl , P. (2005). Capabilities of gPROMS and Aspen Custom Modeler, Using the Sec-Butyl-Alcohol Stripper Kinetics Case Study, Eindhoven Technical University.

Ustun, A. P. and Corvalan, C. (2006). Preventing Disease through Healthy Environment, towards an estimate of the environmental burden of disease. World Health Organization, WHO.

Virella, J. C., Portela, G. and Godoy, L. A. (2006). Toward an inventory and vulnerability of aboveground storage tanks in Puerto Rico, Fourth LACCEI International Latin American and Caribbean Conference for Engineering and Technology (LACCEI'2006), 21-23 June 2006, Mayagüez, Puerto Rico.

Wade, N. M. (2001). Distillation plant development and cost update, *Desalination*, **136**, 3-12.

Wade, N., Willis, J. and Mcsorley, J. (1999). The Taweelah A2 independent water and power project, *Desalination*, **125**, 191-202.

Yasunaga, K., Fujita, M., Ushiyama, T. , Yoneyama, K., Takayabu, Y. N. and Yoshizaki, M. (2008), Diurnal Variations in Perceptible Water Observed by Shipborne GPS over the Tropical Indian Ocean. SOLA, **4**, 97–100.

Zeybeck, Z., Yuse, S., Hapoglu, H. and Albaz, M. (2004). Adaptive heuristic control of batch polymerisation reactor . *Chem. Eng. Processing* 43, 911-920.

Zupan, J. and Gasteiger, J. (1999). Neural network in Chemistry and Drug Design. Weinheim, Germany, Wiley-VCH.



## Appendix

### Publications Made from This Work

- 1 E. A. M. Hawaidi and I.M. Mujtaba, Simulation and optimization of MSF desalination process for fixed freshwater demand: Impact of brine heater fouling, *Chemical Engineering Journal*, (2010), vol. 165, 545 – 553.
- 2 E. A. M. Hawaidi and I. M. Mujtaba, Meeting Variable Freshwater Demand by Flexible Design and Operation of MSF Desalination Process, *Industrial & Engineering Chemistry Research*, (2011), vol. 50, 10604–10614.
- 3 E. A. M. Hawaidi and I. M. Mujtaba, Sensitivity of Brine Heater Fouling on Optimization of Operation Parameters of MSF Desalination Process using gPROMS, in Proceedings of 20<sup>th</sup> European Symposium on *Computer Aided Process Engineering*, pp1787-1792, Eds. S. Pierucci and G. Buzzi Ferraris, Naples, Italy, 6-10 June, 2010.
- 4 E. A. M. Hawaidi and I. M. Mujtaba, Effect of Demister Separation Efficiency on the Freshwater Purity in MSF Desalination Process, In *Computer Aided Chemical Engineering*, vol. 29, 1180-1184, Elsevier B.V., 2011.
- 5 E. A. M. Hawaidi and I. M. Mujtaba, Freshwater Production by MSF Desalination Process: Coping with Variable Demand by Flexible Design and Operation, In *Computer Aided Chemical Engineering*, vol. 29, 895-899, Elsevier B.V., 2011.
- 6 E. A. M. Hawaidi and I. M. Mujtaba, Effect of Brine Heater Fouling on Performance of MSF Desalination Process using gPROMS, International Conference on Energy, Environment and Water Desalination, 8 – 9 December, 2009, Tripoli, Libya

- 7 Effect of Demister Separation Efficiency on the Purity of Freshwater of MSF Desalination Process using gPROMS, *CAPE PhD. Poster Day 2010*, Wednesday 12 May 2010, University of Leeds.
- 8 E. A. M. Hawaidi and I. M. Mujtaba, Impact of Fouling on Flexible Design and Operation of MSF Desalination Process with Variable Freshwater Demand. Submitted to Proceedings of 22<sup>nd</sup> European Symposium on Computer Aided Process Engineering, 17 - 20 June 2012, London.